University of Alberta

A Framework to Improve the Control System Design for Integrated
Residential Heating Systems in Cold Regions

by

Xinming Li

A thesis submitted to the Faculty of Graduate Studies and Research
in partial fulfillment of the requirements for the degree of

Master of Science

in

Construction Engineering and Management

Department of Civil and Environmental Engineering

©Xinming Li
Fall 2013
Edmonton, Alberta

Abstract

Building space heating contributes to high consumption of energy using primarily non-renewable sources. This thesis presents a research study evaluating the design and performance of an integrated heating system utilizing the renewable energy sources of geothermal energy, solar energy, and drain water heat recovery. In general, the usage of geothermal heating in cold regions is challenged by the heat loss from the geothermal field. The proposed integrated system is expected to recover the heat loss from the geothermal field, extend the service life of the geothermal heating system, and provide significantly more energy with higher efficiency. The framework is validated through a residential building under occupancy, where a proposed monitoring system is installed to estimate the performance of the system. Based on the findings, adjustments in the design of the heating system, incorporating an enhanced system control algorithm to enhance system efficiency for energy savings and cost effectiveness, are recommended.

Acknowledgements

Table of Contents

List of Tables

List of Figures

List of Nomenclature

Q: Thermal Energy, kilojoules (kJ)

C: Specific Heat, kJ/kg°C

M: Mass of fluid within a period of time, kg

ΔT: Temperature difference, °C

ρ: Density of fluid, kg/m^3

V: Volume of fluid, m^3

R_m: Mass flow rate of fluid, kg/hr

R_v: Volume flow rate of fluid, m^3/hr

T_{Return}: Temperature of return pipe, °C

T_{Supply}: Temperature of supply pipe, °C

t: serving time or operation time, hrs

Q_{HP}: Energy production from heat pumps, GJ

E_{HP}: Heat pump electricity consumption, kWh

Q_{HP_source}: Energy production from the source side of heat pumps, GJ

$Q_{Building}$: Energy removed from buildings, GJ

E_{HP}: Heat pump electricity consumption, kWh

Q_{Solar}: Energy production from solar energy system, GJ

E_{Solar_pump}: Electricity consumption of solar energy system circulating pumps, kWh

Q_{DWHR}: Energy production from DWHR system, GJ

E_{DWHR_pump}: DWHR system circulating pump electricity consumption, kWh

ε : Efficiency of drain water heat recovery system (%)

Q_{Cold} : Thermal energy absorbed from drain water pipe, J

Q_{Drain} : Thermal energy conducted by drain water pipe, J

C_f : Specific heat of fluid in surrounding pipe, J/g. °C

M_{cold} : Mass of fluid in surrounding pipe, g

$T_{Cold-out}$ and $T_{Cold-in}$: Temperature of fluid out and in the surrounding pipe, °C

C_{Drain} : Specific heat of drain water, J/g. °C

M_{Drain} : Mass of drain water, g

$T_{Drain-in}$ and $T_{Drain-out}$: Temperature of drain water in and out the drain water pipe, °C

$Q_{one\ stack,\ 7\ days}$: Energy production from one stack of DWHR system, GJ

$V_{water,\ 8}$: Water usage from apartment units 1, 2, 3, 4, 5, 8, 10, 12, L

Q_{DWHR}: Energy recycled from one stack of DWHR system, GJ

E_{WHT}: Electricity consumption from water-heating tank, kWh

CHAPTER 1: INTRODUCTION

1.1 Background and Research Motivation

It is widely accepted that our world is facing and will continue to face energy consumption-related atmospheric pollution problems. As major contributors to this energy consumption, buildings are primarily heated using non-renewable sources of energy such as natural gas and diesel. Fuel prices have been increasing as fuel sources become increasingly limited in conjunction with increasing energy demand throughout the world (Aikins and Choi, 2012). The underlying problem is that a greater rate of energy consumption is required than the existing sources can provide (Stein and Powers, 2011). Given this challenge, it is widely advocated that renewable energy utilization replace the usage of non-renewable sources.

Renewable energy sources such as geothermal energy and solar energy are widely used in building heating and cooling systems. However, a number of challenges, such as high initial cost with long-term payback of utilizing renewable sources, constrain their use. This research focuses on evaluating the performance of these renewable sources of energy and improving the efficiency of each heating system for space heating in cold regions.

Among the various technologies for exploiting renewable sources of energy, the ground source heat pump (GSHP), also known as a geothermal heat pump, has significant benefits in terms of energy usage reduction, CO_2 emission reduction, and reduced space requirements (Hepbasli et al., 2003). Geothermal is an effective renewable source of energy which involves extracting heat from the underground field. Interest in geothermal resources has been increasing around the world, and the technology shows significant promise. In Canada, the usage of GSHPs has increased at an annual rate of 10%-15% since 2000 (Lund, 2005). In cold regions, such as Northern Alberta, the usage of geothermal energy reduces potentially available heat over time. The geothermal gradient is 24.2 °C/km in Alberta, Canada, which means the temperature of a given geothermal field from a depth of 100 m ranges from 2°C to13°C, while the temperature of a given geothermal field from a depth of 1000 m ranges from 23°C to 34°C. This source of energy preheats the fluid on the inlet of the heat pump to increase its efficiency. Fort McMurray and Steen River, it should

be noted, are the two communities, which have the highest geothermal gradient in the province (Lam et al., 1984).

In this regard, changes to the underground temperature affect the performance of GSHPs if the GSHP is only using a ground heat exchanger (GHE). GSHPs use the geothermal energy as a heating system in winter and a cooling system in summer, and are powered by electricity using heat pumps, producing a large amount of energy as output. However, it is not easy to balance the heat absorbed from underground and the heat rejected over the years. After long-term operation, if the energy provided from the geothermal field is greater than the energy injected into the field, the field temperature will drop since its self-recovery capacity from the surrounding mass is limited (Wu et al., 2013). Continuous loss of heat will render the geothermal field ineffective as an energy source. This problem is even more pronounced in cold regions since in these cases the heating load is much greater than the cooling load. In this case, a source of heat must be produced to reheat the geothermal field and recover its heating capacity for long-term usage. Most of the other research studies conducted with respect to GSHPs have investigated cases where these systems are used for both heating and cooling. This research, however, investigates the use of a GSHP in an extreme cold region where only heating load is required, which introduces more challenges.

To overcome these challenges, in this research an integrated heating system has been proposed, which has been implemented in a residential building under occupancy in Fort McMurray, Alberta, Canada where heating is a major contributor to the total energy consumption. This integrated heating system includes solar energy and drain water heat recovery (DWHR) assisting the GSHP system and recovering the heat loss of the geothermal field. Solar energy is widely used in many applications in the form of solar radiation for heat, whereas DWHR recycles the wasted energy from drain water. These sources of energy can be used for space heating, can be injected to the geothermal field, and serve to increase the efficiency of heat pumps. Natural gas is also included as a high efficiency non-renewable backup resource. It should be noted that it is generally difficult to predict the performance of a GSHP after only a few years of operation. The development of a sensor-based monitoring framework for estimating the energy performance, which can

also be implemented in other existing building systems, is thus integral to this study. Such monitoring applications are expected to provide useful information about the energy production and efficiency of the existing systems. Based on the information extracted from the monitoring data and unit prices of renewable resources, which are usually higher than the prices of non-renewable resources, an enhanced control system for cost-effectiveness can be achieved. More effective control algorithms can be developed to take full advantage of renewable resources.

1.2 Research Objectives

The framework presented in this thesis is designed to increase the use of renewable resources in place of non-renewable resources in order to reduce greenhouse gas emissions and environmental footprint. Mechanical and system engineers have designed the energy management system to control and monitor the existing system. The standard of this design is part of the National Building Code, but the need for a region-specific design cannot be ignored. Within the context of these considerations, this research is built upon the following **hypothesis**:

Measuring the actual performance of the integrated heating system and geothermal heat loss recovery system allows mechanical engineers to improve the control system design for more efficient heating system operations.

In order to verify this hypothesis, the research encompasses the following objectives:

- Design an experimental system to measure space heating system performance (sensor-based monitoring for data collection and data analysis)
- Analyze the existing design for the control system
- Develop an intelligent control algorithm in order to improve the existing control system design

1.3 Thesis Organization

Chapter 2 (Literature Review) opens with a general summary of renewable and non-renewable sources of energy. A detailed discussion is then presented of the ground source heat pump, solar energy system, and DWHR system which will be implemented in the

case study. Finally, details pertaining to the usage of the integrated system for the special conditions of cold-climate regions are outlined.

Chapter 3 (Proposed Methodology) discusses the proposed methodology used in this research, which is implemented in a real life project in Fort McMurray. The proposed integrated heating system has been designed to achieve energy savings for the operational life of a project under the challenge of extreme cold weather, with the associated increased demand placed on the heating system. Energy production and system efficiency calculations are the two metrics provided in this thesis. Based on these two metrics, a corresponding sensor-based experimental design is created for data collection and data analysis.

Chapter 4 (Implementation Process) discusses the implementation of the proposed methodology with monitoring design in a building under occupancy. Following installation of the sensors, data is collected for analysis of the existing system, and the energy production and efficiency of each heating system are assessed and predicted. To increase the efficiency and cost-effectiveness of the current heating system, suggestions and adjustments are proposed.

Chapter 5 (Conclusions) describes the general conclusions based on the proposed monitoring system, the main contributions of the research, and some recommendations for future research and practical applications.

CHAPTER 2: LITERATURE REVIEW

2.1 Analysis of Each Energy Resource and System

In this section, a general discussion of current renewable and non-renewable energy resources is presented. Their corresponding advantages and disadvantages are also discussed.

2.1.1 Non-renewable Resources: Fossil Fuel

The principal non-renewable energy source is fossil fuels. There are several problems with using non-renewable energy, such as the carbon footprint and the imbalance between increasing energy demand and limited energy resources.

Coal: The use of coal is increasing due to the growth of the world's population and the industrialization of populous developing countries. Although coal is abundant, its usage is limited due to increasingly difficult and expensive mining techniques and environmental damage. Coal has been the principal fuel in industry and power generation plants. 58 million tons of coal was consumed in Canada, in 2006, for instance, of which 51 million tons was used for electricity generation (Natural Resources Canada, 2013). However, feeding the coal and moving the ash to generate electricity requires substantial manual labour or automated machinery (Stein and Powers, 2011).

Oil: Transportation of oil is more convenient compared to coal, and Canada is the sixth largest oil producer in the world (Natural Resources Canada, 2013). In Canada, both the importation and exportation of oil are highly sophisticated due to a number of technical and non-technical factors. Most of the oil reserves in Canada are in the form of oil sands, and 95% of these oil sands are located in Alberta (EIA, 2007). The most popular high quality crude oil end-products are oil and gasoline (Stein and Powers, 2011). Heating oil is a low-viscosity liquid which fuels furnaces or boilers for the heating of buildings. However, compared to natural gas, heating oil is less affordable due to the increasing price and it also generates greater CO_2 emissions.

Natural gas: Natural gas is considered a smart energy due to its abundance, affordability, safeness, cleanness, and reliability (Canadian Natural Gas, 2013), and it has been widely used in Canadian residential, commercial, institutional, and industrial applications. As

indicated by Canadian Natural Gas (CNG), over 30% of energy demand in Canada has been supplied by natural gas. More specifically, over six million homeowners use natural gas appliances to heat their homes and water. Natural gas supplies 47.7% of space heating in Canada, and it also accounts for 48.6% of water heating. Figure 1 and Figure 2 show the distribution of the energy sources used for residential space heating and water heating, respectively. Furnaces are the major equipment used to burn natural gas in residential buildings, and the furnace needs oxygen to support the combustion of the natural gas. Normally, the furnace is divided into direct vent units, which bring air into the burner area via sealed inlets, and non-direct vent units, which use surrounding air for combustion.
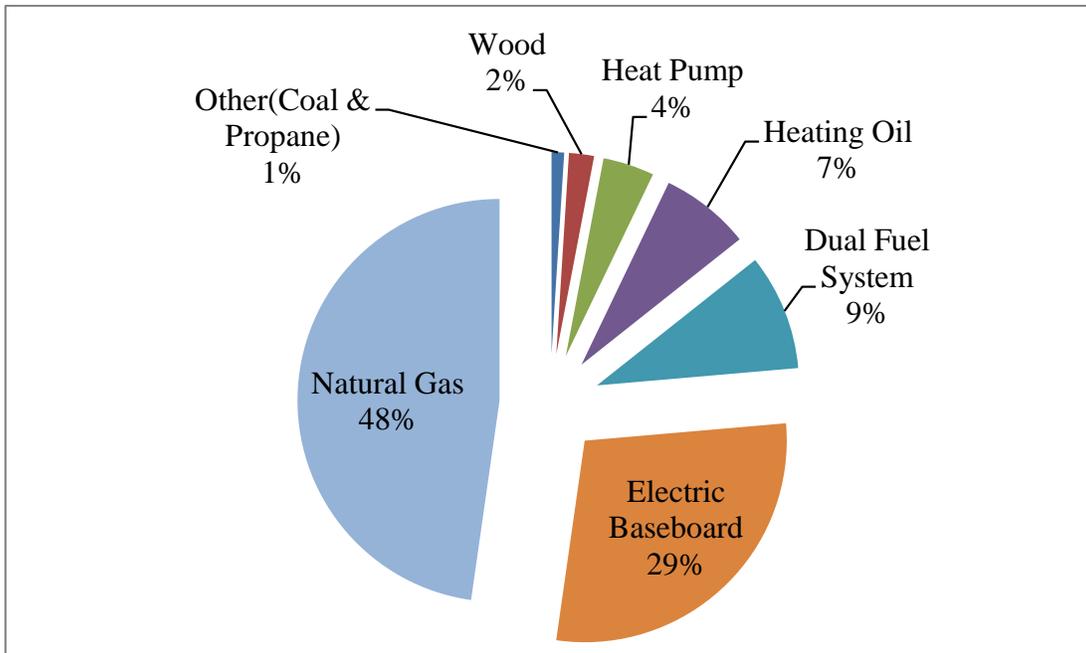
Figure 1: Distribution of residential space heating (Canadian Natural Gas, 2013)
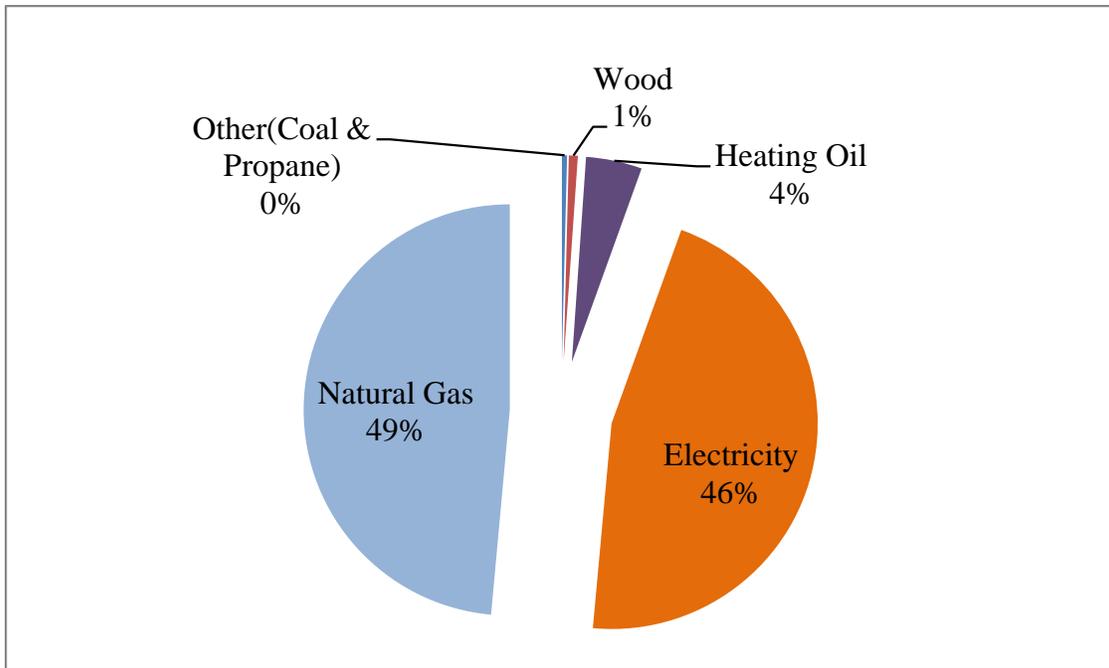
Figure 2: Distribution of residential water heating (Canadian Natural Gas, 2013)

The amount of CO_2 produced by natural gas is half of the CO_2 produced by oil per unit of energy. Due to the decreasing availability of and increasing demand for energy, the costs of both natural gas and oil are increasing. The cost of oil has increased even more rapidly, which makes the utilization of natural gas energy even more attractive (Stein and Powers, 2011).

2.1.2 Renewable Resources

The usage of fossil-based fuels is restricted due to global warming and ecological and economical concerns, and as a result the importance of renewable resources is increasing. Clean and renewable energy is expected to replace the usage of non-renewable sources of energy to some extent, and thus to benefit the global environment. Renewable energy can be obtained from naturally replenished and renewed resources such as sunlight, wind, tides, and geothermal energy (Natural Resources Canada, 2013). Owing to newly developing technologies, renewable energy sources can be converted to usable energy, such as electricity, industrial steam, and space heating. Figure 3 summarizes renewable energy usage in general (Natural Resources Canada, 2013). The renewable resources discussed in this thesis, including solar energy and geothermal energy, will be presented

in later sections (Figure 5). A sustainable water heat recycling system, drain water heat recovery (DWHR), is also detailed in later sections.
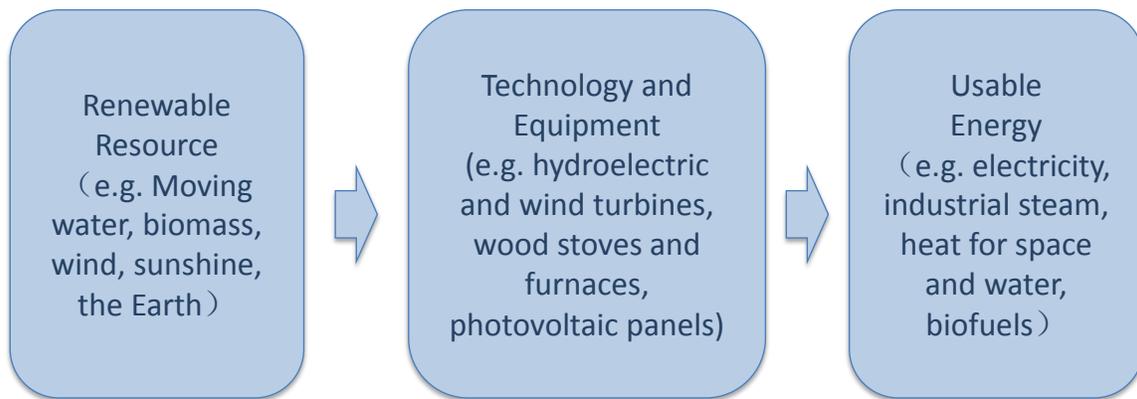
Figure 3: Renewable energy usage (Natural Resources Canada, 2009)

Sunlight: Most of the energy stored in the earth originates from the sun (Stein and Powers, 2011). Solar energy is a clean and renewable resource, and will be an essential component of sustainable energy in the future (Bakirci et al., 2011). Radiant light and heat from the sun provide a large amount of energy that can be utilized for water heating and space heating. Photovoltaic panels and solar thermal collectors can collect the energy from the sun and provide heat to buildings. Solar resources can be utilized most extensively in Eastern Canada (i.e., Ontario and Quebec).

Moving Water: Both falling water and running water can generate power, called hydropower. Run-of-the-river and conventional hydroelectric dams are the most popular methods to generate energy from moving water. Larger dams provide substantial energy and electricity with water driving through the turbines (Stein and Powers, 2011). Currently, hydroelectric power provides most of the electricity in many countries. In the United States, hydroelectric power is the largest renewable resource, accounting for 49% of renewable energy. Canada produced more than 340 billion kilowatt-hours (kWh) in 1999, becoming the world's largest hydroelectric power producer at that time (Water Encyclopedia, 2013). In most Canadian provinces the majority of the energy produced is hydroelectric, and in Manitoba, British Columbia, and Quebec, hydroelectric energy accounts for as much as 90% of the energy produced.

Wind: Diverse temperatures on land and in the ocean cause warm air with less density to move up while cooler air with more density moves down (Stein and Powers, 2011); wind moves the air with unequal thermal energy. Wind energy is a popular renewable source which involves converting wind to electricity. Canada is the world's ninth-largest wind energy producer, while China is the largest wind energy producer, followed by the United States. 2.3% of Canada's electricity was generated from wind in 2011 (The Globe and Mail, 2013).

Geothermal energy: Geothermal heat is an efficient source of energy with significantly lower CO_2 emissions than conventional fossil fuels (Al-Khoury, 2012). Approximately 47% of ground thermal energy is absorbed from the sun (Cooperman et al., 2012). This thermal energy stored in the ground manifests in diverse ways. While the earth surface's temperature fluctuates readily, the ground temperature at only a shallow depth (9 m) remains constant for years (IGSHPA, 2009). Furthermore, geothermal energy classified by source temperature is used for power production as well as for cooling and heating systems. Geothermal sources of temperature above 150°C are used for power production, while moderate temperatures (between 90°C and 150°C) and low temperatures (below 90°C) are suitable for space heating or cooling (Ratlamwala et al., 2012). Hot springs are another geothermal energy source, whereby energy is drawn from naturally heated underground water (Stein and Powers, 2011).

2.1.3 Electricity

Fossil fuels (coal, natural gas, and oil products), nuclear energy, and renewable energy (hydroelectric, geothermal, wind, solar, and their alternatives) are the resources available for producing electricity. The price of electricity is affected by the supply and demand of fuel, transmission, international events, and climate change. It fluctuates through years, seasons, and even days (IGSHPA, 2009).

Canada is a major world producer of hydroelectricity, with hydroelectric power accounting for up to 60% of Canada's electricity generation. The remainder is produced from such sources as coal, nuclear energy, and natural gas, as shown in Figure 4. Households use electricity for heating, lighting, and for powering appliances. According to Statistics Canada, heating of one third of households is supplied by electricity, while others use supplementary heating sources (Statistics Canada, 2012).
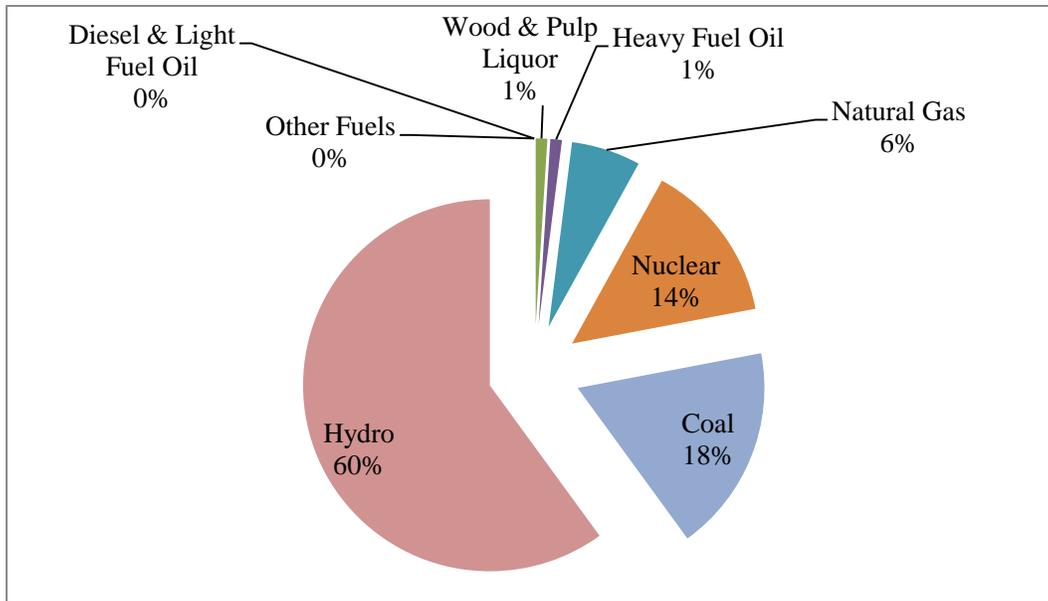
Figure 4: Electricity generation in Canada (Statistics Canada, 2013)

2.2 Renewable Sources and Sustainable Energy Systems in this Thesis

The research presented in this thesis utilizes a number of resources for space heating. In this section, solar energy and electricity-assisted geothermal heat pumps are discussed. As seen in Figure 5, photovoltaic panels are used to collect the thermal energy from sunlight, while heat pumps powered by electricity utilize geothermal sources to produce energy. In this research, both solar and geothermal energy are used for space heating, as is sustainable energy from the DWHR system.
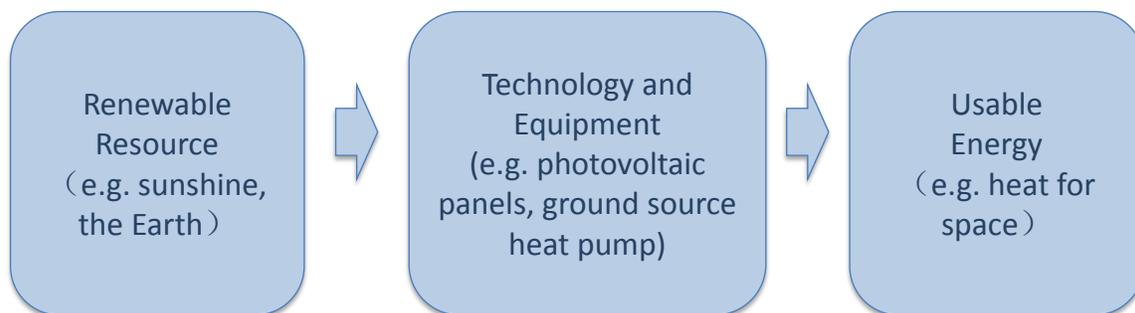
Figure 5: Renewable energy usage in this research

2.2.1 Geothermal energy and ground source heat pump

The ground source heat pump (GSHP) system, which is the geothermal heating system presented in this research, uses low temperature sources of geothermal energy (between 90°C and 150°C or below 90°C) for space heating (Li et al., 2012).

A GSHP comprises three main elements: a ground heat exchanger (GHE), a heat pump, and a distribution system (Choi et al., 2013). The GHE, which is the main component—also called a geothermal field, uses shallow ground geothermal energy as its energy resource and a water/glycol mixture as the transport medium. It should be noted the underground temperature is warmer than the outside air temperature in winter, but cooler than the outside air temperature in summer. The mixed fluid, circulated by a low-power pump, flows through buried piping, storing heat from the soil under the building site in winter. Likewise, the system releases heat into the soil in summer. In winter, a GSHP system can extract heat from shallow ground to provide energy for space heating. In summer, the system is reversed to transfer heat out of the building using the cooler ground as a heat sink (Natural Resources Canada, 2012a; Canadian GeoExchange Coalition, 2012).

The heat pump is operated based on a vapour-compression refrigeration cycle for heating or, in opposite way, for cooling (Banks, 2008). A vapour compression cycle (including an electric motor-driven compressor); condense; and evaporator are required as part of the heat pump's design. During the refrigeration cycle, the heat pump combined with a heat exchanger effectively raises the temperature of the ground source, using electric power to drive the compressor. The lifespan of the mechanical parts involved is approximately 50 years (IGSHPA, 2012). The heat pump provides more efficient heat than does a simple heat exchanger, which normally cannot provide the entire amount of energy required. A heat pump or a GSHP can solve the problem when higher temperatures and greater energy are needed. Since heat pumps consume less primary energy than conventional heating system, less CO_2 emissions are produced in the process (Wood et al., 2010; Bakirci, 2012).

GHEs can be configured as either open-loop or closed-loop (Skouby, 2010), as specified in Figure 6. Open-loop exchangers use surface or underground water sources as a direct heat source. Normally, this operation can be completed at a lower cost and with a smaller loss

during heat transfers than with closed-loop GHEs (Geothermal Heat Pump Consortium, Inc., 2012). However, the open-loop GHE has more potential problems due to its design, which involves bringing outside water into the unit and can result in clogging, mineral deposits, and corrosion more so than with a conventional or closed-loop system. Spatial constraints, such as proximity to a lake, river, or stream, also limit usage of the open-loop GHE, since the water present in the system in these cases usually causes corrosion over time (Geothermal Heat Pump Consortium, Inc., 2012).

The closed-loop system, on the other hand, circulates water through buried or submerged pipes that can be installed either vertically or horizontally, where the heat source can be the earth, a lakes, river, or pond. Geothermal heat pump systems have lower operating costs, lower maintenance costs, and lower life cycle costs compared with conventional systems because all equipment is sealed and installed inside the building or buried underground (Geothermal Heat Pump Consortium, Inc., 2012). The vertical closed-loop is widely used since it is not limited by surface area. However, in this system, initial excavation costs are generally high. In the research presented in this thesis, closed-loop vertical GHEs are utilized due to the given space limitations.

Open Loop   Closed Loop
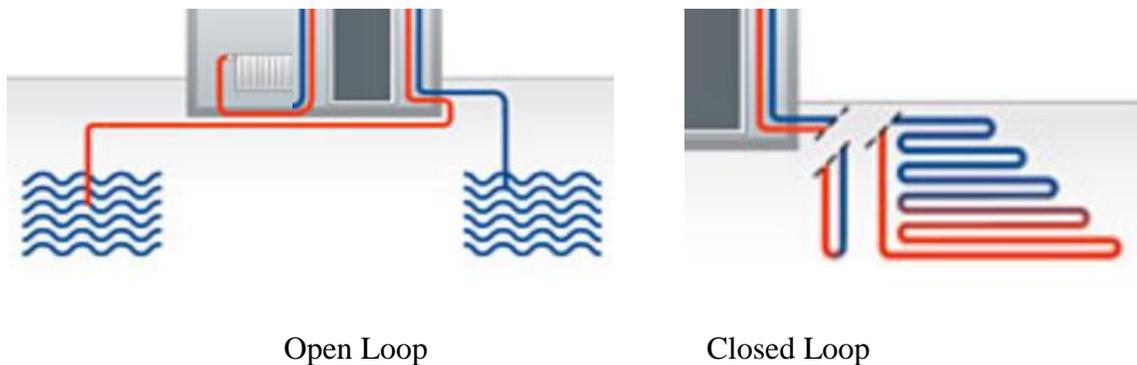
Figure 6: Open-loop and closed-loop ground heat exchanger (Heat pump technology, 2013)

Geothermal energy is a reliable, abundant, and renewable resource. According to IGSHPA (2012), preheating fluid from a ground loop can save 50% in heating fees, decrease repair costs, and reduce total energy consumption by 20%-50%. Geothermal systems also reduce operating costs and CO_2 emissions when compared to traditional heating systems. More specifically, using geothermal energy saves fuel and eliminates CO_2 emissions (Lund and

Freeston, 2001). Previous research shows that annual energy savings in 2001 in fuel oil corresponding to the use of geothermal energy equaled 170 million barrels (25.4 million tons) worldwide, and carbon emissions to the atmosphere were reduced by 24 million tons (Lund et al., 2005). In 2010, the quantity of annual energy due to the use of geothermal energy increased even further. At this time, the annual energy savings equaled 268 million barrels (40 million tons) of fuel oil, which amounted to savings of 38 million tons of carbon emissions and the elimination of 123 million tons of CO_2 emissions annually when compared to fuel oil (Lund and Freeston, 2010). Compared to conventional heating, ventilation and air conditioning (HVAC) equipment, GSHPs consume up to 50% less energy (Cooperman et al., 2012).

In terms of the usage of geothermal energy in Canada, the high-temperature geothermal areas are predominantly located in the western part of the country, while geothermal areas with low and medium temperatures are found throughout Canada. Geothermal heat pumps are now used in all Canadian provinces, and are estimated to save around 600 million kWh (2160 terajoules (TJ)/year) of energy, and around 200,000 tons in greenhouse gas emissions annually in Canada (Lund et al., 2005). Due to these substantial energy and cost savings, geothermal systems are expected to play an important role in heating in the future.

Hepbasli (2007) has summarized advantages of a GSHP compared to an air-source heat pump. Hepbasli has pointed out that earth and groundwater are more stable than air sources of energy, and that a GSHP consumes less energy and requires fewer refrigerants, while there is no demand for additional heat during extreme cold weather. GSHPs also have a simpler design and require less maintenance than do air-source pumps. Although the high initial cost and long-term payback of a GSHP can pose some challenges, it is expected that usage of a GSHP will increase with better design and improved efficiency.

In residential applications, existing ventilating ducts can be utilized for installation of a GSHP. Residents can benefit from the advantages of geothermal, such as providing stable heat for space and water. In addition, preheating water with a GHE can save up to 50% of heating costs, and the lifetime of the mechanical parts can be expected to reach 50 years (IGSHPA, 2012).

13

A coefficient of performance (COP) is used to evaluate the performance of heat pumps. According to previous research, GSHPs have a higher COP than conventional heat pumps, such as air-source heat pumps (Wang et al., 2012). Heating efficiency is indicated by the ratio of the energy output (Btu) to the power input (Btu). Cooling efficiency is indicated by the energy efficiency ratio (EER), which can be calculated by dividing the heat removed (Btu/h) by the electricity required (Watts) to run the unit. According to Energy Star, a heating system with a COP greater than 2.8 or a cooling system with EER greater than 13 is considered efficient (Energy efficiency & renewable energy, 2012).

2.2.2 Solar-assisted ground source heat pump

Solar energy can be collected by photovoltaic panels to provide heat to buildings as direct heating energy. It can also be stored in summer as spare energy and drawn upon by the geothermal field for energy recovery. In cold regions, antifreeze protection is required to avoid freezing of the solar energy systems in winter (Stein and Powers, 2011). Solar energy application combined with a GSHP system, which increases the efficiency of the heat pump, has also been widely used (Omojaro and Breitkopf, 2013).

The first solar-assisted ground source heat pump (SAGSHP) was recommended by Metz (1982). However, Penrod, as cited by Metz, had established decades earlier in 1956 the idea of storing solar energy in the ground (Metz, 1982). As described in more recent scholarship, a direct SAGSHP injects solar heat from the sun to the ground or to underground water (Omojaro and Breitkopf, 2013).

Zhai et al. (2011) have indicated that integrating the GSHP system with a solar thermal system can effectively provide thermal energy for heating-dominated buildings. Such systems can operate with a relatively high COP of 3.5. However, design of the heating system can vary based on the given climatic conditions, building functions, and thermal balance of the ground field. In this thesis, the SAGSHP system has been utilized in an extreme cold region where no cooling load is required in summer. Section 2.3 will further discuss the previous research on SAGSHP in cold regions.

2.2.3 Drain Water Heat Recovery (DWHR) System

Most of the energy used to heat water in residential buildings transfers directly to wastewater, with drain water carrying away valuable energy through the drain pipes. In this context, a DWHR system can be used to recover heat from the wastewater using coiled circulating pipes around the drainage pipe. While the drain water flows down, colder fluid in the coiled circulating pipe moves upward and recollects the heat from the drainage pipe (Figure 7). Both the main pipe and the coiled circulating pipe are usually made of copper in order to ensure effective heat transfer between the two flows. The system is rounded with an insulation layer to improve the efficiency of this heat conduction. Up to half of the energy can be recycled and utilized to preheat or heat cold water going to the water heater, which can reduce the cost of energy usage (Natural Resources Canada, 2012b). Based on the previous data, usage of DWHR systems could save up to 40% of heating costs (SaskEnergy, 2012), and could reduce greenhouse gas emissions significantly. In the case study presented in this thesis, DWHR is found to increase the efficiency of the geothermal system. It should also be noted that the life expectancy of DWHR systems is over 50 years.
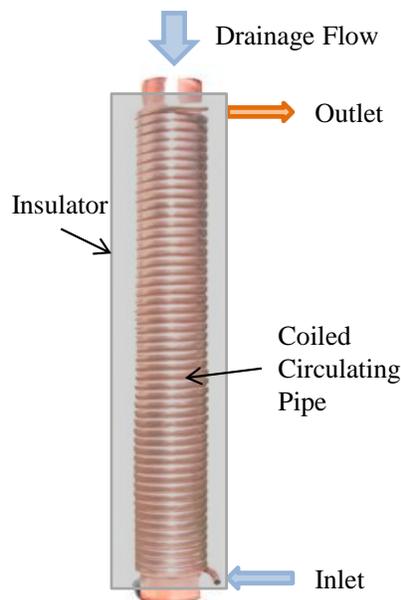
Figure 7: Schematic of DWHR

2.3 Use of Integrated Heating System in Cold Regions

As opposed to hot-climate regions where the heating and cooling systems require almost equivalent loads all year round, in cold-climate regions larger GHEs are required since the heating load is much greater than the cooling load (Zhai et al., 2011). Similarly, Roth et al. (2009) have identified two major challenges related to the use of conventional heat pumps in cold regions: that the heating load is greater than the cooling load, and that heating capacity and COP decrease as the outside temperature drops. Since the cooling load in summer cannot be guaranteed to offset the heating load in winter, long-term operation could result in an irreversible decrease in the temperature of the underground field. In this case, the COP of the heat pump could also be markedly reduced. However, the use of a larger GHE is constrained by the high initial cost and spatial limitations (Zhai et al., 2011). Consequently, the use of an efficiently designed integrated system will supply energy in a manner which ensures energy savings.

Solar energy combined with a GSHP system, which serves to increase the efficiency of the heat pump, is also widely used in cold regions (Bakirci and Colak, 2012). With the assistance of solar energy, this comprehensive utilization not only offsets the deficiency of GSHPs by facilitating soil temperature field recovery, but also provides intermittent heat to the building (Ran et al., 2012). Bakirci et al. (2011), in a study of cold-climate residential heating in Erzurum, Turkey, showed that the COP of a SAGSHP was enhanced to the range of 3.0-3.4, while the overall heating system COP was 2.7-3.0 (Bakirci et al., 2011). Investigating a similar cold-climate region, a research group from Hong Kong, China has utilized TRNSYS simulation software to forecast the performance for 20 years of continuous operation under the climate conditions of Beijing, China (Chen et al., 2011). Compared to a conventional GSHP system, a SAGSHP system for space heating and domestic hot water was found to improve efficiency by a margin of 26.3%. However, results from another study by the same research group simulating the performance of a SAGSHP in the cold-climate region of Harbin, China, showed SAGSHPs to perform with a lower efficiency of 2.84. As such, they recommended against its utilization in extreme weather in the interest of energy savings (Chen et al., 2012). Using the same software, Niu et al. (2011) have concluded that the system

efficiency decreases more rapidly when there is a greater difference between heating load and cooling load exerted on the GSHP. The case that is being addressed in this thesis, moreover, is the special condition when only heating load is required.

In a cold-climate region with very low ambient temperature and relatively low underground temperature in winter, only an optimal integration of a number of renewable energy resources can lead to sufficient energy production (Akpan et al., 2006). Therefore, dealing with cold-climate conditions such as those in Fort McMurray, a proposed integrated heating system including geothermal energy, solar energy, DWHR system, natural gas, and electricity is investigated in this research.

CHAPTER 3: METHODOLOGY

In this chapter, the methodological approaches are presented in detail. Figure 8 shows a visual overview of the methodologies implemented for three main components of this research.

1) Analyze a proposed integrated heating system for cold regions
2) Develop an experimental design to evaluate the existing heating system performance
3) Develop an enhanced control algorithm for existing system operation through monitoring analysis
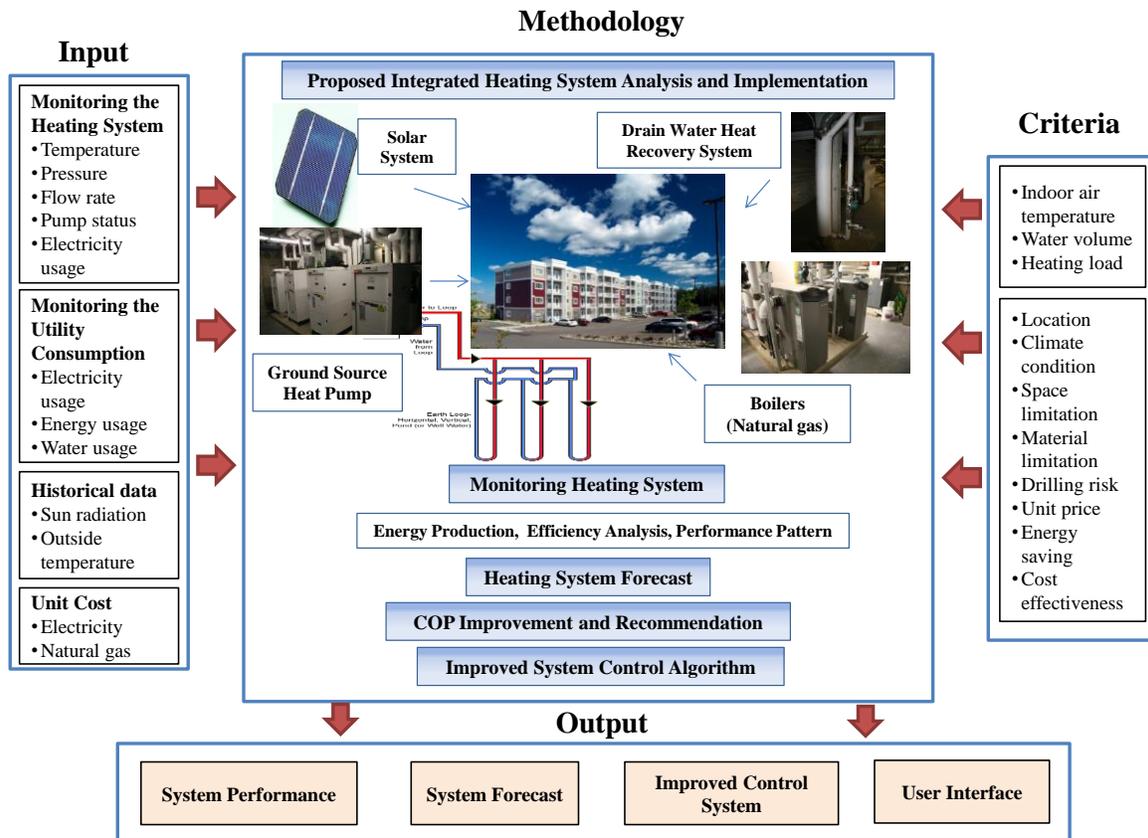
Figure 8: Overview of research approach

In order to gain a better understanding of these heating systems and their performance, a monitoring system has been designed. In this research, four types of inputs are considered: (1) heating system monitoring data, (2) utility consumption monitoring data, (3) historical data, and (4) utility unit costs. More specifically, heating system monitoring data

comprises temperature, pressure, flow rate, pump status, and electricity usage; utility consumption data includes electricity usage, energy usage, and water usage; historical data involves sun radiation data; and utility unit costs are for natural gas and electricity.

Through the monitoring, data collection, and data analysis, a better system control algorithm can be developed for energy and cost savings via coefficient of performance (COP) improvement and other recommendations. The main objective underlying the system control algorithm is to provide the operators or managers (decision makers) with better control over the heating system with higher efficiency.

3.1 Proposed Methodology of the Ground Source Heat Pump System (GSHP)

Geothermal energy is a sustainable and renewable resource which is cost-effective, reliable, and environmentally friendly if the GSHP system is properly designed. The primary challenge related to GSHP systems is the task of maintaining a balance in annual energy. Normally, the ground heat exchanger (GHE) works both as a heating system in winter and as a cooling system in summer in order to make the energy absorbed equivalent to that rejected. Figure 9(a) shows the energy variance in the GHE over one year. The geothermal loop extracts heat from the earth when it is in heating mode in winter and the energy in the field decreases. During summer, the field temperature rises as energy is transferred back into the ground. Figure 9(b) demonstrates how energy in the field fluctuates while the wave range remains relatively consistent throughout the year, (despite the occasional slight decrease observed), if the GHE works efficiently. Unlike typical practice, the GSHP system discussed in this research is not designed for cooling in summer, since heating is more necessary than cooling in cold-climate regions. In this case, the temperature of the GHE will decrease gradually, exerting a negative impact on the efficiency of the geothermal system. Figure 10 demonstrates how the GHE temperature fluctuates under these conditions. As shown by the dashed line in Figure 10(a), if the heating mode is active during the winter months, the energy decreases, followed by only a slight increase in summer due to the characteristics of the earth's surface. Thus, as years pass, the effectiveness of the GSHP system may decline, as shown in Figure 10(b).

19
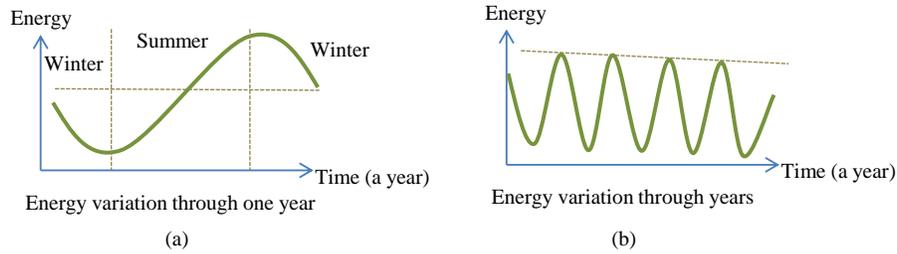
Figure 9: GHE energy distribution using a GSHP for heating and cooling
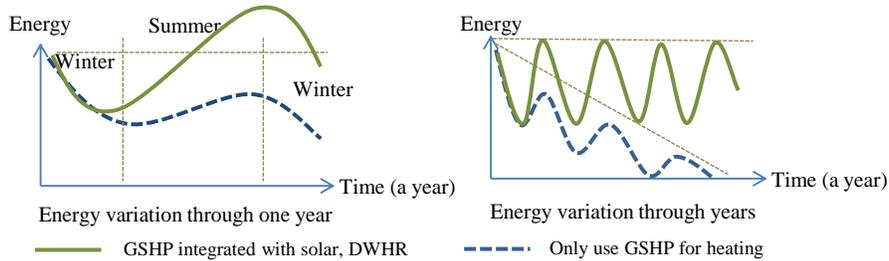
Figure 10: GHE energy distributions using integrated heating system

To address this challenge, solar and DWHR systems are integrated to support the GSHP system. The solar energy system directly injects its produced energy to the GHE, while recycled heat from drain water increases the inlet temperature of the heat pumps and also indirectly injects its energy to the GHE. Energy from both the solar energy and DWHR systems can therefore be collected to recover the heat lost in the underground field. The aim of this approach is to use the integrated heating system to achieve long-term maintenance of the GSHP system (illustrated in Figure 10(a) and Figure 10(b), where solid lines represent the targeted values). As advanced in the above discussion, in combining the GSHP system with solar energy and drain water systems, the lifetime of the GSHP system is extended, and it provides significantly more thermal energy than can an independent GSHP heating system. Integrating these four main systems is expected to ensure energy efficiency and to provide thermal energy within the constraints of budget, space, and energy resource availability. The following sections provide a more detailed discussion of the integrated heating system in the case study.

3.2 Methodology for the Developing an Experimental Design for Existing System

An effective heating system is determined either by proper system design or an efficient operation system. For better system operation control, mechanical engineers usually

install sensors on the control set point and operation pumps. However, for the research presented in this thesis, sensors are required for two metrics, energy production and COP. These two metrics are developed in this thesis research and can be implemented in an existing heating system in order to evaluate the system performance and to improve the existing system control.

3.2.1 Energy Production and Experimental Design

By monitoring the supply (from heating system resources to the main heating loop) and return (from the main heating loop to the heating system resource) pipes of the integrated heating system, the thermal energy generated from each system is evaluated by means of a specific heat equation. Based on the specific heat equation, energy production can be estimated based on temperature difference, fluid specific heat, and circulated fluid mass. Temperature data from the supply and return pipes on each system is required in order to obtain the temperature difference. The entire methodology is based on the first law of thermodynamics, whereby thermal energy input should be equal to energy output through an insulated system. Based on the law that energy cannot be created or destroyed (Stein, 2011), this research assumes there is no heat loss through transmission.

The energy production equation is derived to estimate the energy generation from each heating system. Thermal energy loss or gain (Q) in the pipes can be calculated using Equation (1). It should be noted that the specific heat capacity (C) in Equation (1) is defined as the amount of heat required to raise the temperature of the unit mass of a substance by 1°C. The total thermal energy loss or gain is calculated satisfying Equation (3), which is derived from Equations (1) and (2).

$$Q = C \times M \times T \tag{1}$$

$$M = \rho V \tag{2}$$

$$\sum_{i=1}^{n} Q = \sum_{i=1}^{n} C_i \times M_i \times \Delta T_i = \sum_{i=1}^{n} C_i \times R_{m_i} \times t_i \times \left(T_{Supply_i} - T_{Return_i} \right)$$

$$= \sum_{i=1}^{n} C_i \times \rho_i \times R_{v_i} \times t_i \times \left(T_{Supply_i} - T_{Return_i} \right)$$

$$\tag{3}$$

Where

Q: Thermal Energy, kilojoules (kJ)

C: Specific Heat, kJ/kg°C

M: Mass of fluid within a period of time, kilograms (kg)

ΔT: Temperature difference, °C

ρ: Density of fluid, kg/m^3

V: Volume of fluid, m^3

R_m: Mass flow rate of fluid, kg/hr

R_v: Volume flow rate of fluid, m^3/hr

T_{Return}: Temperature of return pipe, °C

T_{Supply}: Temperature of supply pipe, °C

t: serving time or operation time, hr

In the experiment, multipliers, such as specific heat, density, flow rate of fluid in the testing period, and temperature difference, are required. Specific heat and density are defined by the fluid type and concentration.

Each system operates different circulating fluid with different specific heat and density. The serving time (t) can be provided by each of the operation pumps. The temperature difference between the return and supply pipes $(T_{supply} - T_{return})$ that connect to each heating system, along with the flow rate (R_v), should therefore be determined in the experiment. In this case, temperature sensors should be installed at the connection between each heating system and the main heating loop, while flow rate sensors can be installed on either the supply or return pipe since the flow rates for the two pipes are the same. In the case study, the flow rate is assumed to remain constant during operation, thus the flow rate samples were measured. From these equations and the experiment data collection, the thermal energy generated by each system can be evaluated in terms of kilojoules (kJ).

In the case study, temperatures and flow rate samples were measured on the supply and return pipes of the solar energy system, where the solar heat transfer station connects to

the main heating loop, as "T_{Supply}" and "T_{Return}" for the solar energy system. In terms of the DWHR system, these required sensors were installed on the inlet and outlet of the coiled circulating pipes on the stack. It is also practical to measure the performance of GHE by installing temperature sensors and flow rate meters on the geothermal loops where the end of the loop links to the mechanical room in the building. However, due to a technical problem in this case study, energy production of the geothermal loops was not measured, but was instead estimated based on the outputs and inputs of the heat pumps.

Heat pumps and boilers connect to the water storage tank directly in order to elevate the temperature in the tank. Therefore, the outlet temperature of the tank is the temperature of the return pipes (T_{Return}) for both heat pumps and boilers. The supply temperatures (T_{Supply}) for both heat pumps and boilers are the temperatures on their outlet pipes, correspondingly.

Based on the above sensor-based monitoring design and data collection, the energy production of solar energy system, DWHR system, GHE, heat pumps, and boilers can be calculated based on Equation (3). A detailed experimental design is further discussed in the next chapter, including heating system schematic drawings.

3.2.2 Coefficient of Performance and Experimental Design

COP is another metric by which to evaluate the performance of the heating system. The COP of the heat pump (*HP*) is the ratio of heat supplied (energy production) and electricity consumed by the heat pump (IGSHPA, 2009). The heat supplied in Equation (4) is the sum of the heat extracted from the ground and the electric demand of the heat pump. For a heating system, based on Equations (3) and (5), the COP of the heat pump can be derived from Equation (6).

$$COP \ of \ HP = \frac{Q_{HP} \times 277.78}{E_{HP}} \tag{4}$$

Where
Q_{HP}: Energy production from heat pumps, GJ
E_{HP}: Heat pump electricity consumption, kWh

$$COP \ of \ HP(heating) = \frac{Q_{HP\_source} \times 277.78 + E_{HP}}{E_{HP}} \tag{5}$$

$$COP \ of \ HP(heating) = \frac{\sum_{i=1}^{n} C_i \times \rho_i \times R_{v_i} \times t_i \times \left(T_{Supply_i} - T_{Return_i}\right) \times 10^{-6} \times 277.78 + E_{HP}}{E_{HP}}$$

$$\tag{6}$$

Grounded by the energy production measurement, which is discussed in the previous experimental design in Section 2.2.1, the additional measurement records the electricity consumption of heat pumps as "E_{HP}".

The COP of a cooling system, which is given in Equations (7) and (8), is calculated as the energy removed from the building divided by the heat pump electricity consumption. In the case study, only the COP of the heat pump for heating is utilized, since the GSHP is not designed to function as a cooling system.

$$\boldsymbol{COP \ of \ Heat \ Pump(cooling)} = \frac{Q_{Building} \times 277.78}{E_{HP}} \tag{7}$$

$$COP \ of \ Heat \ Pump(cooling) = \frac{\sum_{i=1}^{n} C_{B\_i} \times \rho_{B\_i} \times R_{vB\_i} \times t_{B\_i} \times \left(T_{Supply_{B\_i}} - T_{Return_{B\_i}}\right) \times 10^{-6}(GJ) \times 277.78}{E_{HP}}$$

$$\tag{8}$$

Where

Q_{HP_source}: Energy production from the source side of heat pumps, GJ

$Q_{Building}$: Energy removed from buildings, GJ

E_{HP}: Heat pump electricity consumption, kWh

A COP can also be used to indicate the performance of any other systems. In general, the COP of a given system is the ratio between energy production and circulating pump power consumption. The COP of the solar energy system is illustrated in Equation (9), where Q_{Solar} can be calculated using the energy production experimental design. An additional electricity consumption meter is required to be installed on the system circulating pump in order to collect data as "E_{Solar_pump}". The COP of the DWHR system follows the same experimental methodology. A detailed monitoring design is discussed in the case study chapter.

$$COP \; of \; Solar \; Energy \; System = \frac{Q_{Solar} \times 277.78}{E_{Solar\_pump}} \tag{9}$$

Where

Q_{Solar}: Energy production from solar energy system, GJ

E_{Solar_pump}: Electricity consumption of solar energy system circulating pumps, kWh

$$COP \; of \; DWHR \; System = \frac{Q_{DWHR} \times 277.78}{E_{DWHR\_pump}} \tag{10}$$

Where

Q_{DWHR}: Energy production from DWHR system, GJ

E_{DWHR_pump}: DWHR system circulating pump electricity consumption, kWh

3.3 Methodology for Improving the Control System

Following the data collection, data calculation, and data analysis from the experimental monitoring design, the next objective is to investigate an enhanced heating system control. This improved system control algorithm should prevent energy waste and unnecessary power consumption during operation. The objective is achieved through the following steps:

(1) Compare the temperature data from the supply and return pipes for each system. The system should operate when the temperature on the supply pipe (from resource to heating loop) is higher than the temperature on the return pipe (from heating loop to resource).

(2) Evaluate energy production by using a specific heat equation (see Section 2.2.1).

(3) Calculate the power consumption of corresponding pumps from monitoring and estimation.

(4) Estimate the COP and annual system performance pattern of each system.

(5) Check if the corresponding circulating pump is worth running with sufficient energy production.

(6) Determine a new set point of temperature difference (ΔT) between the supply and return pipes that increases the COP.

(7) Set ΔT as a set point for running the corresponding circulating pumps and turn off the pumps when they are operating at a low COP.

25

(8) Adjust and fine-tune the system algorithm based on the analysis results obtained from the above steps.

(9) Estimate the expected COP improvement based on the current system recommendations.

In addition, the unit prices of natural gas and electricity, as well as energy savings and cost effectiveness, are considered for the analysis of the existing system. A user interface to display the performance of the existing system is also developed in collaboration with researchers from the Department of Computing Science at the University of Alberta.

3.4 Other Supplementary Calculations

3.4.1 Production Cost

The production cost discussed in this thesis reflects the total energy cost for the energy production of the system. This figure is used for a cost comparison between electricity and natural gas production. The production cost of natural gas can be estimated by Equation (11), while the production cost of electricity can either be calculated by Equation (11) or Equation (12).

$$\textbf{Production Cost} = \frac{Energy\ source\ unit\ cost\ (\$) \times Energy\ source\ quantity}{Energy\ production\ (GJ)} \tag{11}$$

$$\textbf{Production Cost} = \frac{Energy\ source\ unit\ cost\ (\$) \times \mathbf{1}}{COP\ of\ the\ corresponding\ system} \tag{12}$$

3.4.2 Efficiency of Boilers

The efficiency of boilers is calculated by the ratio of energy output over input, where an effective boiler is defined as one which can achieve a high efficiency of 95%.

$$\textbf{Thermal Efficiency}(\%) = \frac{Energy\ output}{Energy\ input} \times \mathbf{100}\% \tag{13}$$

3.4.3 Drain Water Heat Recovery Efficiency

The efficiency of DWHR depends on the heat conduction performance between the drain water pipe and the surrounding energy recycling pipe. Temperature and flow rate sensors are installed on these pipes to monitor performance. However, the flow of the drain water

pipe is intermittent, necessitating the insertion of a permanent meter on the pipe. Unfortunately, for this case study, the researchers were not permitted to cut the pipes on the existing system in order to insert a permanent meter. Due to this practical limitation, the flow rate on the drain water pipe is difficult to determine. Although the following calculation will not be used in this case study due to the limitation mentioned above, the methodology may be still valuable and practical for implementation in other systems.

$$\boldsymbol{\varepsilon} = \frac{Q_{Cold}}{Q_{Drain}} = \frac{C_f M_{Cold}(T_{Cold-out}-T_{Cold-in})}{C_{Drain} M_{Drain}(T_{Drain-in}-T_{Drain-out})} \qquad (14)$$

Where:

ε: Efficiency of drain water heat recovery system (%)

Q_{Cold} : Thermal energy absorbed from drain water pipe, J

Q_{Drain} : Thermal energy conducted by drain water pipe, J

C_f : Specific heat of fluid in surrounding pipe, J/g. °C

M_{cold} : Mass of fluid in surrounding pipe, g

$T_{Cold-out}$ and $T_{Cold-in}$: Temperature of fluid out and in the surrounding pipe, °C

C_{Drain} : Specific heat of drain water, J/g. °C

M_{Drain} : Mass of drain water, g

$T_{Drain-in}$ and $T_{Drain-out}$: Temperature of drain water in and out the drain water pipe, °C
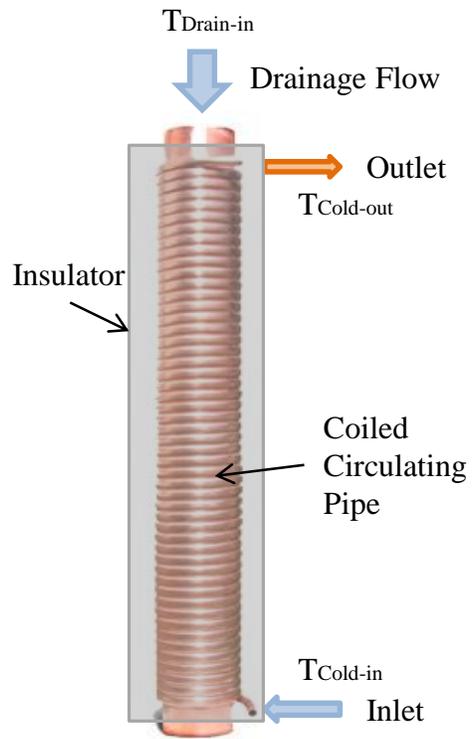
Figure 11: Schematic of DWHR

CHAPTER 4: IMPLEMENTATION

In this chapter, the implementation of the proposed integrated heating system in a building under occupancy is discussed in detail. After two years of operation utilizing the methodology given in Chapter 3, the monitoring system was installed on site in order to evaluate the performance of the existing heating system. A good understanding of the performance has been achieved after analyzing the data collected over more than three months. Better understanding is expected to be achieved based on long-term data, but this is beyond the scope of this thesis.

By analyzing the monitoring data, the efficiency of the individual systems and how the systems work together can be investigated. As a result, the monitoring system and proposed data analysis results are expected to benefit engineers by improving the existing system with an enhanced heating control algorithm, providing them with a valuable resource for better future designs. Similar monitoring designs can be implemented in other existing systems based on the same approach.

4.1 Introduction

This case study describes the details of the monitoring approach for integrated heating source-assisted GSHP systems for space heating in residential buildings in a cold-climate region. The project, "Stony Mountain Plaza" (Cormode & Dickson, 2013), comprises two 4-storey residential buildings located in Fort McMurray, Alberta, Canada (56°43′35″N 111°22′49″W). The entire project has been designed based on the principles of energy saving, high efficiency, and low operational cost. It has been built based on a wood-framed modular construction approach in order to reduce construction cost and cycle time; (Figure 12 illustrates the modular construction process). The modules were built in Lethbridge, Alberta, and then transported to Fort McMurray. A large crane was used to erect the buildings on site within only five weeks (Cormode & Dickson, 2013).

Figure 12: Modular construction process

Figure 13: Selected case-study building

One of these two residential buildings has been chosen for the research presented in this thesis (Figure 13). The heating system used in this building provides space heating and hot water for the multi-family residence of 106,600 ft^2. This project utilizes the GSHP system as the main heating system. Ten geothermal vertical circuit loops with 8 boreholes at a depth of 91.44 metres (300 feet) and diameter of 12.7 centimetres (5 inches) per circuit are installed under the building. 1.91-centimetre (3/4-inch) high-density poly-ethylene (HDPE) pipes are installed inside the boreholes, and these pipes transport the circulating fluid of 13.6% methanol. At this point, it is important to note two main challenges regarding this project: (1) GSHP systems are not designed to function as cooling systems to recover heat from buildings in summer, and (2) the extreme dry-cold weather in Fort McMurray results in a large amount of energy consumption for building space heating. To overcome these challenges, an integrated system is proposed to bolster the GSHP system, including renewable energy from solar and a sustainable drain water heat recovery (DWHR) system.

The main idea is to inject solar energy to recover the heat loss of the ground heat exchanger (GHE) and indirectly retain the sustainability of the GSHP system. In addition, the DWHR

system provides thermal energy on the source side of the heat pump to recover the heat loss of the GHE secondarily. Finally, the non-renewable source of natural gas is also included as a backup source for heating. This resource fuels boilers to generate energy and to heat water, which can be used for various purposes such as space heating. Moreover, this integrated system uses several energy sources. Although a significant number of research studies have investigated geothermal systems, few investigations have been conducted on integrated systems which use several sources, and none of those studies are comparable to the integrated system investigated in this project.

4.1 Heating System Schematic and Specifications

In this section, details of the heating system connection schematic and existing system control algorithm will be clarified, along with a system layout chart and a control system flow chart. All of the equipment discussed in this section is in the mechanical room, which is in the basement of the building.

4.1.1 Heating System Schematic

As mentioned above, the buildings under investigation are designed to be served by an integrated heating system which combines geothermal, solar, DWHR, and conventional electric or natural gas energy. Figure 14 depicts the heating system schematic. On the source side of the heat pumps, the system includes solar panels mounted on the roof of the building. The azimuth angle of the solar energy system is 45° south-facing, with a total surface area of 28.7 m^2. During operation of the solar panels, heated Tyfocor-L fluid is circulated through a solar heat transfer station (SHTS) to the upper panels on the roof in order to prevent freezing. The SHTS also circulates 13.6% methanol with the collected energy to recover the heat to the GHEs and indirectly increase the entering temperature of the water-to-water heat pumps.

The DWHR system, including eleven stacks that recycle heat from the 70 apartment units' drainage through parallel copper loops, increases the temperature from the GHE to the heat pumps and indirectly recovers the heat to the GHE. Gathering the source-side energy from the solar energy system, DWHR system, and the GHE, four heat pumps powered by electricity produce thermal energy with an expected coefficient of performance (COP) of

31

2.8, a threshold which indicates that the multiple-source heat pump system is working effectively. The heat pumps transfer water heat further to two water storage tanks, each with a capacity of 1000 gallons, as shown in Figure 15.

In addition to these renewable energy sources and purchased electric power, natural gas-burning boilers are utilized to provide additional heat to the building when needed. The driving power to operate pumps in each loop is supplied by electricity. 24 temperature sensors and seven pressure sensors were added to the heating system machines in the mechanical room during the initial installation for control of the existing system. During operation, water storage tanks collect the thermal energy from each heating system, and the temperature on the bottom of the water storage tank (T10 in Figure 14 and Figure 15) is increased to a set point which satisfies occupant requirements. The set point of each heating system is specified in the following section. (A detailed engineering heating system schematic drawing is provided in Appendix A, with a description of equipment tags in Appendix B.)
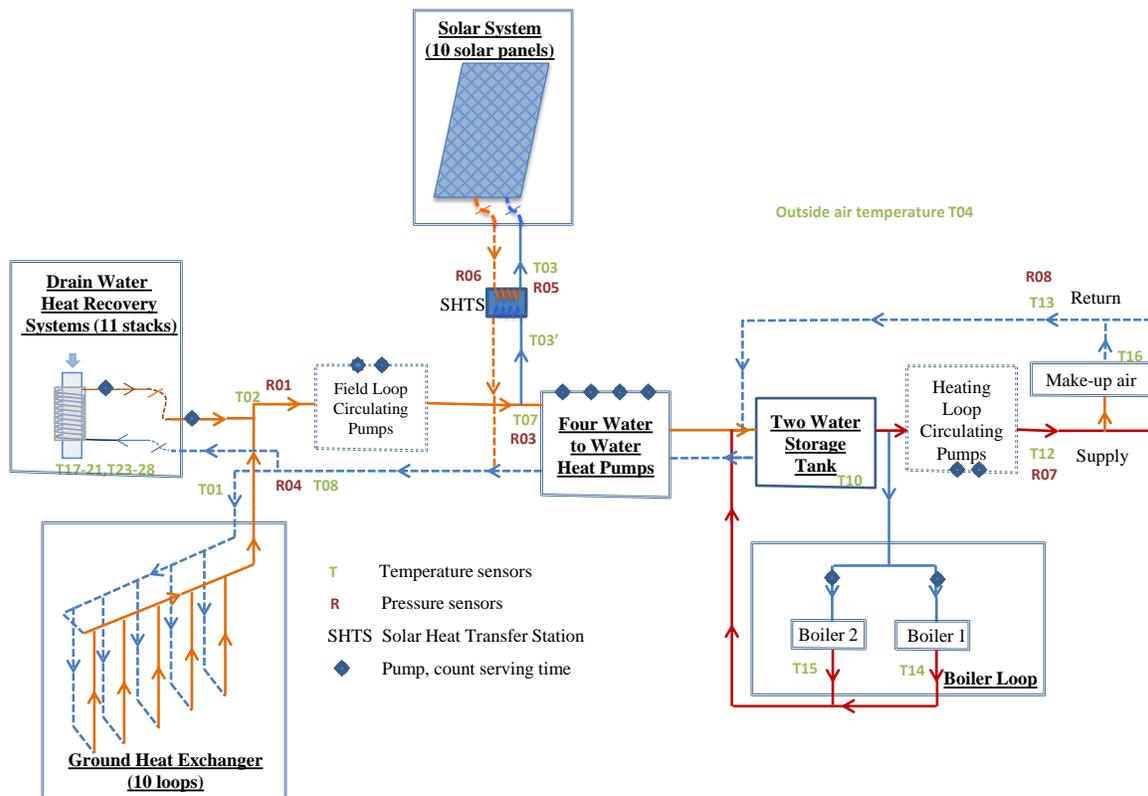
Figure 14: Heating system schematic with existing sensors
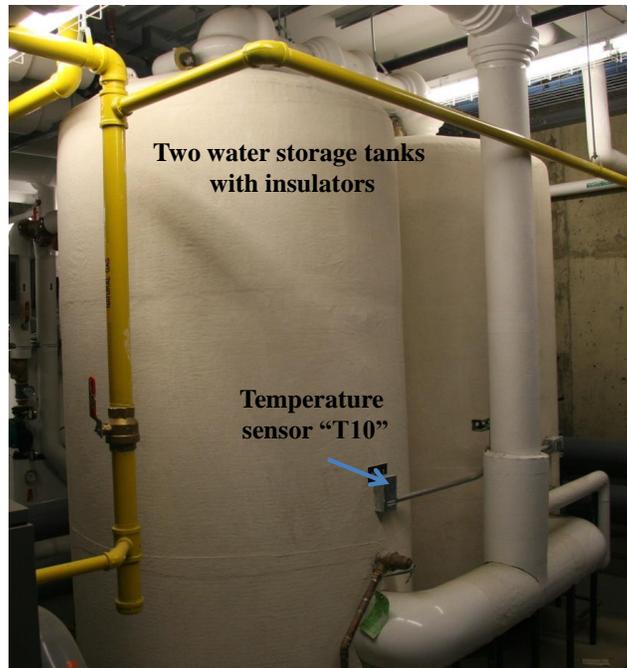
Figure 15: Water storage tanks with installed temperature sensors

4.1.2 System Specifications

Each system is designed to operate under precise control rules pertaining to the outside temperature and the hot water storage tank set point temperature control for the heating mode. When the outside temperature decreases below 15°C, the GSHP system heating mode turns "on" and four heat pumps begin operating based on various tank temperature set points. When the outside temperature falls below -20°C, the GSHPs switch "off" while two natural gas-burning boilers turn "on". The heat pumps (numbers 1, 2, 3, and 4) and boilers (numbers 1 and 2) begin to heat the water and transfer it to the water tank when the temperature of the water tank falls below the specific set points of 44-47°C and 63-71°C, respectively. For instance, the first heat pump turns on when T10 is lower than 47°C, and the second heat pump turns on when T10 is lower than 46°C. Boiler 1 operates when T10 is lower than 71°C while Boiler 2 works when T10 is lower than 63°C.

Regarding the solar panels, the solar heat transfer system is switched on to bolster the GHE loop when the temperature in the GHE loop falls below the temperature in the monitored solar panels. Freeze protection is also considered in order to protect the pipe from freezing. In addition, the DWHR system is activated whenever water drains, and the

recovered heat is recycled to preheat the water in the tanks. Figure 16 shows the flowcharts of the original heating system control algorithms for each of three main heating systems. These algorithms specify how the systems connect and collaborate with one another. (A detailed control algorithm summarized from the project is provided in Appendix C.) However, in reality, based on the performance of each heating system in the winter months, recommendations to change each set point have been proposed in the interest of energy saving, as discussed in later sections. Further suggestions are still anticipated following further data calibration analysis in the next few years of this study.
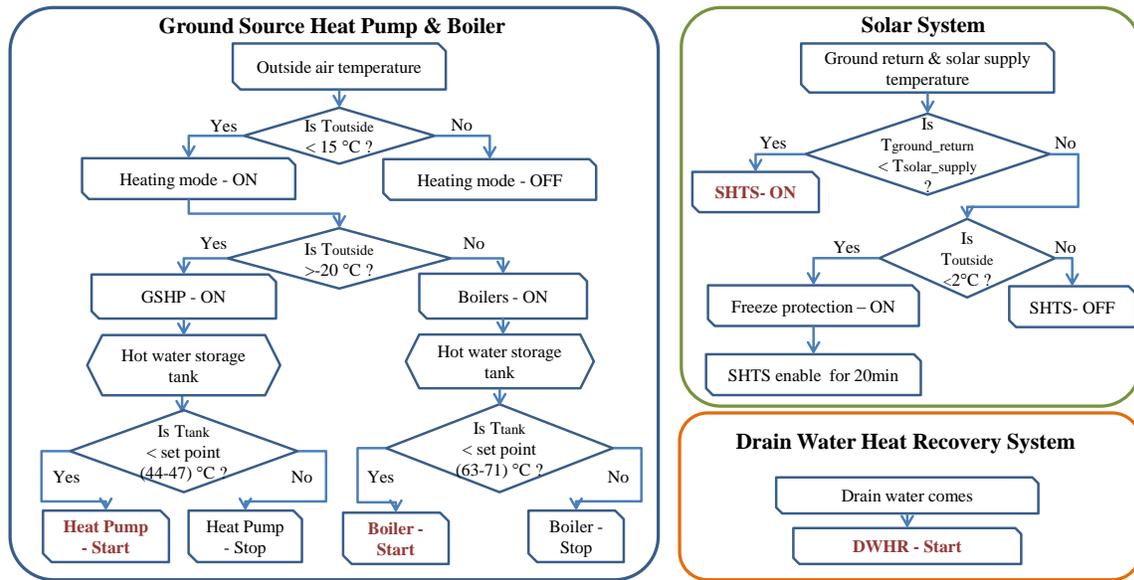
Figure 16: Original heating system control algorithm

4.2 Experimental Design, Data Collection, and Assumptions

At the initial phases of this project, some temperature and pressure sensors had already been installed in the basement by building management for system control. However, the installed sensors were not adequate for the purpose of this research since some of the critical parameters needed for the calculations had not been measured. These readings, though, can still be considered for reference. A brief overview of the initial system is given below, along with recent additional instrumentation implemented to the system.

As explained in in detail Chapter 3 with respect to the equations, it is necessary to obtain the temperature difference and flow rate for supply and return pipes for each component

in order to calculate the energy production from the system using the specific heat equation. The same methodology can be implemented to each heating system. To calculate the COP of a heating system, electricity usage should also be measured. Underground field loop circulating pumps and heat pumps are the main power consumers in the entire system. Small power pumps such as the DWHR stack circulating pumps and the solar energy system circulating pumps consume small amounts of electricity, which can be neglected or calculated approximately based on the pump capacity and pump running status (i.e., whether the pump is running or not). The serving time can be determined from the operation of the pumps.

Since the initial installed temperature and pressure sensors were not adequate to conduct the analysis discussed in the previous chapter, additional sensors were installed as shown in Figure 17. "T+number" shows the location and tag of the temperature sensor, while the label, "Flow+number", represents the location and tag of the flow rate sensor. "CT+number" and "ST+number" illustrate the location and tag of electricity usage and pump status meters, respectively. The following paragraphs discuss the sensor architecture process (Figure 18) and data collection. Reasonable assumptions, such as circulating pump operation performance and flow rates, which will be further explained in each analysis, have been made in order to predict the results.
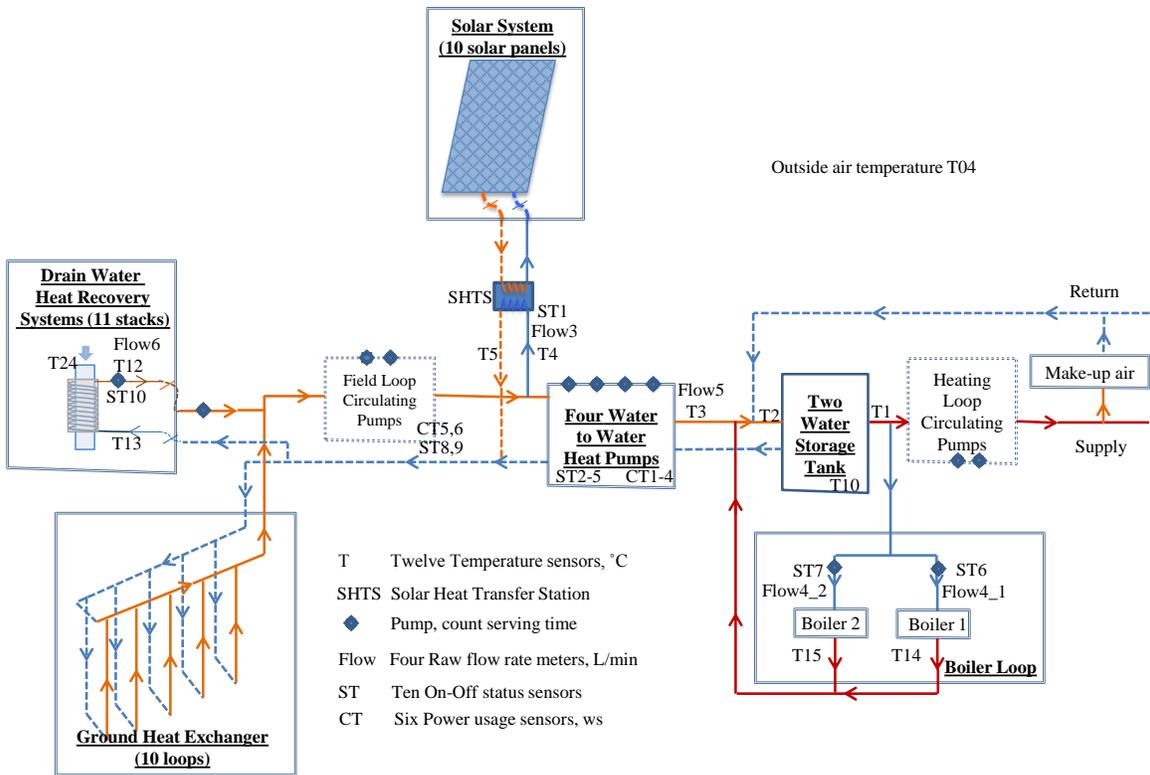
Figure 17: Heating system schematic with the additional instrumentation
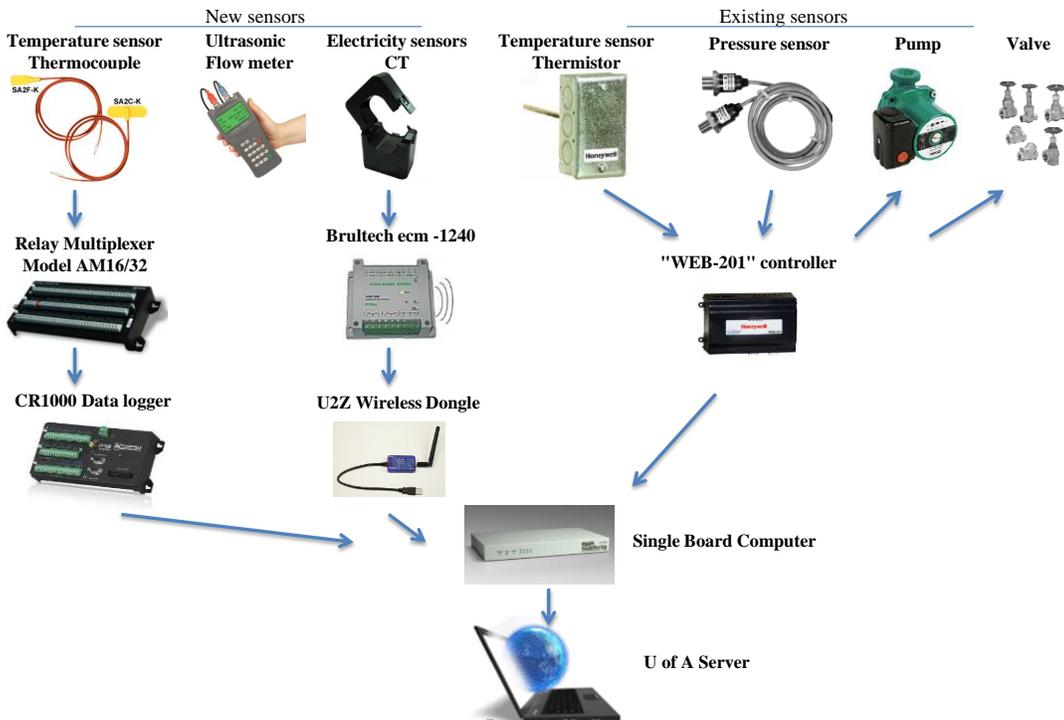
Figure 18: Monitoring system architecture

In addition to four existing temperature sensors, eight new temperature sensors, ten on-off status sensors, and six power meters were installed in the mechanical room on March 15, 2013, in order to monitor the performance of energy generation from each heating system and calculate the COPs. In addition, four flow rate samples were measured on the corresponding pipes, which are used in the calculations, assuming that they are constant over time.

Since the monitoring system and sensors had to be installed in such a manner as to avoid any damage to the existing equipment, e.g., cutting of the pipes, and considering that the pipes are not always running at full capacity, thermocouples were installed at the bottom of the pipes to capture the most accurate temperature readings possible. Insulators were added back to the pipes after the installation of these thermocouples in order to avoid the influence of surrounding air temperature and to prevent monitoring noise.

Data from the thermocouples were recorded with a data logger-CR1000 by Campbell Scientific, which is connected to a single-board computer. The AM16/32B Relay Multiplexer was also used to increase the number of channels that can be measured by the data logger. In addition, an ultrasound flow rate meter was utilized for one-time measurement of the fluid flow rate. The accuracy of ultrasound flow meter FDT-21 is within 1%, and the current transformer (CT) is measuring the electric currents utilizing the same single-board computer to collect data.

Figure 19 shows the screenshots from the database with the temperature data collected from the new sensors. Temperature was collected in 30-second intervals, and the average temperatures of these 30-second intervals were recorded. Based on the status of the pumps, raw data for flow rates were created using the previously taken measurements with the assumption that when a pump runs, it runs with the same capacity as had been measured; otherwise, there is no flow in the pipes (zero flow). A linear flow rate increase was assumed when the number of working heat pumps increased from one to four; (i.e., if one heat pump operates with a flow rate of x, then the flow rate of four heat pumps will be $4x$). Based on this assumption, a database for flow rate has been created (see Figure 20). Flow rate data is updated in 1-minute intervals in the database and electricity usage data is recorded in 10-second intervals, and cumulative data is also updated in the

database (Figure 21). Pumps, which consume a small amount of energy and thus are not recorded in the database, are also considered in these calculations. The maximum power capacity of each small pump is assumed and taken into account in the calculation in order to make the final results more accurate and realistic. Since data have been collected at various intervals, one minute has been selected as the interval for all calculations, and data has thus been averaged on a per-minute basis for each calculation.

Figure 19: Sample temperature data from database

Figure 20: Sample flow rate data from database

Figure 21: Sample electricity data from database

Figure 22 and Figure 23 show the screenshots of the database, which can be accessed at <https://smartcondo.ca/ssrg9_pma/> with a valid user name and password. Data can be downloaded and exported to MS Excel, Word, PDF, and other files formats using SQL code; (detailed SQL codes are provided in Appendix D of this thesis).

38
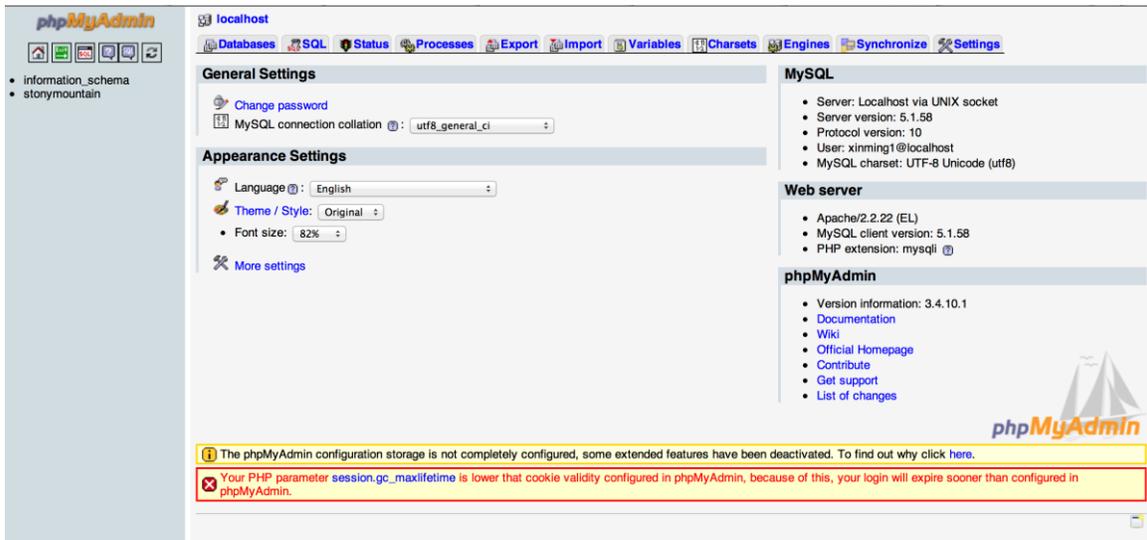
Figure 22: Screenshot of database home page
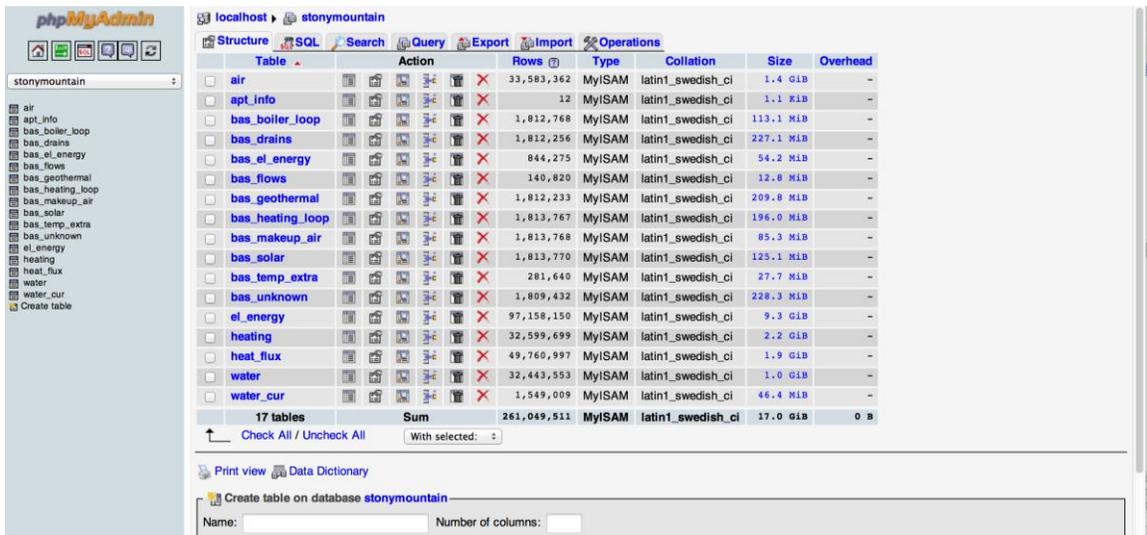
Figure 23: Screenshot of the database for Stony Mountain Plaza

In addition, electrical meters, energy meters, and water usage meters which correlate to this heating system analysis were installed in 12 out of 70 apartment units to monitor their utility consumption, including electricity usage, energy usage, and water usage from (Sharmin et al., 2012). A detailed discussion of these sensors is beyond the scope of this thesis.

4.3 Analysis of the Monitoring Data

The objectives underlying the monitoring are to estimate the energy generation and to evaluate the heating efficiency of each system. The study has been designed to measure the temperature and flow rate in the pipes, as well as the electricity usage of the equipment that consumes most of the power, in order to obtain the results to be discussed in the previous section. As mentioned above, the additional sensors were installed in the mechanical room on March 15, 2013. Since then, data is being collected by the data management system and transferred to the University of Alberta server at 10-second to 1-minute intervals. By analyzing the data obtained using the monitoring system, the production and efficiency of the individual systems, as well as of the integrated system, can be ascertained. As a result of this research, valuable system performance patterns, a user interface, and an enhanced control system can be obtained, by which engineers can make further adjustments to heating system designs. The following paragraphs discuss the weekly production analysis results for each heating resource and system based on the data collected during the period of March 15 to July 4, 2013. (A monthly performance analysis is attached in Appendix G.) Circulating fluid, corresponding sensors, and multipliers for each system are provided in Table 1. Legends "T" and "Flow" in Table 1 are explained in the monitoring design in Figure 17 with the locations of sensors. Also, for the analysis it is assumed that there is no heating loss through transmission.

Table 1: Circulating fluid, corresponding sensors and multipliers

(Legends refer to Figure 17)

System	Fluid	Supply Temp (°C)	Return Temp (°C)	Flow Rate (L/min)	Specific Heat (kJ/kg °C)	Density (kg/ m³)
Solar Energy System	13.6% Methanol	T5	T4	Flow3	4.00	971.68
DWHR System	13.6% Methanol	T12	T13	Flow6	4.00	971.68
GSHP	15% Glycol	T3	T1	Flow5	3.90	1,016.98
Boilers	15% Glycol	T14, T15	T1	Flow4	3.90	1,016.98

4.3.1 Renewable Sources of Energy

4.3.1.1 Solar panels

Ten solar panels with a combined total area of 28.7 m^2 have been installed on the roof of the building to collect solar energy. The solar panels connect to an SHTS, which is a preinstalled and leak-tested unit with the integrated heat exchanger and Tyfocor-L fluid circulating through a primary loop. The SHTS transmits thermal energy to the underground field through supply and return pipes on the secondary loop with 13.6% methanol. The amount of energy generated from the solar energy system can be calculated by monitoring the temperatures of the supply and return pipes on the secondary loop. Figure 24 illustrates the SHTS loops, and outlines the data being collected from the installed sensors.
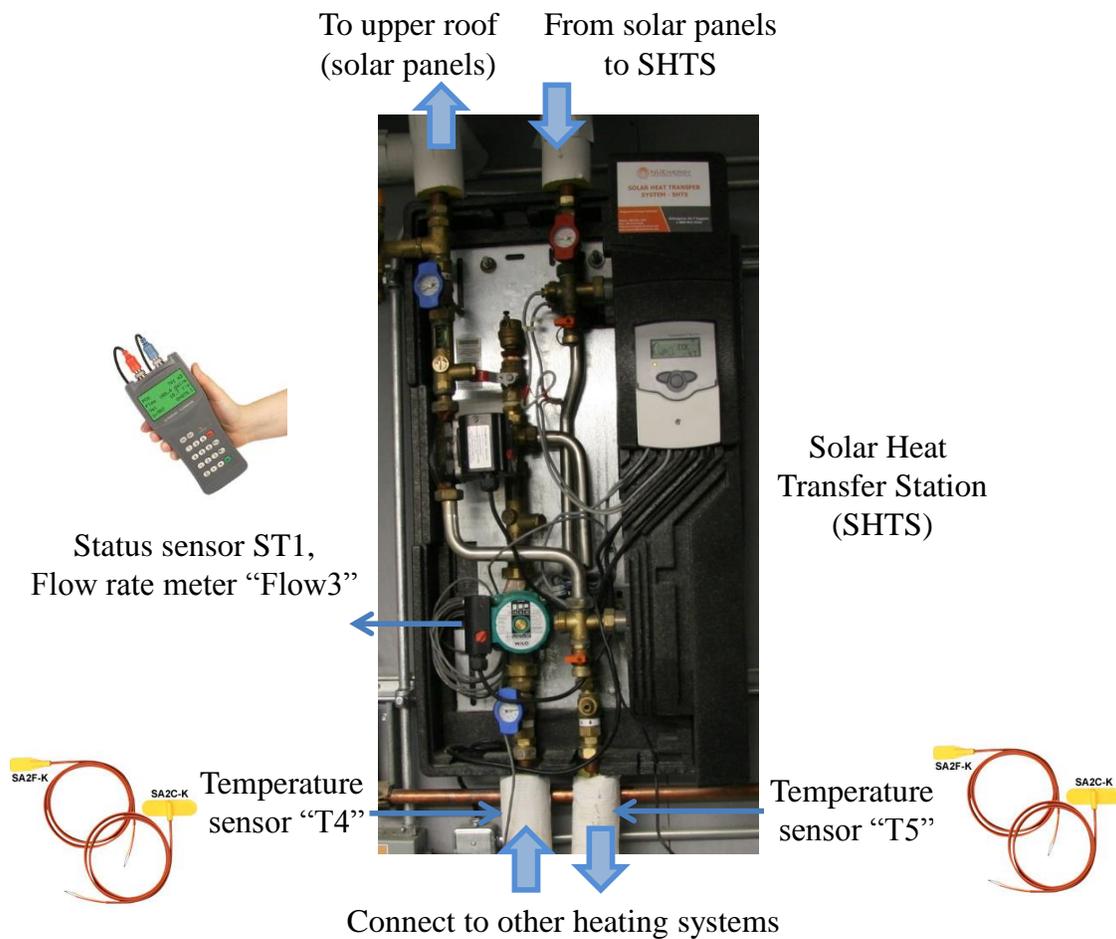
Figure 24: Solar heat transfer station loops with sensors locations

For this thesis, the solar energy system production is calculated on a weekly basis as presented in Figure 25. During the monitoring time period, energy was generated by the SHTS from late-winter to spring and early-summer. It is also observed that the wasted energy percentage decreased in this period. In general, during the late-winter and spring, the SHTS was wasting energy at nights and early mornings because it was required to run the system every 20 minutes when the outside temperature was below 2°C for freeze protection. In fact, 10% to 20% of energy from the heating loop has been wasted by the solar energy system at night in winter and spring for freeze protection, while no energy has been wasted in summer. Also, since the circulating pumps continued to operate, this has also led to electricity wastage.
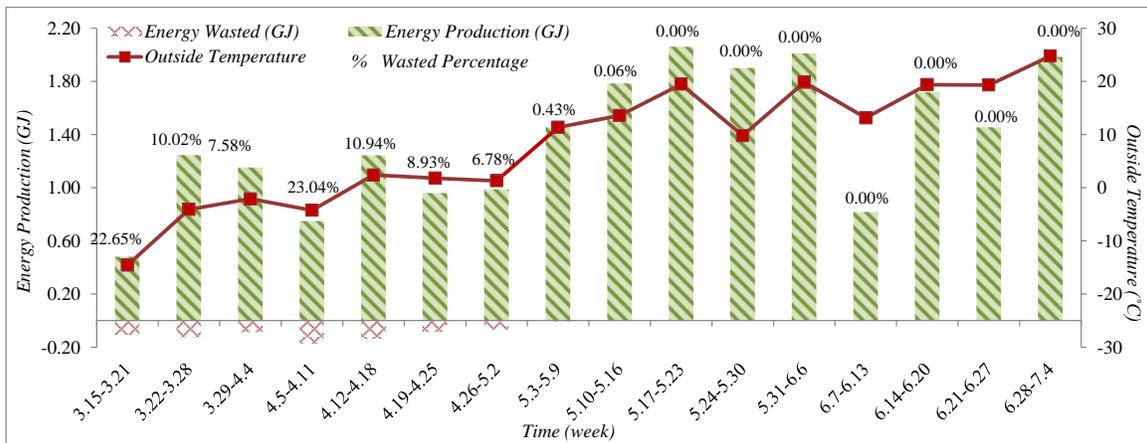
Figure 25: Solar energy system production and energy wasted

The corresponding COP of the solar energy system fluctuated between 7 and 30 with an increasing trend as illustrated in Figure 26, corresponding to seasonally increasing temperatures. Note that there is an unexpectedly low COP for the week of June 7, when the solar energy system performed with lower production and efficiency due to the unusually heavy rains experienced in Fort McMurray during this period. The solar energy system also performed with less efficiency in late winter than it did in spring or summer. In order to improve the COP of the solar energy system, more effective control of operation should be implemented based on the results obtained from the monitoring. Suggested adjustments are discussed in the latter portion of this section.
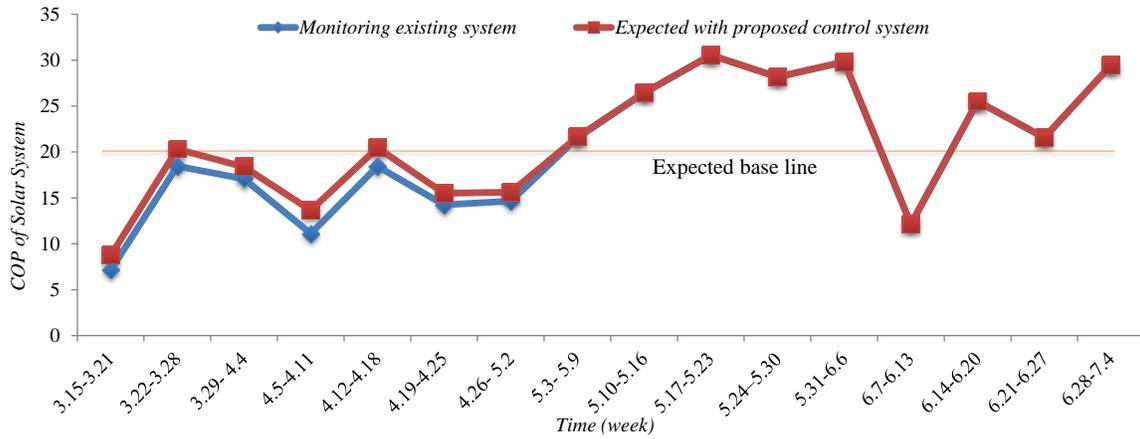
Figure 26: COP improvement of the solar energy system

A clear energy production pattern is observable in Figure 27, which presents sample solar energy production performances for every Friday of the monitoring duration. The efficient operating period expands corresponding to the overall increase in the daylight duration from March to June. In winter and spring (including March and April), low solar heating system production is encountered between 6 p.m. and 10 a.m. During this period, energy waste can be circumvented by avoiding running the primary loop. This adjustment can save a considerable amount in annual operational costs and improve the COP of the solar energy system by a margin of between 1 and 2. In addition, during summer nights due to the cooler fluid coming from GHE loop, the solar energy system can provide a small amount of energy for recovery of the GHE.
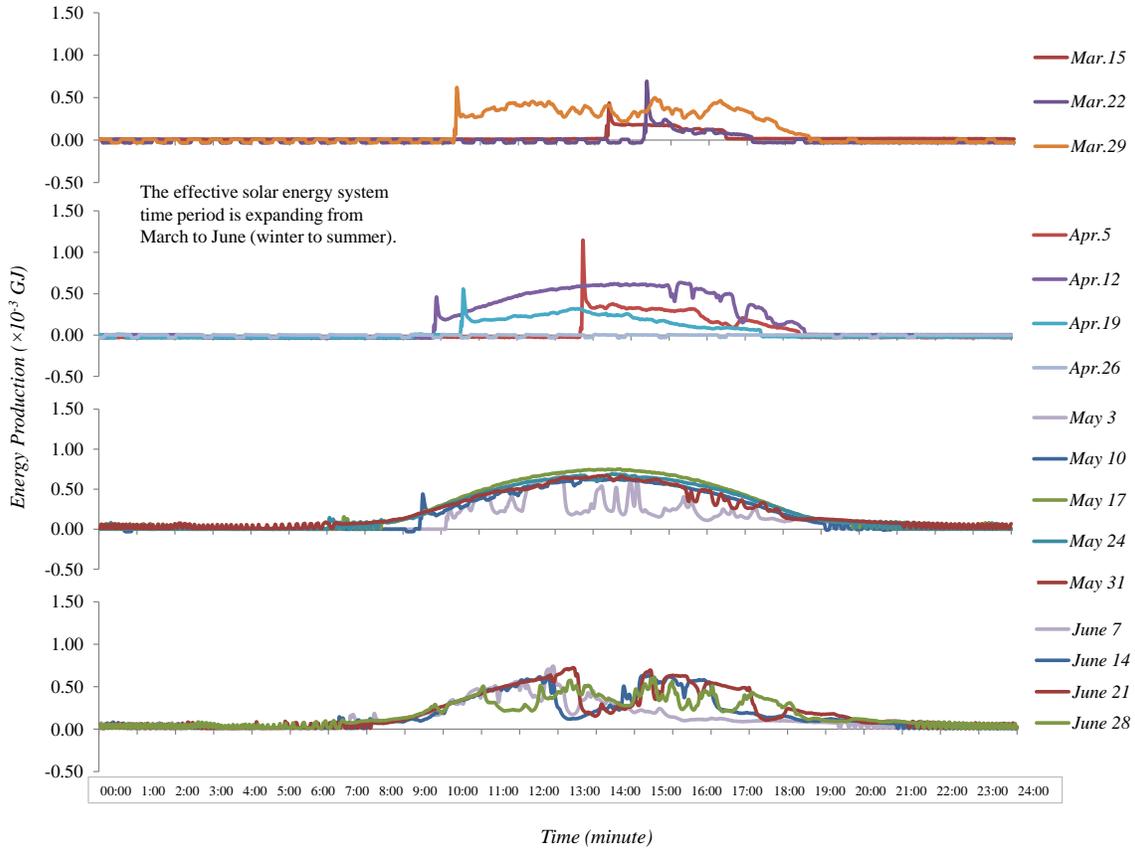
Figure 27: Solar energy system production performance (sample data for Friday of every week)

Adjustments should be made to avoid energy wasting and increase the efficiency of the system operation. The concentration of Tyfocor-L fluid in the solar primary loop may be increased and the set point for freezing protection may be decreased. In this case, the solar energy system should run only when the temperature of T5 is greater than that of T4 (Figure 24); in this case, the COP of the solar energy system can be increased by 1-2 from the blue-diamond line to the red-square line, as in Figure 26. The solid yellow line with a COP of 20 is the expected to be the baseline efficiency of this system.

After calculating the monthly productions based on the monitoring data, annual solar energy production is estimated based on the annual sun radiation information from NASA Surface Meteorology and Solar Energy (ASDC, 2008) and the heat production rates from measurements for April, May, and June, 2013. The following points summarize the forecasting steps:

(1) Calculate monthly energy production (Q), energy wasted percentage ($W\%$), and average daily energy production (Q_daily) of each testing month.

(2) Calculate the energy receiving rate ($kWh/m^2/day$), which can be calculated from the ratio of average daily energy production $Q\_daily*(1+W\%)$ to solar panel area ($A=28.7m^2$).

(3) Estimate the energy-receiving efficiency factor (E) of the solar energy system using an energy receiving rate divided by historical radiation data and average efficiency factors ($Avg(E)$) among the testing months. The efficiency factor has been calculated as 0.37 for the testing period.

(4) Plot the outside temperature vs. energy wasted percentage by minute, and obtain a trend line (Figure 28).
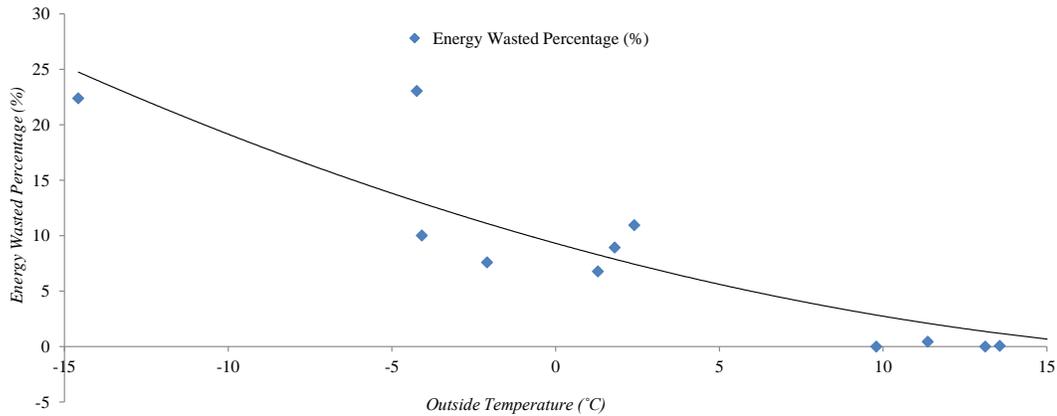
Figure 28: Solar energy system energy wasted percentage vs. outside temperature

(5) Derive an equation to estimate the monthly energy wasted percentage based on the historical outside temperature data. Based on the following equation, the energy wasted percentages can be estimated for other months.

$$W\%=0.0164T^2-0.8206T+9.312 \ (R^2=0.8307) \tag{15}$$

(6) Energy production estimation can be calculated using historical radiation data (Ra) and the following equation: $Ra\times Avg(E)\times A\times t\ /(1+W\%)$, where t is the number of days in the corresponding month.

Detailed calculation processes are attached in Appendix F. Figure 29 shows the monthly production from the solar energy system with an annual production of up to 50 GJ based on the forecasting model.

45
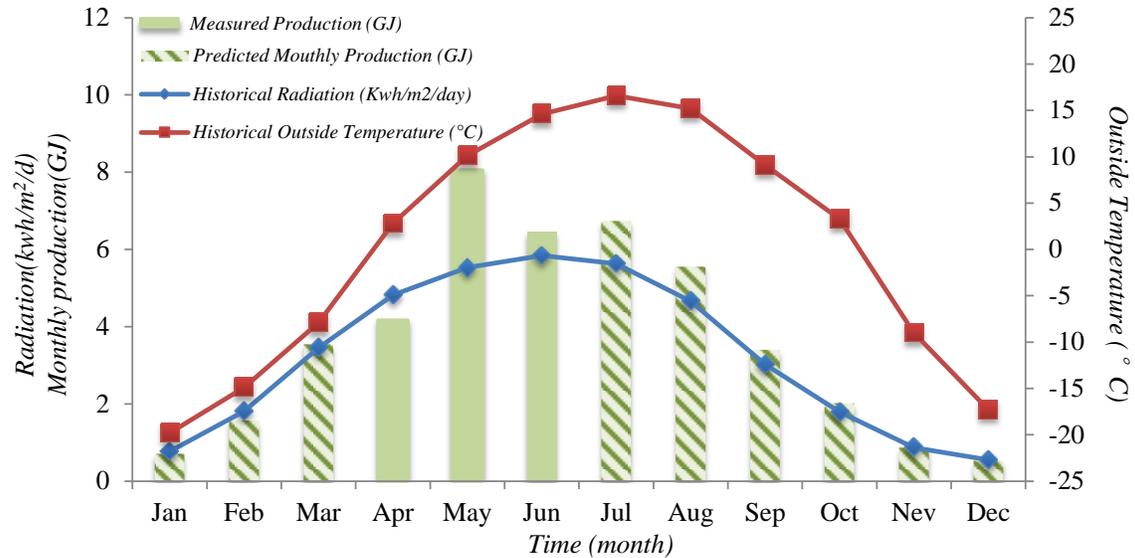
Figure 29: Solar system production prediction based on annual sun radiation estimations and monitoring data (NASA)

4.3.1.2 Drain water heat recovery

The building includes 11 DWHR stacks which recycle heat from drain water from the 70 apartment units (43 one-bedroom and 27 two-bedroom units). Each drain water pipe is entwined with coil which contains circulating fluid. The DWHR systems are wrapped with insulation to prevent energy loss to the ambient environment, and each heat recovery unit ultimately connects to the main heat loop. Figure 30 illustrates the DWHR system, along with the sensor locations. By monitoring the drain water pipes and heat loop pipes, data regarding the amount of thermal energy recycled from the drain water pipe, thermal energy transferred to the heat loop, and the efficiency of the heat transfer can be obtained. Therefore, the total energy savings from this system can be estimated by adding up the heat recovery from each DWHR stack.
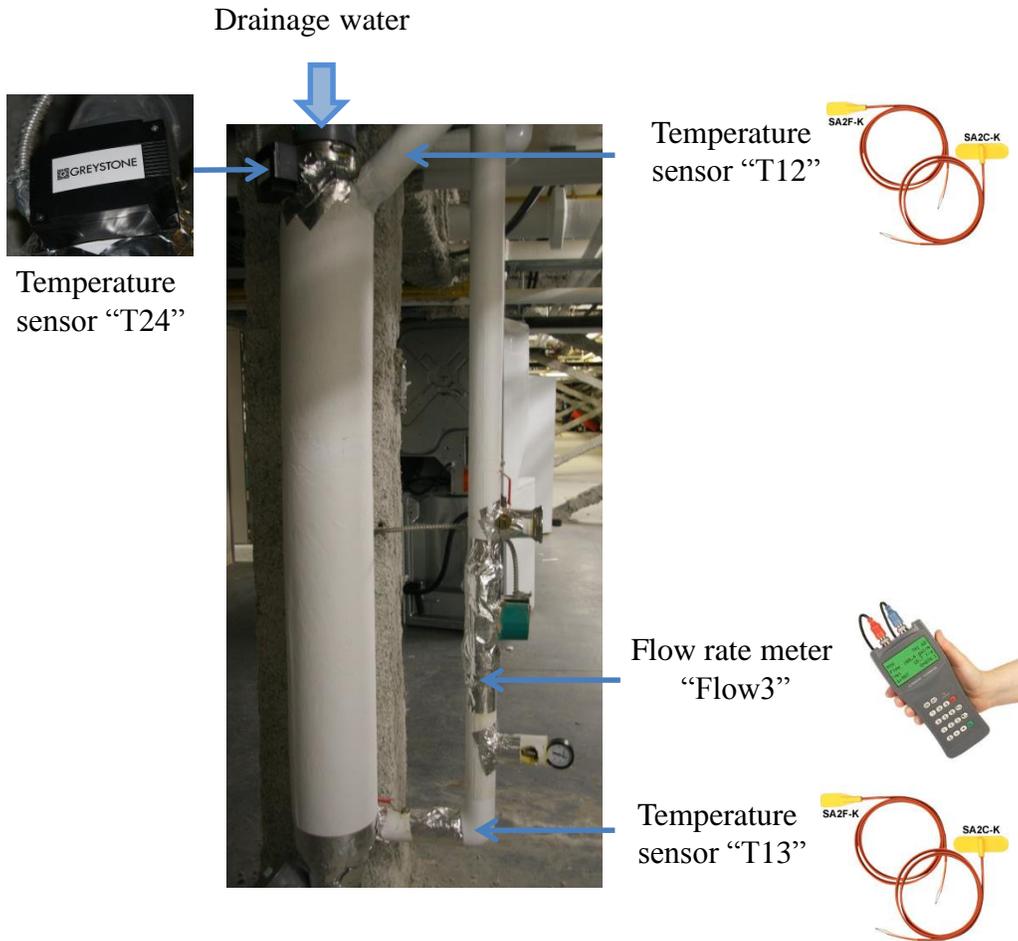
Figure 30: Selected one stack of DWHR system with sensors location

A particular DWHR stack, which connects with four one-bedroom south-facing units and four two-bedroom south-facing units, has been chosen for monitoring. Temperature sensors have been installed on corresponding supply and return pipes as shown in Figure 31. During late-winter and spring, this DWHR stack alone could result in 0.5 to 0.7 GJ in weekly-recycled energy based on the multipliers provided in Table 1, while the production decreases to a range from 0.3 to 0.7 GJ in summer.
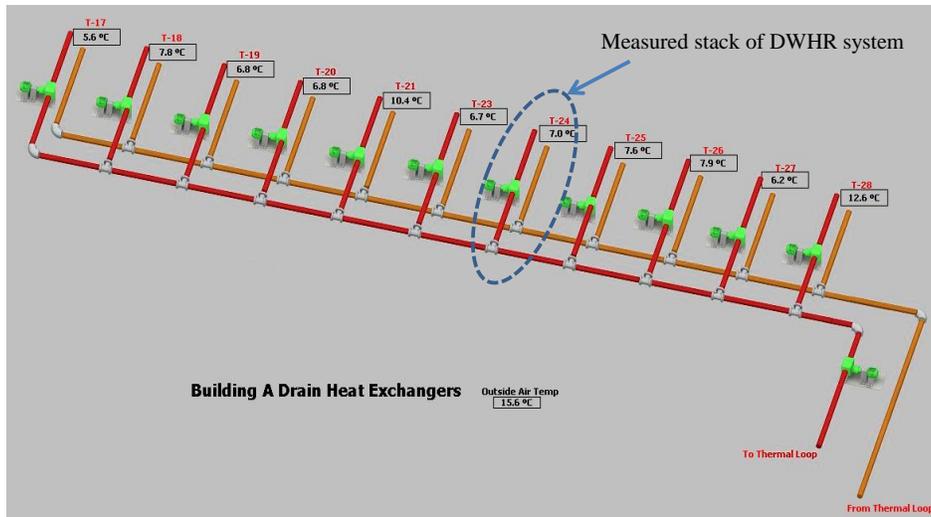
Figure 31: 3D model of measured one stack of DWHR system

In addition, average water usage from each apartment unit is measured and calculated. Water usage from 12 out of 70 apartment units has been measured from the end of December, 2011. Based on these measurements, the average daily hot water usage of a one-bedroom apartment unit has been estimated to be 100 litres, while a two-bedroom can be expected to use up to 117 litres per day. A clear direct relationship between water usage and DWHR recycled energy production is apparent as observed in Figure 32. Based on this correlation, it is expected that energy production of entire DWHR systems can be estimated using the water usage data.
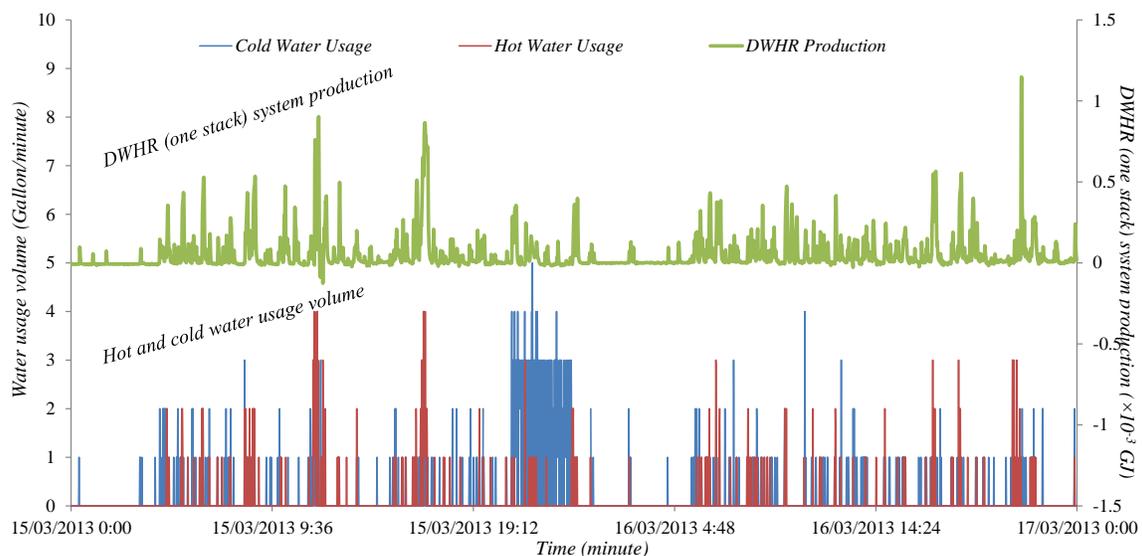
Figure 32: Relationship between water usage and DWHR production

48

Based on the ratio of water usage volume from one stack to the total water usage of 70 apartment units, the corresponding system production of eleven DWHR systems is estimated for the testing period (March 15 to July 4, 2013). The weekly water usage from apartment units is found to be approximately constant throughout the year. Using the water usage and heat recovery information from one stack of DWHR system, estimation of the total production of the 11 DWHR systems has been obtained based on the flowing steps:

Estimation steps:

(1) Find the average of the water usage of one-bedroom and two-bedroom units from data in 2012, where "A" represents one-bedroom units while "B" represents two-bedroom units.

A = 100 litres/day; B(two-bedroom) = 117 litres/day.

(2) Calculate the water usage from eight units (units 1, 2, 3, 4, 5, 8, 10, and 12), which connect to the DWHR stack that is being tested. Data for unit 10 is missing due to a technical problem. However, the average usage of unit 10 is calculated as 82.57 litres/day using historical data.

(3) Determine the average daily water usage of the entire building by using "43×A+27×B" (43 one-bedroom and 27 two-bedroom apartment units). Constant daily water usage is assumed for this calculation.

(4) Estimate the energy production from the 11 DWHR systems by multiplying the energy recycled from one stack of a DWHR system by the ratio of average water usage of the entire building and water usage from eight apartment units in the selected testing period.

With respect to the above steps, if we take one week as an example, estimation can be achieved using Equation (16).

$$11 \; DWHRs \; production = Q_{one \; stack,7 \; days} \times \frac{(43 \times 100 + 27 \times 117) \times 7 days}{V_{water,8}} \qquad (16)$$

Where

$Q_{one \; stack, \; 7 \; days}$: Energy production from one stack of DWHR system, GJ

$V_{water, 8}$: Water usage from apartment units 1, 2, 3, 4, 5, 8, 10 (added manually due to missing data), and 12, L

Figure 33 presents the weekly energy production estimation from the eleven DWHR systems, which range from 6.0 to 7.5 GJ in winter and spring and decrease to the range of 3.5 to 6.5 GJ in summer. The most probable causes of lower production in summer are the higher inlet temperature (T13) to the DWHR systems and the smaller temperature difference between the drain water (T24) and inlet (T13).
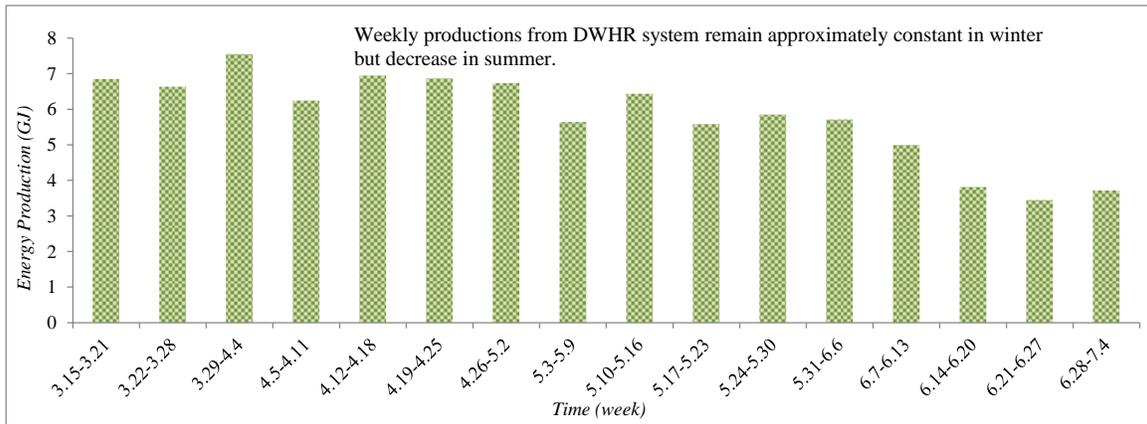
Figure 33: DWHR system energy production

Water is heated in the water-heating tank in each apartment unit, and this heating is measured using electricity meters for the selected 12 apartment units. In addition to the thermal energy recovered from wasted hot water, DWHR systems are able to recycle a small amount of thermal energy from wasted hot water and a small amount of thermal energy even from cold water when the temperature of the incoming water from the GHE is lower than the temperature of the cold water. The thermal energy in the hot water can be estimated by the electricity usage of the water-heating tank. A 95% heat dissipation factor is assumed for hot water use. Equation (17) calculates the ratio of the recycled energy from the DWHR system to the electricity usage for heating the water. The ratio indicates how much energy can be recycled by the DWHR system, as shown in Figure 34 and Table 2. The ratio is approximately stable at 60% in the first two months. Higher percentages in the last four weeks occur because more cold water has been used and it does not consume electric energy.

$$E = \frac{Q_{DWHR} \times 277.78}{E_{WHT} \times 95\%} \times 100\% \tag{17}$$

Where,

Q_{DWHR}: Energy recycled from one stack of DWHR system, GJ

E_{WHT}: Electricity consumption from water-heating tank, kWh

Table 2: The energy recycled percentage from water-heating tank by DWHR system

Time	3.15 -3.21	3.22 -3.28	3.29 -4.4	4.5 -4.11	4.12 -4.18	4.19 -4.25	4.26 -5.2	5.3 -5.9	5.10 -5.16	5.17 -5.23	5.24 -5.30	5.31 -6.6	6.7 -6.13	6.14 -6.20	6.21 -6.27	6.28 -7.4
Water-heating Tank (kWh)	269	257	294	303	312	321	252	276	270	296	195	188	196	225	173	169
DWHR(GJ)	0.54	0.53	0.58	0.58	0.62	0.69	0.56	0.54	0.56	0.61	0.59	0.55	0.50	0.38	0.30	0.32
E(%)	55	57	55	53	55	60	62	55	58	57	84	81	70	46	48	53
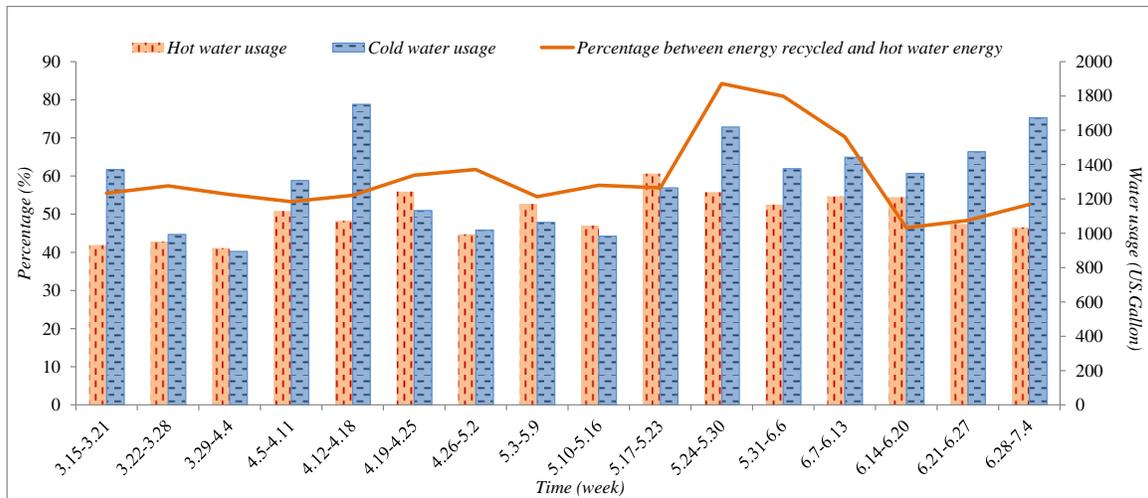
Figure 34: Fraction between hot water tank power usage and DWHR system energy recovery (one stack)

The COP of the DWHR system ranges from 4 to 8, as shown by the blue line with diamond markers in Figure 35. Since the circulating pumps on each unit and the pump on the main DWHR heat loop are always "on", a considerable amount of energy is wasted during this process. If the recycled heat cannot exceed the electric energy usage to power the circulating pump, it is not worthwhile to operate the DWHR system. It is thus suggested that the DWHR system be controlled by the temperature difference between

the supply and return pipe. To achieve energy production that is triple the rate of electricity consumption, each DWHR system has to run when the difference between the supply and return pipes on the energy collection loop (T12 - T13) reaches 0.35°C. In this case, the COP of a DWHR system can increase to 16-20 with a 5%-8% reduction in energy production compared to current system performance. To attain a higher COP, each DWHR system should run when the temperature difference between the supply and return pipes on the energy collection loop reaches 1.37°C, in which case the COP of a DWHR system can increase to 28-32 with a 23%-30% reduction in energy production.

Considering that the purpose of utilizing DWHR is not to provide heat to the building directly but to recover the GHE and enhance the efficiency of the GSHP, even a small amount of energy injected to the GHE can assist with GHE energy recovery. As such, a COP of 16-20 is adequate for this project. Figure 35 illustrates the expected COP increase based on the proposed adjustments from the blue-diamond line to the red-square line.
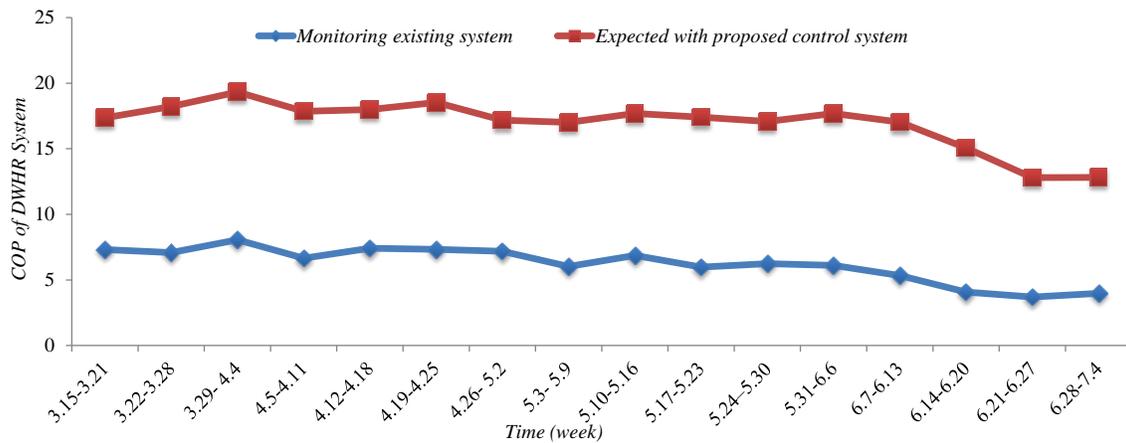
Figure 35: COP improvement of DWHR system

4.3.1.3 Ground source heat pump

10 underground geothermal loops with 8 boreholes on each loop (80 boreholes in total) at a depth of approximately 90 metres (300 feet) serve as heat exchangers under the building. Four water-to-water heat pumps, which gather heat from the DWHR systems and solar heating system, are located in the basement of the building. Figure 36 shows the 3D model of the GSHP system with the water storage tank. On the source side of the heat pumps, a circulating pipe connects to the geothermal GHE, DWHR system, and solar heating system.

On the load side of the heat pumps, the water storage tank links to the heat pumps through the supply and return pipes. Figure 37 shows the 10 geothermal loops in the basement, which are further connected to the underground loops.

When the outside temperature is below 15°C but above -20°C, heat pumps are ready to operate. With the assumed flow rate range of 147 to 170 litres per minute (L/min) per heat pump during the testing period, the heat pumps generated 173.07 to 199.7 GJ as output. Figure 38 presents the weekly production from the heat pumps with the flow rate of 170 L/min. The majority of outside temperatures in the testing period fluctuate below 15°C, and it is during these conditions that the multi-source (solar energy, DWHR energy, and geothermal energy) heat pumps produce the majority of the energy needed to satisfy the heating load requirement. As given in Figure 38, the production from heat pumps is inversely proportional to outside temperature. The total COP of the GSHP is approximately 2.1 to 2.5, with an average production rate of 2.6 to 3.0 MJ per minute per heat pump. The COPs of heat pumps are lower in summer due to the cooler GHE. However, the temperature of the GHE is expected to increase after operations in summer with the integration of the solar energy system and DWHR system.
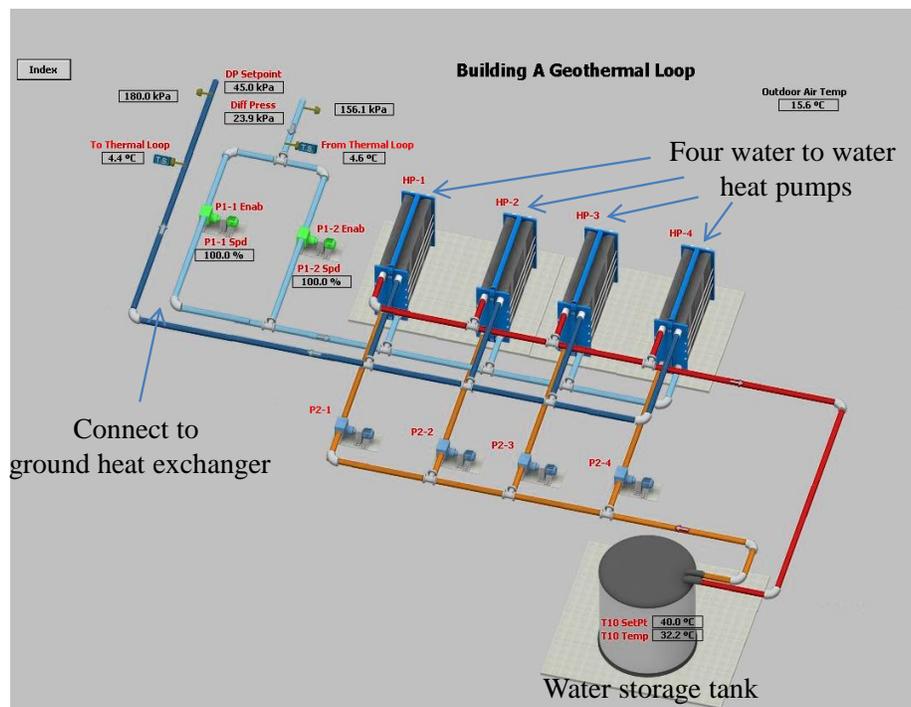
Figure 36: 3D model of the GSHP with water storage tank

53
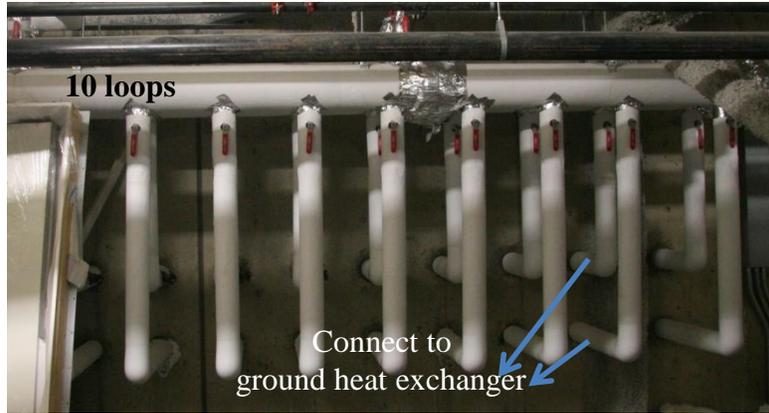
Figure 37: Ten ground heat exchanger loops in the basement
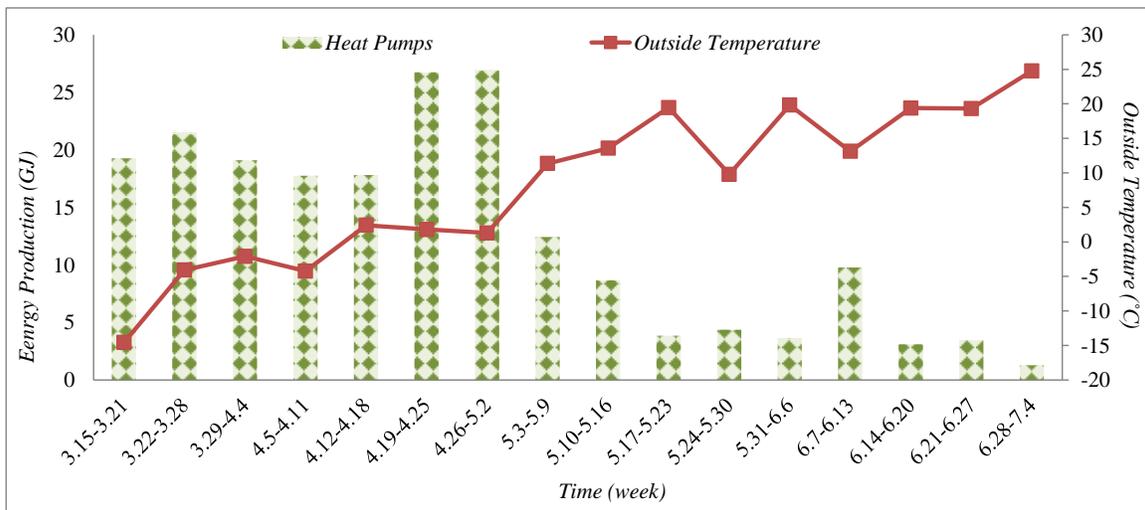
Figure 38: Heat pumps energy production vs. outside temperature

The calculated COP of the multi-source heat pump (2.1 to 2.5) is lower than expected. As can be seen in Figure 39, the entering source temperature (EST) fluctuated from 3 °C to 4 °C in winter while the entering load temperature (ELT) or leaving load temperature (LLT) of these heat pumps was around 40°C. These three temperature settings are the main factors that result in low COP. Adjustments should be made to add more source energy, e.g., energy from solar panels, in order to increase the EST. In addition, actions should be taken to reduce the ELT or LLT by decreasing the heating load. In this case, the COP of heat pumps is expected to increase to 3.2 to 3.3.

		Load Flow - 30GPM					Load Flow - 45GPM					Load Flow - 60GPM				
EST(°C)	Flow(GPM)	ELT(°C)	LLT(°C)	Power(KW)	COP	LST(°C)	ELT(°C)	LLT(°C)	Power(KW)	COP	LST(°C)	ELT(°C)	LLT(°C)	Power(KW)	COP	LST(°C)
-1	45	15.6	23.1	12.6	4.7	-7.0	15.6	20.6	12.4	4.9	-5.2	15.6	19.4	12.2	5.0	-4.2
		26.7	33.8	16.6	3.4	-6.0	26.7	31.5	16.3	3.5	-4.6	26.7	30.3	16.0	3.6	-3.7
		37.8	44.4	20.6	2.6	-5.0	37.8	42.3	20.2	2.7	-3.9	37.8	41.0	19.8	2.8	-3.3
		48.9					48.9					48.9				
	60	15.6	23.3	12.7	4.8	-7.0	15.6	20.8	12.5	4.9	-5.3	15.6	19.5	12.3	5.1	-4.3
		26.7	34.0	16.7	3.5	-6.0	26.7	31.6	16.4	3.6	-4.7	26.7	30.4	16.1	3.7	-3.8
		37.8	44.7	20.7	2.6	-5.0	37.8	42.4	20.4	2.7	-4.1	37.8	41.3	20.0	2.8	-3.4
		48.9					48.9					48.9				
10	30	15.6	24.9	13.3	5.6	2.3	15.6	21.9	13.1	5.7	4.8	15.6	20.3	12.9	5.9	6.1
		26.7	35.0	17.3	4.1	3.2	26.7	32.7	16.9	4.2	5.4	26.7	31.2	16.6	4.3	6.5
		37.8	46.1	21.2	3.1	4.3	37.8	43.4	20.8	3.2	6.1	37.8	42.1	20.4	3.3	7.0
		48.9	56.7	25.1	2.5	5.3	48.9	52.2	24.6	2.6	6.8	48.9	52.9	24.2	2.7	7.4
	45	15.6	25.2	13.4	5.7	2.0	15.6	22.1	13.2	5.8	4.6	15.6	20.4	13.0	6	5.9
		26.7	35.8	17.4	4.1	3.0	26.7	32.8	17.1	4.3	5.3	26.7	31.3	16.8	4.4	6.4
		37.8	46.3	21.4	3.2	4.1	37.8	43.6	21.0	3.3	5.9	37.8	42.2	20.6	3.4	6.9
		48.9	56.9	25.3	2.5	5.2	48.9	54.3	24.8	2.6	6.6	48.9	53.1	24.3	2.7	7.4
	60	15.6	25.4	13.5	5.8	1.8	15.6	22.2	13.3	5.9	4.4	15.6	20.6	13.1	6.1	5.8
		26.7	36.0	17.5	4.2	2.9	26.7	32.9	17.2	4.3	5.2	26.7	31.4	16.9	4.5	6.3
		37.8	46.6	21.5	3.2	3.9	37.8	43.7	21.1	3.3	5.8	37.8	42.3	20.7	3.5	6.8
		48.9	57.1	25.5	2.6	5.0	48.9	54.5	25.0	2.7	6.5	48.9	53.2	24.5	2.8	7.3

Figure 39: Heat pump performance table screenshot (water furnace)
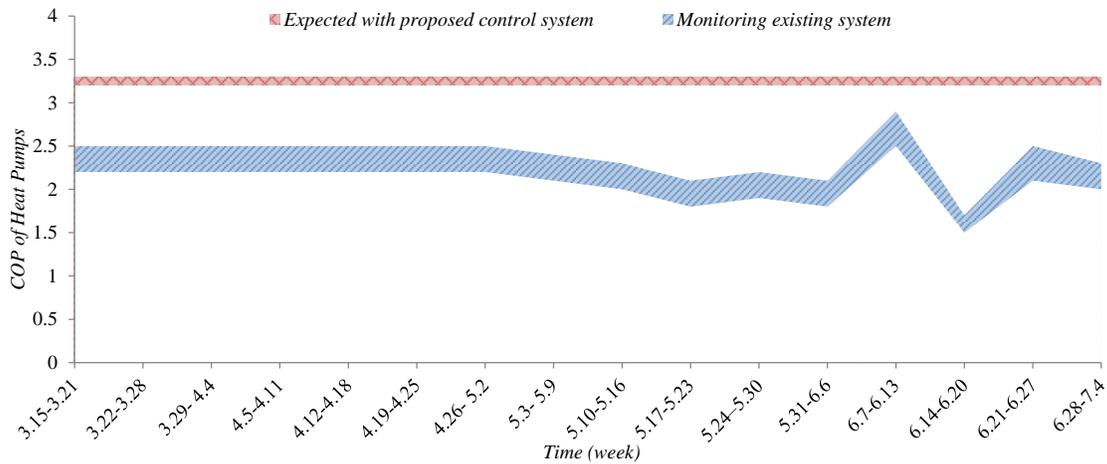
Figure 40: COP improvement of heat pumps

The output energy of a heat pump is equal to the source input plus the electricity usage of the heat pump (first law of thermodynamics, Kittel and Kroemer, 1980). Using this principle, the energy generated from the GHE can be estimated, as illustrated in Figure 41. It is clearly observable that the production of the GHE decreases in the spring and summer with the warmer outside temperatures, which is in accordance with the previous theoretical analysis.

However, it should be noted here that the accuracy of these results may be improved once long-term data is available. Reliable forecasting of the performance of the geothermal heating system will be carried out after collecting at least one full year of data. For instance, if the amount of energy injected to the underground field in summer is much greater than the amount of energy extracted in winter, the effectiveness of the GHE will

not decline. Otherwise, precautions should be taken before system performance further declines.
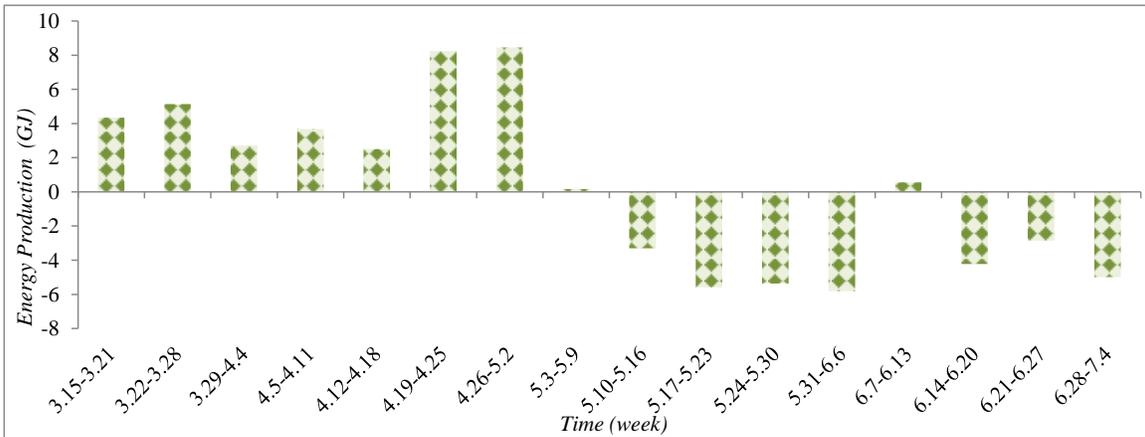
Figure 41: Geothermal GHE energy production
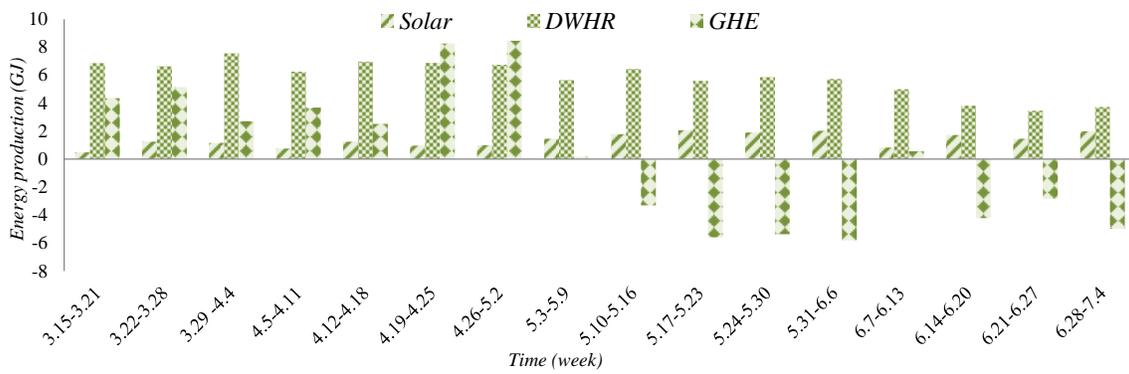
Figure 42: Heat energy production from each renewable source on the source side of heat pumps
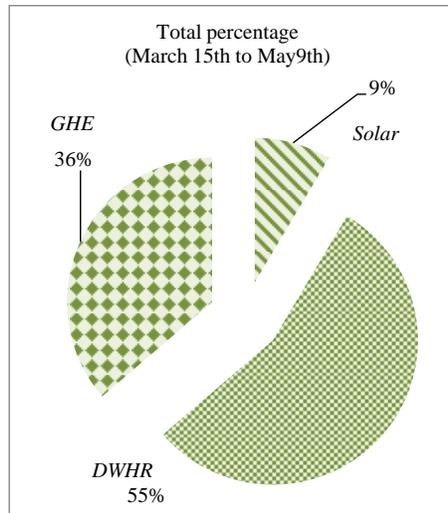
Figure 43: Energy production percentage from each renewable source (during testing period from March 15 to May 9)
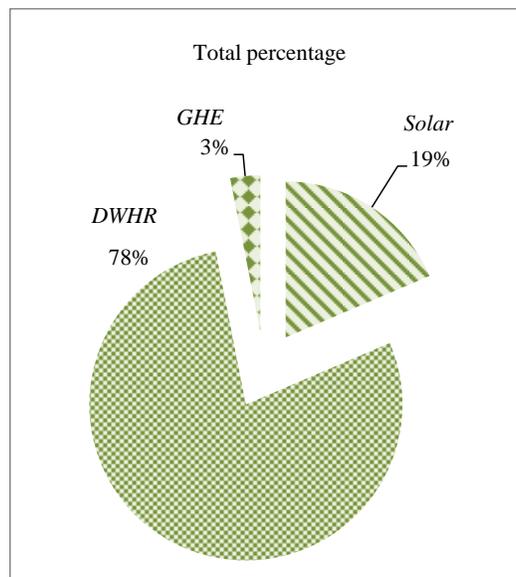
Figure 44: Total production percentage from each renewable source

Based on the 16 weeks of monitoring (from March 15 to July 4), the energy production of each renewable source from the source side of the heat pumps is calculated (Figure 42, Figure 43, and Figure 44). In the winter and spring, the solar energy system provided 9% of energy while the GHE contributed 36% of energy (Figure 43). The balance of the energy, 55%, was recycled from the DHWR systems. However, in summer, the productivity of the GHE dropped to a negative value. As a result, the solar energy system, DWHR system and the GHE drew 3%, 78% and 19% of source-side production for heat

pumps, respectively, during the testing period (Figure 44). The production from the GHE is expected to increase in the winter again. In summary, the solar energy system production varies from week to week with the sun radiation. The DWHR system continuously recycles energy based on the approximately constant weekly water usage from apartment units and produces a slightly decreasing amount of energy from winter to summer; the GHE energy production will be further derived after a longer period of monitoring.

4.3.2. Non-renewable Source of Energy

The only non-renewable source of energy that is utilized for heating in this case study is natural gas. It is used to fuel the Lochinvar-Knight boilers, which have a very high efficiency of 95%.

Boiler Loop

Boilers are used for generating heat for residential unit purposes by heating mixed fluid (15% glycol) to a preset temperature and circulating that fluid throughout the building. Natural gas is widely used as an important energy resource, and Fort McMurray is no exception, given that this particular geographic area has significant natural gas reserves. Two boilers are installed in the basement to provide heat to the building. These play an important role when the GSHP cannot satisfy the heat requirements of occupants. When the outside temperature is lower than -20°C, natural gas is selected as a more cost-effective heating resource than electricity, which is used to power the heat pumps. Figure 45 shows the connections among the heat pump, tank, and boilers while Figure 46 is the 3D model of the boiler loop.
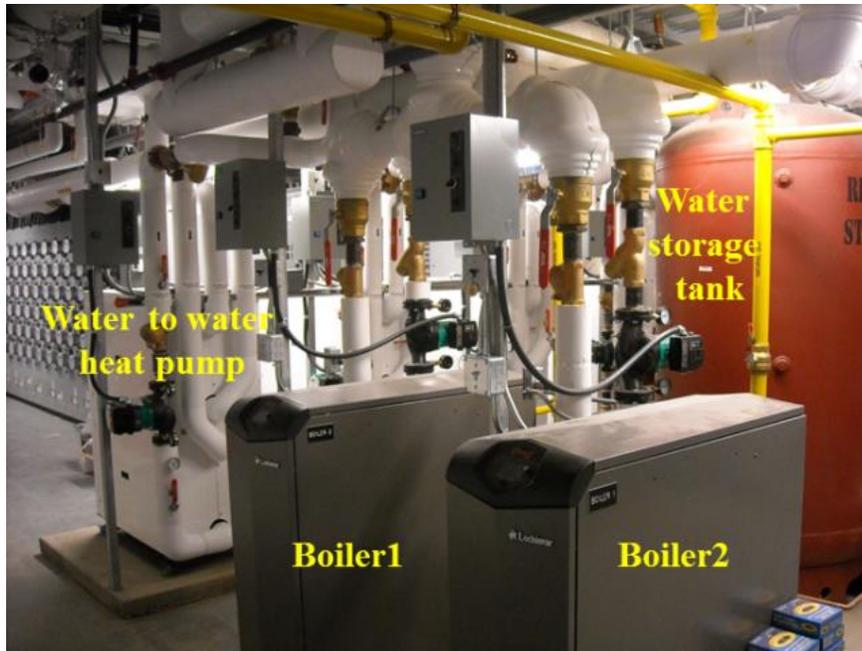
Figure 45: Heat pump, tank, and boiler in the basement
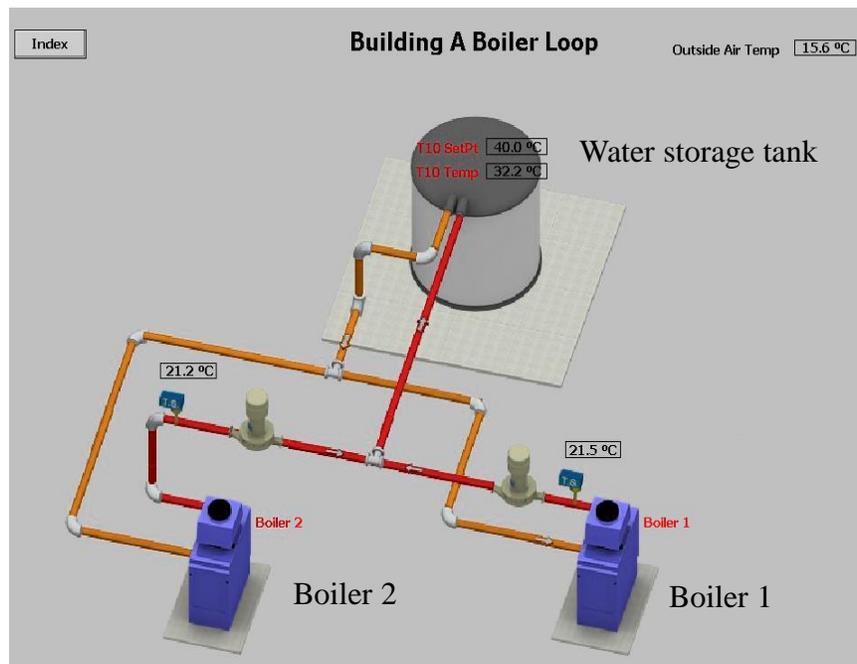
Figure 46: 3D model of the boiler loop

Following the same principles as given in other systems, by measuring the temperature difference and flow rate on the circulating pipes, the thermal energy generated from the boilers can also be estimated. Each boiler works with a flow rate of 303 L/min.

Temperatures of the supply and return pipes for Boiler 1 and Boiler 2 are measured. The production results indicate that the boilers were active at the beginning of the testing period in March with an average production rate of 5.5 MJ per minute per boiler, which doubles the production rate of the heat pump. However, in mid-June, the boilers worked for 30 minutes once the heating mode switched from "off" to "on", which resulted in heat loss. This trend is due to the fact that the boiler is self-maintaining, which means that the boiler's circulating pump, after two months of dormancy, is set to run and clean itself without using natural gas or producing heat.

A comparison between the paid resources of electricity and natural gas is made according to the given energy production from the heat pumps and boilers. Heat pumps are found to operate with an average production rate of 3.0MJ/min when the outside temperature is above -20°C, and the boilers operate as the sole source of heat when the temperature falls below this threshold, with an average production rate of 5.5MJ/min. Figure 47 shows the energy production percentage between renewable and paid resources. Within the 16 weeks of monitoring, renewable resources produced up to 57% of energy, while the other 43% of energy was provided by the paid resources, comprising electricity (33%) and natural gas (10%).
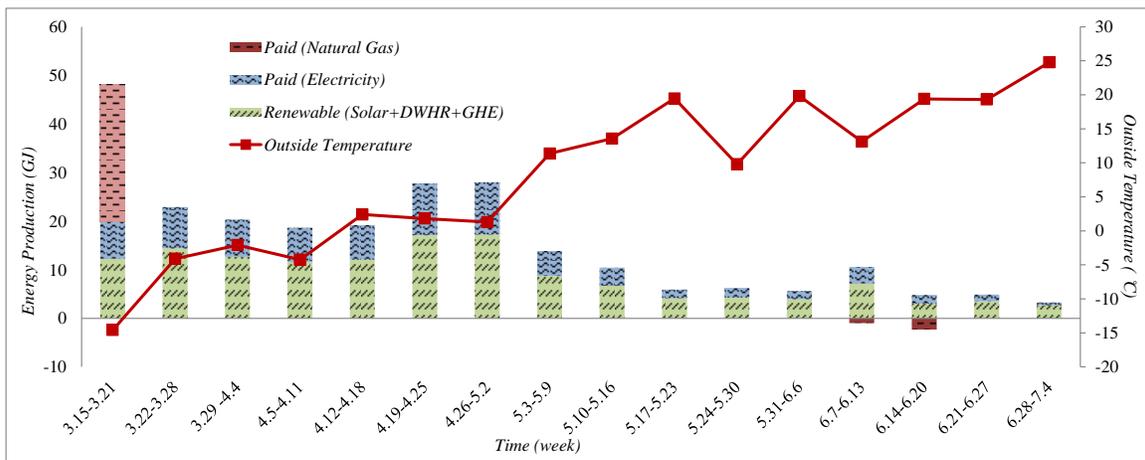
Figure 47: Energy production comparison between renewable and paid resources

Total percentage
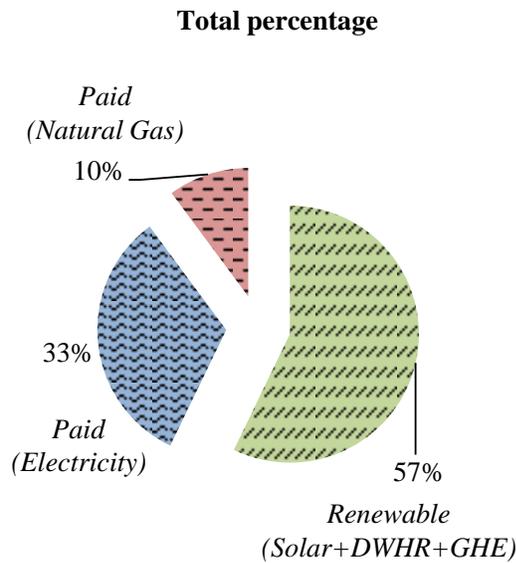
Figure 48: Energy production percentages between renewable and paid resources

4.4 Cost Comparison of Electricity and Natural Gas

Taking the electricity and natural gas prices into consideration, a comparison of cost-effectiveness between electricity and natural gas is made, as illustrated in Figure 49. It should be noted that the flow rate is one of the factors affecting the production of the heat pump. When the sample measurements were taken, the flow rate was measured as 148 L/min, whereas the designed flow is 227 L/min. The electricity-associated costs given in Figure 49 are thus estimated by the range of flow rates from 148 L/min to 227L/min in order to support decision-making by facility management. The heat pumps could achieve a total production cost of $7.4/GJ to $11.4/GJ with the current Direct Energy electricity price vacillating between $0.073/kWh to $0.085/kWh. On the other hand, the total cost for natural gas would be $3.9/GJ with an average boiler efficiency of 85%, according to Gas Alberta Inc. natural gas price range of $2.9/GJ to $3.6/GJ for Alberta delivery. If the COP of the heat pump can be increased to 3.2 to 3.3, then the expected production cost will be in the range of $7.0/GJ to $7.2/GJ, as shown in Figure 50. It is therefore more cost-effective to use boilers as the only heaters for space heating for the entire building

61

unless natural gas prices increase beyond the threshold of $7.0/GJ. However, the use of solar- and DWHR-assisted GSHP systems is much more environmentally-friendly, provided the COP of the heat pumps can be increased. Recommendations for the improvement of COPs will be further discussed in the following section.
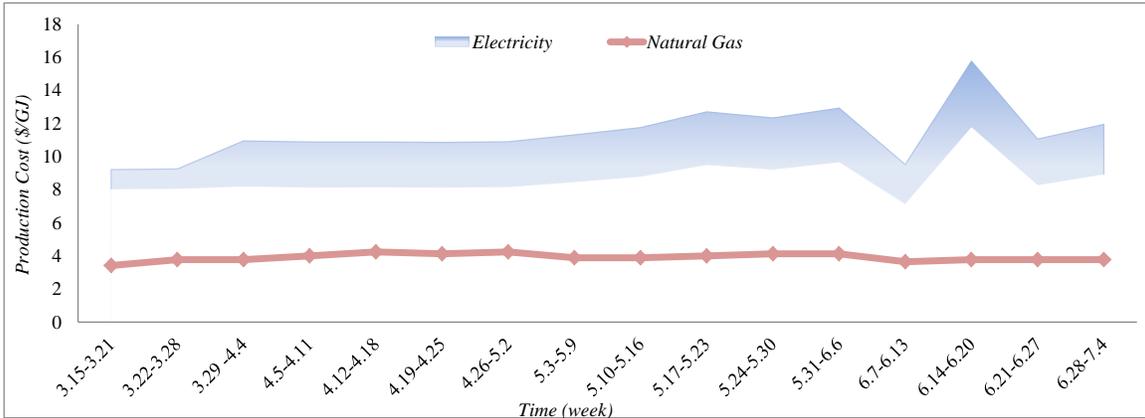
Figure 49: Production cost comparison between electricity and natural gas
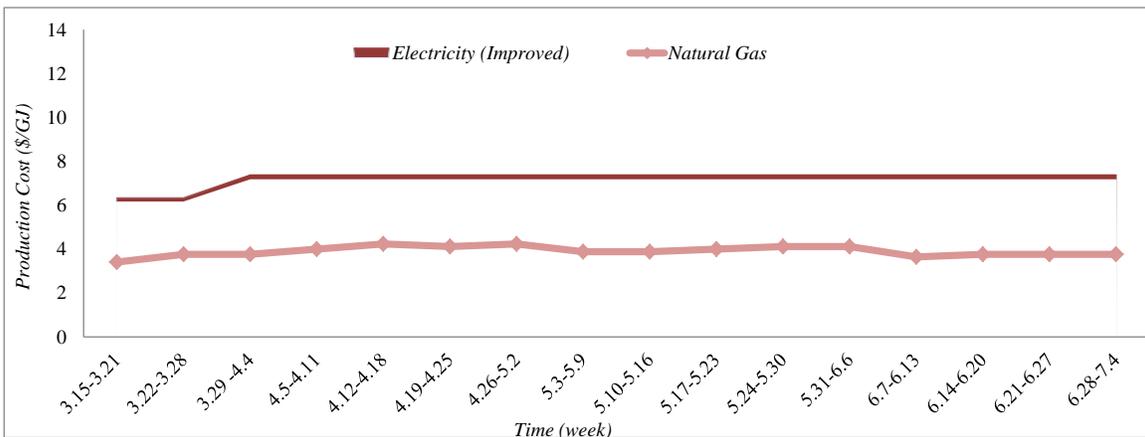
Figure 50: Production cost comparison between electricity and natural gas after proposed adjustments

4.5 Heating Consumption

Space heating energy usage meters were installed in 12 out of 70 apartment units at the end of December, 2011 in order to obtain their annual heating consumption. As expected, it is found that a significant heating load is required for winter while no cooling load is needed for the summer. From the average hourly heating consumption of one-bedroom and two-bedroom units, it is estimated that the entire building could consume up to 500

GJ per year, with the peak monthly load of approximately 110 GJ in December, as illustrated in Figure 51, not including energy consumption for the basement, where only mechanical equipment is located.

	May-12	Jun-12	Jul-12	Aug-12	Sep-12	Oct-12	Nov-12	Dec-12	Jan-13	Feb-13	Mar-13	Apr-13
Monthly heating load	2.04	0.07	0.00	0.00	0.00	30.77	73.93	110.46	101.20	56.51	74.05	47.22
Outside Temperature (℃)	13.55	18.61	21.69	18.73	12.48	-0.06	-11.64	-20.29	-18.23	-8.93	-8.73	-0.34
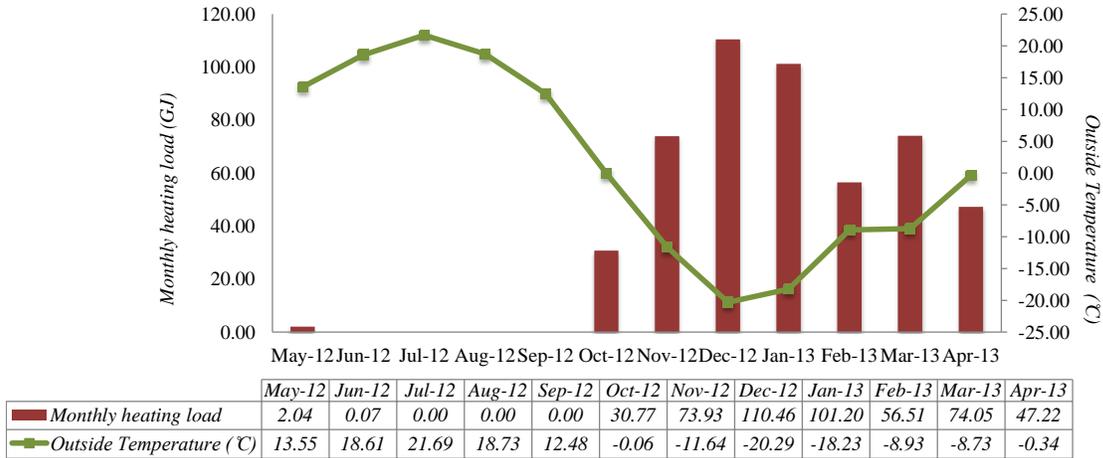
Figure 51: Monthly building heating load vs. outside temperature
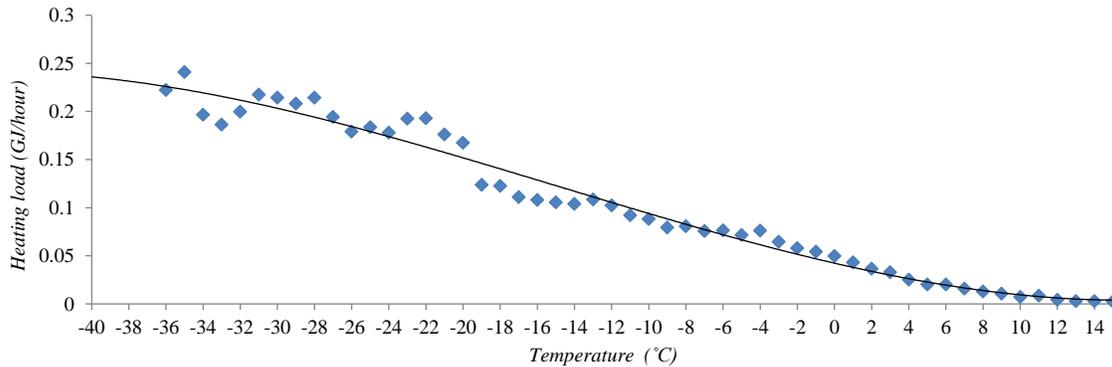
Figure 52: Building heating loads vs. outside temperature

The relationship between hourly heating load and outside temperature is also investigated, as shown in Figure 52, with outside temperature on the *x*-axis and hourly heating load on the *y*-axis. It is determined that no heating load is required when the outside temperature is above 15°C. A clear pattern is identified by the trend line, which subsequently leads to the polynomial presented in Equation (18). It is observed from this equation that higher outside temperature is a requirement for lower heating loads, as expected. Using this equation and the outside temperature, heating load demand can be calculated. The heating system control algorithm can thus be adjusted according to this

63

equation. Since the water storage tank stores the thermal energy from the resources and provides heat to the building based on the heating requirements, the tank has to be heated to a higher set point (temperature) when a larger heating load is required. When the required heating load is lower, the tank does not have to reach such a high temperature set point. In this case, various set points of the water storage tank can be defined based on this equation in order to avoid excessive energy production and waste.

$$Load(T) = 2 \times 10^{-6}T^3 + 9 \times 10^{-5}T^2 - 0.0044T + 0.042 \qquad (18)$$

Where *Load* shows the hourly heating load requirement in GJ and T shows the outside temperature in °C.

4.6 Recommendation for Coefficient of Performance Improvement

The COP represents the thermal efficiency for power cycles by calculating the ratio of the heating output over the electrical energy consumed. The COPs for the solar energy system, DWHR system, and heat pumps based on the current monitoring results in the testing period are 20.4, 6.2, and 2.1-2.5, respectively (given in Table 3). It should be noted that these COP values are smaller than expected, i.e., than the design values. However, based on the following recommendations, the COPs are expected to be improved to some extent.

Table 3: Coefficient of performance of solar energy system, DWHR system and heat pumps

Weeks (2013)	Results	3.15-3.21	3.22-3.28	3.29-4.4	4.5-4.11	4.12-4.18	4.19-4.25	4.26-5.2	5.3-5.9	5.10-5.16	5.17-5.23	5.24-5.30	5.31-6.6	6.7-6.13	6.14-6.20	6.21-6.27	6.28-7.04	Average
COP of Solar	Monitoring existing system	7.1	18.5	17.1	11.1	18.4	14.2	14.6	21.6	26.4	30.5	28.2	29.8	12.1	25.5	21.6	29.4	20.4
	Expected with proposed control system	8.7	30.3	18.4	13.7	20.4	15.5	15.6	21.6	26.5	30.5	28.2	29.8	12.1	25.5	21.6	29.4	21.1
COP of DWHR	Monitoring existing system	7.3	7.1	8.1	6.7	7.4	7.3	7.2	7.19	6.9	6.0	6.2	6.1	5.3	4.1	3.7	4.0	6.2
	Expected with proposed control system	17.4	18.2	19.3	17.9	18.0	18.5	17.2	17.0	17.7	17.4	17.1	17.7	17.7	17.7	12.8	12.8	17.1
COP of HP	Monitoring existing system	2.2-2.5	2.2-2.5	2.2-2.5	2.2-2.5	2.2-2.5	2.2-2.5	2.2-2.5	2.1-2.4	2.0-2.3	1.8-2.1	1.9-2.2	1.8-2.1	2.5-2.9	1.5-1.7	2.1-2.5	2.0-2.3	2.1-2.5
	Expected with proposed control system	3.2-3.3	3.2-3.3	3.2-3.3	3.2-3.3	3.2-3.3	3.2-3.3	3.2-3.3	3.2-3.3	3.2-3.3	3.2-3.3	3.2-3.3	3.2-3.3	3.2-3.3	3.2-3.3	3.2-3.3	3.2-3.3	3.2-3.3

Based on the current performance of each heating system, some energy-wasting problems are identified. In the interest of energy saving and cost efficiency, corresponding suggestions are specified in terms of the following two aspects:

(1) Avoid unnecessary power consumption and energy wasting.

Due to the freeze protection operation, the solar heating system is found to have wasted energy through the circulating pipes during nights, which drew 10% to 20% of the weekly solar energy production in winter. Based on the preliminary results observed from the data analysis, the solar loop circulating pump should run when the temperature of the solar supply pipe is greater than the temperature of return pipe. In addition, the concentration of Tyfocor-L fluid in the solar primary loop may be increased in order to decrease the set point of freezing protection, which would in return reduce the number and duration of the anti-freeze system runs.

During the monitoring period, the DWHR system kept running at all times, and sometimes consumed more power energy than recycled energy. Based on this observation, each DWHR stack should run only when there is drain water flow and when the difference between the temperatures of the supply and return pipes is greater than 0.35°C. Detailed suggestions are summarized in Figure 53. With these recommendations, COPs of the solar energy system and DWHR system can be improved, with the expected results of 21.1 and 17.1, respectively, as detailed in Table 3.

(2) Increase the COP of multi-source heat pumps.

Low EST and high ELT of heat pumps are the main factors causing the low COP of the heat pumps. Adjustments should be made either by adding more solar panels or large condensers on the source side of the heat pumps to increase the EST, or by modifying the set point of the tank temperature based on the heating load requirement for any specific outside temperature (Figure 52) to reduce the ELT. These recommendations can improve the COP of the heat pumps to 3.2 - 3.3 according to heat pump performance data. Furthermore, four heat pumps are currently in activation mode, while generally only two heat pumps are required for heating in winter. In order to support self-maintenance of the heat pumps, the four heat pumps can be grouped into two pairs that alternate operation, switching every three months.

Ground Source Heat Pump & Boiler

Is $T_{outside}$ < 15 °C ?
— Yes → Heating mode - ON
— No → Heating mode - OFF → GSHP and Boilers - OFF

Is $T_{outside}$ > -20 °C ?
— Yes → Is T_{tank} < set point (36-45) °C ?
— No → Tank set point – 42.5°C GSHP -OFF

Is T_{tank} < set point (36-45) °C ?
— Yes → **Four Heat Pumps – ON** (group four pumps into two, switch group mode every 3month)
— No → Heat Pumps - OFF

Is T_{tank} < set point (63-71) °C ?
— Yes → **Two Boilers – ON** (priority goes from 1 to 2, switch sequence every half year)
— No → Boilers - OFF

Solar System

Is $T_{solar-supply}$ > T_{solar_return} ?
— Yes → Is T_{solar_supply} > T_{ground_return} ?
— No →

Is T_{solar_supply} > T_{ground_return} ?
— Yes → **Solar Heat Transfer Station- ON**
— No → Is T03 < -35°C ?

Is T03 < -35°C ?
— Yes → Freeze protection – ON → Solar Heat Transfer Station enable for 20min
— No → Solar Heat Transfer Station- OFF

Drain Water Heat Recovery System

Drain water comes

Is T_{D_suppy} - T_{D_return} > 0.3C ?
— Yes → DWHR Pump8- ON → **DWHR - Start** / Injection Pump7- ON
— No → DWHR - OFF

Figure 53: Proposed heating system control algorithms

4.7 User Interface

With the help of our collaborators in the University of Alberta's Department of Computing Science, a user interface has been established as a product of this research. The data analysis methodology proposed and implemented in this thesis constitutes the backbone of the heating system component of this user interface, which is available online at <https://smartcondo.ca/HomeWatch/>. Figure 54 shows a screenshot from the home page of this user interface. Engineers, building owners, and researchers can obtain access to the interface by simply inputting a username and password. "Graphs" and "Energy Calculations", which are related to the research in this thesis, are provided in this interface. In terms of the heating system performance, the user can click "Energy Calculations" to select the desired time period for the performance evaluation as shown in Figure 55. Following selection of time period and calculation type, the results of energy production, power usage information, and COPs of systems can be displayed in different formats, such as bar graphs. Additional formulae can be manually added using the function "Formula Configuration".

Figure 54: User interface screenshot - home page

Figure 55: User interface screenshot – testing period setting

CHAPTER 5: CONCLUSIONS

5.1 Research Results

This research has investigated an integrated heating system comprising a solar energy system, drain water heat recovery (DWHR) system, and ground heat exchanger (GHE) as the source-side renewable resources of the heat pumps. Electricity drives the heat pump and produces the required heat, which is then stored in water storage tanks. One of the unique aspects of this integrated heating system is that solar and DWHR assist the ground source heat pump (GSHP) systems to ensure that the energy in the geothermal field is sustained over the years. Boilers work as an auxiliary heater in winter, generating heat by burning natural gas. The heating system performance has been evaluated by analyzing the monitoring data to obtain the weekly energy production and coefficient of performance (COP) of each heating system. In addition, an enhanced control system has been derived based on the data analysis results and observations, which is expected to improve the COP of the heating system in the interest of energy saving and cost-effectiveness. The following conclusions have been drawn based on the results obtained using the monitoring data.

1. The proposed monitoring system design and developed data analysis strategy can capture the performance of the heating system with energy production results and efficiency, which provides valuable outcomes to the engineers and decision makers for adjustment in the current system and future heating system designs.

2. Annual production from the solar energy system can be up to 50 GJ based on 28.7 m^2 solar panels. The monthly production from the solar energy system varies through the year from less than 1 GJ to the peak production of 8 GJ. However, research results show that there is some energy waste during the nights in winter, which can be minimized by implementing the control system proposed in this study.

3. The DWHR system continuously recycles heat from drainage, which is approximately consistent from winter to spring and has a slight decrease in summer. Energy from either hot water or cold water can be recycled. This system can generate an impressive amount of energy (0.3-0.7 GJ per stack per week), which is equivalent to more than 60% of the thermal energy used for heating hot water.

4. With the existing control algorithm, the COPs of the solar and DWHR systems are 20.4 and 6.2, respectively. Data analysis results show that unnecessary power usage could be avoided when operating renewable resources, which can enhance the corresponding COPs to 21.1 and 17.1.

5. With long-term operation of the GSHP, its low efficiency may be attributable to unbalanced heating and cooling load (or no cooling load) to the GHE. GSHP systems face such risks in cold-climate regions unless a better-designed integrated system can be widely embraced and implemented.

6. The COP of the integrated heating system with solar- and DWHR-assisted GSHPs can achieve a COP of 2.1-2.5 when it is designed only for heating, as in the extreme cold-climate region of Fort McMurray, Alberta. This integrated heating system still needs improvement for the purpose of energy saving.

7. In terms of the environmental aspects and CO_2 emissions reduction, renewable resources are to be considered to be of the highest priority for use as energy sources. In the interest of cost savings, however, considering the high cost of electricity and the low cost of natural gas in Fort McMurray, using only natural gas for heating of this building is more cost effective unless either the price of natural gas increases beyond the threshold of \$7.0/GJ or measures are taken to significantly improve the COP of the GSHPs.

It is acknowledged that 16 weeks of data may not be adequate to accurately predict the performance of the GHE. However, it should be noted that the developed data analysis strategy can be used to obtain more accurate results when long-term monitoring data is available.

5.2 Research Contributions

The proposed strategy of using renewable sources of energy—i.e., solar energy and geothermal energy—is practical and benefits the occupants living in cold-climate regions. Through the proposed strategy, solar and DWHR systems assist the GSHP to recover the heat loss of the geothermal field. The developed monitoring design and data analysis strategies presented in this thesis can provide a better understanding of the existing

system, thereby addressing the economic concerns that may constrain the use of sustainable heating system design. The contributions are summarized below:

(1) A framework of experimental design and data analysis of control system design for space heating;

(2) Analysis of data to evaluate the efficiency of the existing design of the space heating system in the case study;

(3) A framework for assessment of collected data and the development of the metrics for energy production and COP;

(4) The development of a control system to improve the energy production and COP;

(5) Development of forecast models for energy production; and

(6) Establishment of a user interface by which for mechanical engineers to evaluate the performance of the existing heating system through the experimental design.

5.3 Future Direction

Once comprehensive long-term data is collected, it will be possible to observe the performance of the GHE and compare the energy production and energy recovery from the GHE with annual results. Both the potential risk that there is heat loss in the geothermal field after a few years of operation and the estimated extent of annual heat loss can thus be determined. This will provide valuable information for the future design of the GSHP system, as well as for predicting the efficiency of solar- and DWHR-assisted GSHPs in the coming years.

In addition, initial cost of renewable resources is not considered in this research. The payback of the GSHP system and the integrated heating system will be estimated after taking into account the initial costs, such as material cost, installation cost, and maintenance cost.

Thirdly, the percentage of energy production from the solar energy system and DWHR system will also be clarified, which will support subsequent source-side design by engineers of the heat pump based on cold-climate heating demands. The annual heating load from the boiler under the current system operation (i.e., boiler works when outside temperature drops to -20°C) can be calculated. An annual comparison between electricity and natural gas will be achieved as well.

Finally, through annual data analysis, more accurate and proper improvement of the existing control algorithm can be developed and further implemented to the existing control system one accepted by mechanical engineers. Under this circumstance, the effectiveness of the research results will be validated.

References

Al-Khoury, R. (2012). "Computational modeling of shallow geothermal systems." CRD Press/Balkema.

Aikins, K.A. and Choi, J.M. (2012). "Current status of the performance of GSHP (ground source heat pump) units in the Republic of Korea." *Energy*, 47, 77-82.

Atmospheric Science Data Center (2008). "Surface meteorology and solar energy." https://eosweb.larc.nasa.gov/sse/RETScreen/ (Accessed Apr., 2013).

Akpan, I.E., Sasaki, M., and Endoh, N. (2006). "Optimization of domestic size renewable energy system design suitable for cold climate regions." *Japan Society of Mechanical Engineers (JSME) International Journal Series B*, 29(4), 1241-1252.

Banks, D. (2008). "An Introduction to Thermogeology: Ground Source Heating and Cooling". Blackwell Publishing, Oxford, UK.

Bakirci, K. and Colak, D. (2012). "Effect of a super heating and sub-cooling heat exchanger to the performance of a ground source heat pump system." *Energy*, 44, 996-1004.

Bakirci, K., Ozyurt, O., Comakli, K., and Comakli, O. (2011). "Energy analysis of a solar-ground source heat pump system with vertical closed-loop for heating applications." *Energy*, 36, 3223-3232.

Cormode & Dickson (2013). "Featured project - Stony Mountain Plaza." http://www.cormode.com/featured-projects/project/stony-mountain-plaza/ (Accessed Jun., 2013).

Cooperman, A., Dieckmann, J., and Brodrick, J. (2011). "Drain water heat recovery." *ASHRAE Journal*, 53(11), 58-64.

Cooperman, A., Dieckmann, J., and Brodrick, J. (2012). "Residential GSHPs." *ASHRAE Journal*, 72-79.

Canadian GeoExchange Coalition (2012). "Geothermal Energy". http://www.geo-exchange.ca/en/ (Accessed Mar., 2013).

Canadian Geothermal Energy Association (2012). "Geothermal energy." http://www.cangea.ca/geothermal-energy/ (Accessed May, 2013).

Chen, X., Lu, L., and Yang, H. (2011). "Long term operation of a solar assisted ground coupled heat pump system for space heating and domestic hot water." *Energy and Buildings*, 43, 1835-1844.

Canadian Natural Gas, "Natural gas use-electricity". http://www.canadiannaturalgas.ca/natural-gas-use/electricity (Accessed Jun., 2013).

Choi, J.C., Park, J., and Lee, S.R. (2013). "Numerical evaluation of the effects of groundwater flow on borehole heat exchanger arrays." *Renewable Energy*, 52, 230-240.

Chen, X. and Yang, H. (2012). "Performance analysis of a proposed solar assisted ground coupled heat pump system." *Applied Energy*, 97, 888-896.

Direct Energy (2013). "Alberta natural gas and electricity plans." http://residential.directenergy.com/EN/Energy/alberta/Pages/Dereg/ELE/Energy-Products-Electricity.aspx (Accessed May, 2013).

Desideri, U., Sorbi, N., Arcioni, L., and Leonardi, D. (2011). "Feasibility study and numerical simulation of a ground source heat pump plant, applied to a residential building." *Applied Thermal Engineering*, 31, 3500-3511.

Energy Efficiency & Renewable Energy, "Geothermal heat pumps." http://www.energysavers.gov/your_home/space_heating_cooling/index.cfm/mytopic=12640 (Accessed Apr., 2012).

Eco Innovation, "Thermo Drain residential solution", http://www.ecoinnovation.ca/residential-solutions/ (Accessed May, 2012).

Gas Alberta Inc. (2013). "Current AECO C (wholesale) prices for Alberta delivery." http://www.gasalberta.com/pricing-market.htm (Accessed May, 2013).

Geothermal Heat Pump Consortium, Inc. Ground water source (open loop) heat pump systems, http://bge.apogee.net/ces/library/tcwshp.asp (Accessed Apr., 2012).

Geothermal Heat Pump Consortium, Inc. Ground-coupled (closed-loop) systems, http://bge.apogee.net/ces/library/cchl.asp (Accessed Apr., 2012).

Geothermal Heat Pump Design Manual, Application guide, AG31-008, Staunton, VA, USA.

Gerber, L. and Maréchal, F. (2011). "Defining optimal configurations of geothermal systems using process design and process integration techniques." *Applied Thermal Engineering*, 43, 29-41.

Hepbasli, A., Akdemir, O., and Hancioglu, E. (2003). "Experimental study of a closed loop vertical ground source heat pump system." *Energy Conversion and Management*, 44, 527-548.

Hepbasli, A. and Balta, M.T. (2007). "A study on modeling and performance assessment of a heat pump system for utilizing low temperature geothermal resources in buildings." *Building and Environment*, 42, 3747-3756.

Heat pump technology (2013). "Ground Source Heating & Hot Water System Design." http://www.icsheatpumps.co.uk/residential/system_design_ground_source.php (Accessed May, 2013).

ICAX international Heat Transfer, "Ground Source Heat Pump", http://www.icax.co.uk/gshp.html (Accessed May, 2012).

International Ground Source Heat Pump Association (2009). "Ground Source Heat Pump Residential and Light Commercial Design and Installation Guide." Oklahoma State University, Engineering Technology, Stillwater, OK, USA.

International Ground Source Heat Pump Association (2012). "Ground Source Heat Pump." http://www.igshpa.cn/htdocs/pages.asp?id=12 (Accessed Apr., 2012).

Kittel, C. and Kroemer, H. (1980). *Thermal Physics*, second ed., W.H. Freeman, San Francisco, CA, USA, ISBN 0-7167-1088-9, pp. 49.

Kim, E., Lee, J., Jeong, Y., Hwang, Y., Lee, S., and Park, N. (2012). "Performance evaluation under the actual operating condition of a vertical ground source heat pump system in a school building." *Energy and Buildings*, 50, 1-6.

Kim, U.S., Park, T.C., Kim, L.H., Kim, W.H., and Yeo, Y.K. (2009). "Optimization of the heat plant of district energy systems." *Korean Journal of Chemical Engineering*, 26(4), 955-962.

Lam, H.L. and Jones, F.W. (1984). "Geothermal gradients of Alberta in Western Canada." *Geothermics*, 13(3), 181-192.

Lee, C.K. (2011). "Effects of multiple ground layers on thermal response test analysis and ground-source heat pump simulation." *Applied Energy*, 88, 4405-4410.

Lund, J.W. and Bertani, R. (2010). "Worldwide geothermal utilization 2010." *Proceedings, Geothermal Resources Council Annual Meeting*, 34(1), 182-185.

Lund, J.W. and Freeston, D.H. (2001). "World-wide direct uses of geothermal energy 2000." *Geothermics*, 30, 29-68.

Lund, J.W., Freeston, D.H., and Boyd, T.L. (2005). "Direct application of geothermal energy: 2005 worldwide review." *Geothermics*, 34, 691-727.

Li, X., Sharmin, T., Gökçe, H. U., Gül, M., Al-Hussein, M., and Morrow, D. (2012). "An integrated monitoring framework for geothermal space-heating systems in residential buildings, Fort McMurray." *Proceedings, 11th International Conference on Sustainable Energy Technologies*, Vancouver, BC, Canada, Sep. 2-5.

Metz, P.D. (1982). "The use of ground-coupled tanks in solar-assisted heat-pump systems." *Solar Energy Engineering*, 104(4), 366-72.

Natural Resources Canada (2013). "Energy resources." http://www.nrcan.gc.ca/energy/sources/1330 (Accessed Jun., 2013).

Natural Resources Canada (2012a). "Earth energy, ground-source/geothermal heat pumps, geoexchange." http://www.nrcan.gc.ca/home/ (Accessed May, 2012).

Natural Resources Canada (2012b). "Drain water heat recovery". http://www.nrcan.gc.ca/science/expert/video/3668 (Accessed Jun., 2012).

Natural Resources Canada. (2009) "About renewable energy". http://www.nrcan.gc.ca/energy/renewable/1297 (Accessed May, 2013).

Niu, F., Ni, L., Yao, Y., Jiang, Y., and Ma, Z. (2011). "Thermal accumulation effect of ground-coupled heat pump system." *Proceedings, International Conference on Electric Technology and Civil Engineering*, Lushan, China, Apr. 22-24, 1805-1807.

Ochsner, K. (2008). "Geothermal Heat Pump-A Guide for Planning and Installing." Earthscan, London Sterling, VA, UK.

Omojaro, P. and Breitkopf, C. (2013), "Direct expansion solar assisted heat pumps: A review of applications and recent research." *Renewable and Sustainable Energy Reviews*, 22, 33-45.

Ozgener, O. and Hepbasli, A. (2007). "A review on the energy and exergy analysis of solar assisted heat pump systems." *Renewable & Sustainable Energy Reviews*, 11, 482-496.

Picard, D., Delisle, V., Bernier, M., and Kummert, M. (2004), "On the combined effect of wastewater heat recovery and solar domestic hot water heating." *Proceedings, Canadian Solar Buildings Conference*, Montréal, QC, Canada, Aug. 20-24.

Roth, K., Dieckmann, J., and Brodrick, J. (2009). "Heat pumps for cold climates." *ASHRAE Journal*.

Ratlamwala, T.A.H., Dincer, I., and Gadalla, M.A. (2012). "Performance analysis of a novel integrated geothermal-based system for multi-generation applications." *Applied Thermal Engineering*, 40, 71-79.

Ran, C., Wang, Z., and Zhang, L. (2012). "The solar assisted ground-source heat pump heating applied research of cold regions." *Advanced Materials Research*, vols. 424-425, 844-847.

SaskEnergy (2012). "Discover how DWHR System can improve your home energy." http://www.saskenergy.com/saving_energy/drainwaterheatrecovery.asp (Accessed May, 2012).

Skouby, A. (2010). "Closed-Loop/Geothermal Heat Pump Systems." *Design and Installation Standards*. International Ground Source Heat Pump Association.

Statistics Canada (2012). "Households and the Environment: Energy Use". http://www.statcan.gc.ca/pub/11-526-s/2010001/part-partie1-eng.htm (Accessed Jun., 2013).

Sharmin, T., Li, X., Gökçe, H. U., Al-Hussein, M., and Gül, M. (2012). "Monitoring building energy performance under occupancy in Fort McMurray, Alberta." *Proceedings, 11th International Conference on Sustainable Energy Technologies*, Vancouver, BC, Canada, Sep. 2-5.

Stein, R.S. and Powers, J. (2011). "The Energy Problem." World scientific Publishing Co. Pte. Ltd.

The Geoexchanger, "Installing the geothermal heat pump". http://www.thegeoexchange.org/installation/index.html (Accessed May, 2012).

The Globe and Mail, "Wind power sails on despite local buffeting", http://www.theglobeandmail.com/report-on-business/industry-news/energy-and-resources/wind-power-sails-on-despite-local-buffeting/article2330974/?%20Resources (Accessed Jul., 2013).

U.S. Energy Information Administration, "Country Analysis Brief: Canada." http://www.eia.gov/404r.cfm?v=http://www.eia.gov/emeu/cabs/canada/oil.html (Accessed Oct., 2007).

Water Encyclopedia (2013). "Hydroelectric Power", http://www.waterencyclopedia.com/Ge-Hy/Hydroelectric-Power.html (Accessed Jul., 2013).

Wang, E., Fung, A.S., Qi, C., and Leong, W.H. (2012). "Performance prediction of hybrid solar ground-source heat pump system." *Energy and Buildings*, 47, 600-611.

Wood CJ, Liu H, and Riffat, S.B. (2010). "An investigation of the heat pump performance and ground temperature of a piled foundation heat exchanger system for a residential building." *Energy*, 35, 4932-4940.

Wu, W., Wang, B., You. T., Shi, W., and Li, X. (2013). "A potential solution for thermal imbalance of ground source heat pump systems in cold regions: Ground source absorption heat pump." *Renewable Energy*, 59, 39-48.

Yao, C. and Hao, B. (2012). "Ground-source heat pump performance analysis based on building-integrated renewable energy demonstration projects." *Advanced Materials Research*, vol. 354-355, 766-722.

Yang, H., Cui, P., and Fang, Z. (2010). "Vertical-borehole ground-coupled heat pumps: A review of models and systems." *Applied Energy*, 87, 16-27.

Zhai, X.Q., Qu, M., Yu, X., Yang, Y., and Wang, R.Z. (2011). "A review for the applications and integrated approaches of ground-coupled heat pump systems." *Renewable and Sustainable Energy Reviews*, 15, 3133-3140.

Appendices:

A: System Schematic from Project Mechanical Drawings
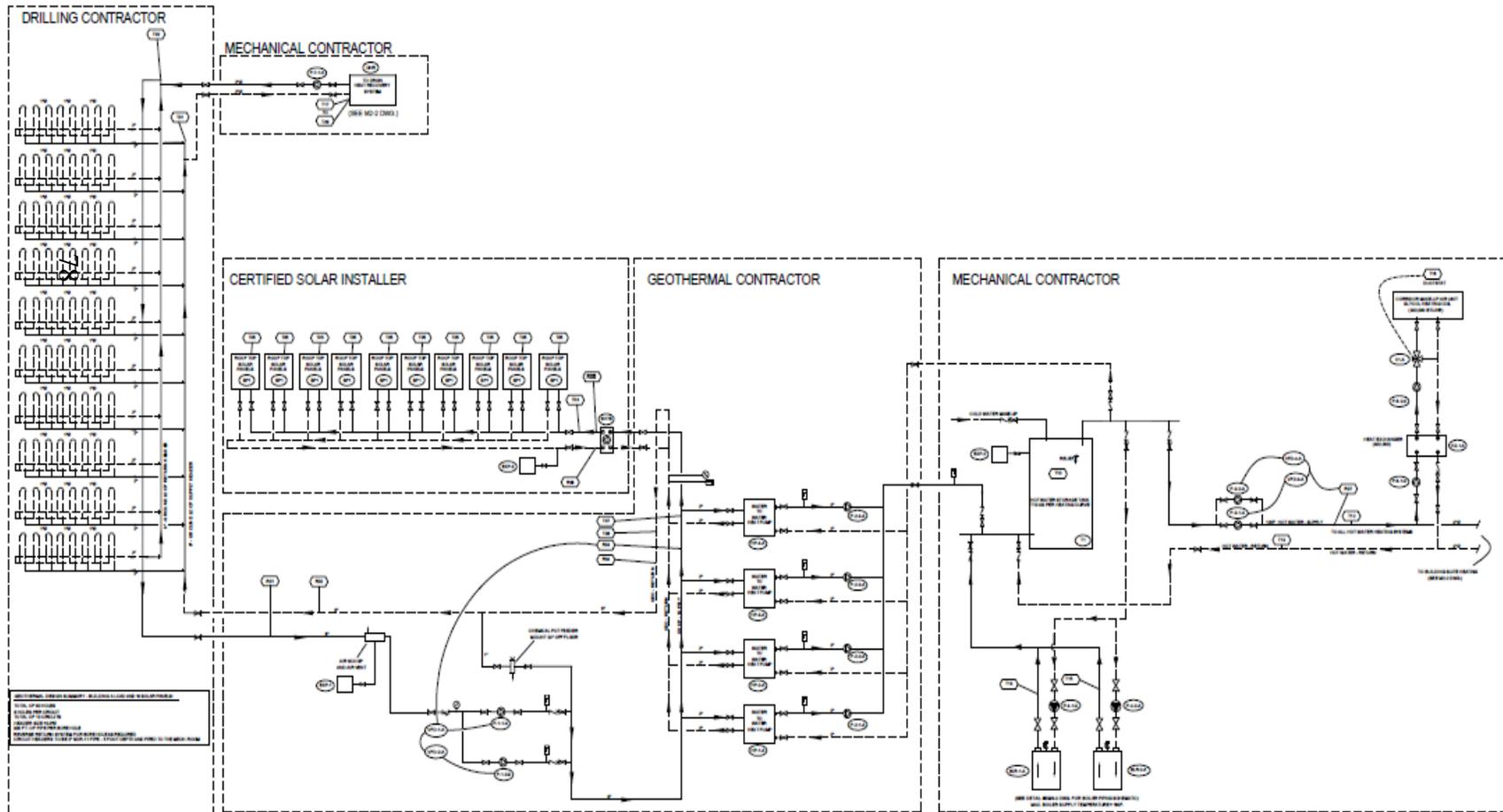
B: Description of Equipment Tags for Figure 14

HEATING SYSTEM EQUIPMENT SCHEDULE	
TAG	**DESCRIPTION**
P-1-1-A	LOOP FIELD CIRCULATING PUMP # 1-1-A
P-1-2-A	LOOP FIELD CIRCULATING PUMP # 1-2-A
P-2-1-A	WATER TO WATER CIRCULATING PUMP - HEATING WATER
P-2-2-A	WATER TO WATER CIRCULATING PUMP - HEATING WATER
P-2-3-A	WATER TO WATER CIRCULATING PUMP - HEATING WATER
P-2-4-A	WATER TO WATER CIRCULATING PUMP - HEATING WATER
P-3-1-A	HEATING SYSTEM CIRCULATING PUMP
P-3-2-A	HEATING SYSTEM CIRCULATING PUMP
P-4-1-A	BOILER #1 CIRCULATION PUMP
P-4-2-A	BOILER #2 CIRCULATION PUMP
P5	N/A
P-6-1-A	HX-1 WATER SIDE CIRCULATION PUMP
P-6-2-A	HX-1 GLYCOL SIDE CIRCULATION PUMP
P-7-1-A	DRAIN HEAT RECOVERY CIRCULATION PUMP
BLR-1-A	BOILER 1
BLR-2-A	BOILER2
EXP-1	EXPANSION TANK #1
EXP-2	EXPANSION TANK #2
EXP-3	EXPANSION TANK #3

HEATING SYSTEM CONTROL POINTS	
TAG	**DESCRIPTION**
T01	TEMPERATURE - GROUND LOOP SUPPLY
T02	TEMPERATURE - GROUND LOOP RETURN
T03	TEMPERATURE - SOLAR PANEL LOOP SUPPLY
T04	OUTSIDE AIR TEMPERATURE
T05	TEMPERATURE - SOLAR PANELS
T06	N/A
T07	TEMPERATURE - GEO BUILDING LOOP SUPPLY
T08	TEMPERATURE - GEO BUILDING LOOP RETURN
T09	N/A
T10	TEMPERATURE - HEATING WATER TANK
T11	N/A
T12	TEMPERATURE - HEATING LOOP SUPPLY
T13	TEMPERATURE - HEATING LOOP RETURN
T14	TEMPERATURE - BLR-1 SUPPLY
T15	TEMPERATURE - BLR-2 SUPPLY
T16	TEMPERATURE - CORRIDOR MAKE-UP AIR HEATING COIL SUPPLY
T17 TO T29	DWR PIPE TEMPERATURE (12 DHR UNITS)

HEATING SYSTEM EQUIPMENT SCHEDULE	
TAG	DESCRIPTION
HP-1-A	WATER/WATER HEAT PUMP #1
HP-2-A	WATER/WATER HEAT PUMP #2
HP-3-A	WATER/WATER HEAT PUMP #3
HP-4-A	WATER/WATER HEAT PUMP #4
SP1	SOLAR PANEL
VFD-1-A	VARIABLE FREQUENCY DRIVE #1 - FOR PUMP #P-1-1-A
VFD-2-A	VARIABLE FREQUENCY DRIVE #2 - FOR PUMP #P-1-2-A
VFD-3-A	VARIABLE FREQUENCY DRIVE #3 - FOR PUMP #P-3-1-A
VFD-4-A	VARIABLE FREQUENCY DRIVE #4 - FOR PUMP #P-3-2-A
HX-1-A	CORRIDOR MAKE-UP AIR HEAT EXCHANGER
SHTS	SOLAR HEAT TRANSFER STATION
V1-A	3-WAY MODULATING VALVE (MUA GLYCOL HEATING COIL)

HEATING SYSTEM CONTROL POINTS	
TAG	DESCRIPTION
R01	PRESSURE - GROUND LOOP HEADER - RETURN
R02	PRESSURE - GROUND LOOP HEADER - SUPPLY
R03	PRESSURE - GEO BUILDING LOOP SUPPLY
R04	PRESSURE - GEO BUILDING LOOP RETURN
R05	PRESSURE - SOLAR PANEL LOOP SUPPLY
R06	PRESSURE - SOLAR PANEL LOOP RETURN
R07	PRESSURE - HEATING BUILDING LOOP SUPPLY

C: Original Heating System Specification

Mode	Description
Winter / Summer Switchover	The system is in heating mode when outside air temperature is less than 50°F (15°C).
GSHP / Boiler Switchover	Boiler is being used when outside air temperature is less than -10°F (-20°C).
Zone Thermostats	Room Thermostats control the zone valve for the perimeter radiation in each area.
Main Building Geo Loop 82		Building Geo Loop pressure is controlled by pump (P-1). Variable frequency drive (VFD), which controlled by pressure sensor (R03), keeps the loop pressure constant.
Heating Water-Geo Mode		Hot water storage tank temperature is to be maintained as per heating curve. If hot water storage tank temperature drops to set point 40°C, then the heat pump (HP 1-4) is open and pumps (P-2) are ON.
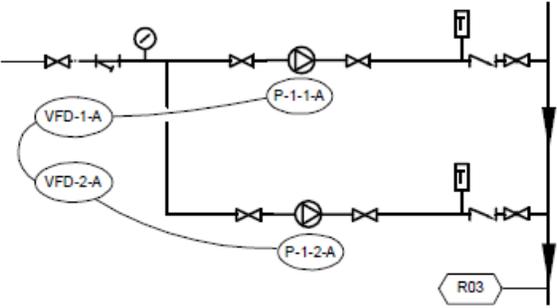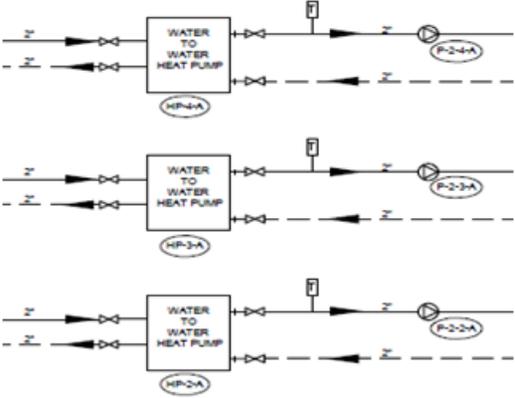
Mode	Description
Heating Water-Boiler Mode 83	(SEE DETAIL #SM9-3 DWG. FOR BOILER PIPING SCHEMATIC) MAX. BOILER SUPPLY TEMPERATURE = 160F.	Hot water storage tank temperature is to be maintained as per heating curve. IF the temperature in the tank drops below set point 40°C, then the boiler system is enabled and pumps P4 are ON.
Solar Panel Control		IF the Building Geo Loop Supply Temperature is less than the Solar Panel Temperature (T05), then pumps in the SHTS are ON (solar transfer to heat).
Solar Panel Freeze Protection		IF Solar Panel Temperature (T05) is less than 35°F (2°C), then pumps in the SHTS (solar heat transfer system) are ON for 20 min.
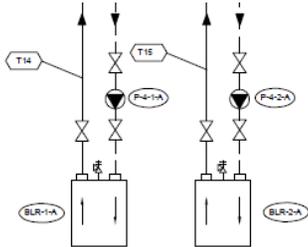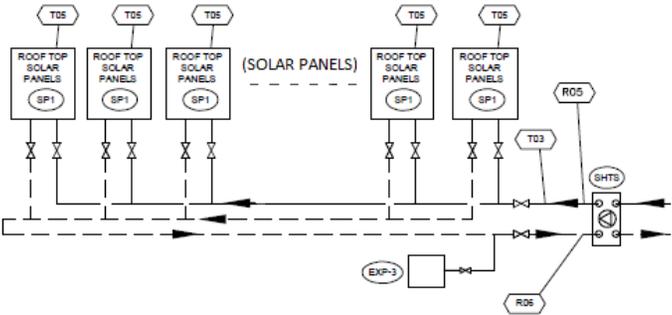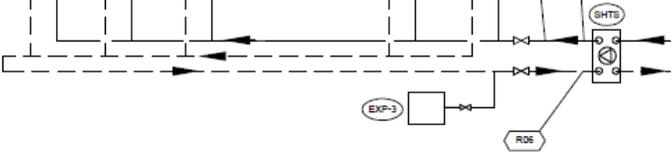
Mode		Description
Drain Water Heat Recovery		Whenever drain water comes, pumps (P-7) are on.
Mode	**Description**	
Main Building Geo Loop over Temperature 84		IF the Building Geo Loop Return Temperature (T08) is greater than 60°F (15°C), then the loop field is shut down and pumps P1 are turned "off".
HotWater Pump Control		In Heating Mode, either Geo or Boiler, the System HotWater pumps (P3) are ON
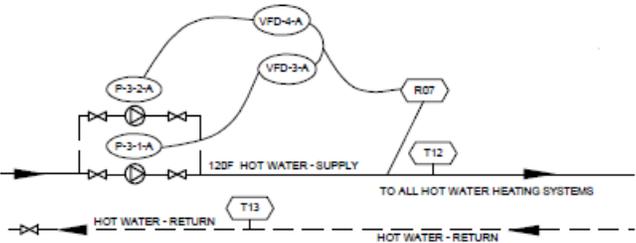
D: SQL code

Detail SQL codes are presented in this section for averaging data by one minute and downloading data from different database.

Temperature data：

```
SELECT CONCAT( YEAR( ts ) , '-', MONTH( ts ) , '-', DAY( ts ) , ' ', HOUR( ts ) ,
':',MINUTE(ts),':00' ) AS time, AVG(`t1`) , AVG(`t2`) , AVG(`t3`) ,
AVG(`t4`),AVG(`t5`),AVG(`t6`),AVG(`t7`),AVG(`t8`),AVG(`t9`),AVG(`t12`),AVG(`t13`)

FROM `bas_temp_extra`

Where ts >= '2013-03-15  00:00:00'

AND ts < '2013-07-04 00:00:00'

GROUP BY YEAR( ts ) , MONTH( ts ) , DAY( ts ) , HOUR( ts ),MINUTE(ts),':00'
```

Flow rate data：

```
SELECT CONCAT( YEAR( ts ) , '-', MONTH( ts ) , '-', DAY( ts ) , ' ', HOUR( ts ) ,
':',MINUTE(ts),':00' ) AS time, AVG(`flow1`) , AVG(`flow2`) , AVG(`flow3`) ,
AVG(`flow4_1`),AVG(`flow4_2`),AVG(`flow5_1`),AVG(`flow5_2`),AVG(`flow5_3`),AVG(`fl
ow5_4`),AVG(`flow6`)

FROM `bas_flows`

Where ts >= '2013-03-15  00:00:00'

AND ts < '2013-07-04 00:00:00'

GROUP BY YEAR( ts ) , MONTH( ts ) , DAY( ts ) , HOUR( ts ),MINUTE(ts),':00'
```

Boiler data:

```
SELECT CONCAT( YEAR( ts ) , '-', MONTH( ts ) , '-', DAY( ts ) , ' ', HOUR( ts ) ,
':',MINUTE(ts),':00' ) AS time, AVG(`BO_Blr_1_Enable`) ,
AVG(`BO_Blr_2_Enable`),AVG(`AI_T14_Blr1_Supply`),AVG(`AI_T15_Blr2_Supply`)

FROM `bas_boiler_loop`

Where ts >= '2013-03-15  00:00:00'
```

AND ts <= '2013-07-04 00:00:00'

GROUP BY YEAR(ts) , MONTH(ts) , DAY(ts) , HOUR(ts),MINUTE(ts),':00'

Geothermal data：

SELECT CONCAT(YEAR(ts) , '-', MONTH(ts) , '-', DAY(ts) , ' ', HOUR(ts) , ':',MINUTE(ts),':00') AS time, AVG(`BO_P1_1_Enab`) , AVG(`BO_P1_2_Enab`) , AVG(`BO_HP_1_Enable`) , AVG(`BO_P2_1_Enable`),AVG(`BO_HP_2_Enable`),AVG(`BO_P2_2_Enable`),AVG(`BO_HP_3_Enable`),AVG(`BO_HP_4_Enable`),AVG(`BO_P2_3_Enable`),AVG(`BO_P2_4_Enable`), AVG(`AV_Tank_10_Setpoint`),AVG(`AV_T10_Temp`),AVG(`AI_T07_Geoloop_supT`),AVG(`AI_T08_Geoloop_retT`),AVG(`AO_P1_1VFD_Cntl`),AVG(`AO_P1_2_VFD_Cntl`)

FROM `bas_geothermal`

Where ts >= '2013-03-15 00:00:00'

AND ts <= '2013-07-04 00:00:00'

GROUP BY YEAR(ts) , MONTH(ts) , DAY(ts) , HOUR(ts),MINUTE(ts),':00'

DWHR data:

SELECT CONCAT(YEAR(ts) , '-', MONTH(ts) , '-', DAY(ts) , ' ', HOUR(ts) , ':',MINUTE(ts),':00') AS time, AVG(`BO_P8_1_DHR_Hx_EN`) , AVG(`BO_P8_2_DHR_Hx_EN`) , AVG(`BO_P8_3_DHR_Hx_EN`) , AVG(`BO_P8_4_DHR_Hx_EN`),AVG(`BO_P8_5_DHR_Hx_EN`),AVG(`BO_P8_7_DHR_Hx_EN`),AVG(`BO_P8_8_DHR_Hx_EN`),AVG(`BO_P8_9_DHR_Hx_EN`),AVG(`BO_P8_10_DHR_Hx_EN`),AVG(`BO_P8_11_DHR_Hx_EN`),AVG(`BO_P8_12_DHR_Hx_EN`),AVG(`BO_P7_1_DHR_Circ_EN`),AVG(`AI_T24_DWR_Temp`),AVG(`AI_T04_Outside_Air`)

FROM `bas_drains`

Where ts >= '2013-03-15 00:00:00'

AND ts <= '2013-07-04 00:00:00'

GROUP BY YEAR(ts) , MONTH(ts) , DAY(ts) , HOUR(ts),MINUTE(ts),':00'

Heating loop:

```
SELECT CONCAT( YEAR( ts ) , '-', MONTH( ts ) , '-', DAY( ts ) , ' ', HOUR( ts ) ,
':',MINUTE(ts),':00' ) AS time,
AVG(`AI_T12_HWS_T`),AVG(`AI_T13_HWR_T`),AVG(`AO_P3_VFD_Ctrl`),AVG(`AO_P3
_2_VFD_Ctrl`)

FROM `bas_heating_loop`

Where ts >= '2013-03-15 00:00:00'

AND ts <= '2013-07-04 00:00:00'

GROUP BY YEAR( ts ) , MONTH( ts ) , DAY( ts ) , HOUR( ts ),MINUTE(ts),':00'
```

Water usage data:

```
SELECT TIME, SUM( hot_water )

FROM (

SELECT FROM_UNIXTIME( FLOOR( (

UNIX_TIMESTAMP( ts ) -14400 ) /86400 ) *86400 +14400

) AS TIME, (

SUM( `hot` )

) AS hot_water

FROM `water_cur`

WHERE ts >= '2013-03-15 00:00:00'

AND ts < '2013-07-04'

AND apt

IN ( 1, 2, 3, 4, 5, 8, 10, 12 )

GROUP BY TIME, apt

) AS hot

GROUP BY TIME
```

Daily hot water tank power consumption data:

```sql
SELECT time, SUM( HWT_energy )
FROM (
   SELECT FROM_UNIXTIME( FLOOR(( UNIX_TIMESTAMP( ts )-14400) /86400 )
*86400+14400 ) AS time,

   apt, 2 * ( MAX( aux4 ) - MIN( aux4 ) ) AS HWT_energy
   FROM `el_energy`
   WHERE ts >= '2013-03-15 00:00:00'
   AND apt IN ( 1, 2, 3, 4, 5, 8, 10, 12 )
   AND phase = 'B'
   GROUP BY time, apt
   ) AS HWT
GROUP BY time
```

Hot water and cold water usage data:

```sql
SELECT ts, SUM( hot ) , SUM( total )
FROM `water_cur`
WHERE apt IN ( 1, 2, 3, 4, 5, 8, 10, 12 )
GROUP BY ts
ORDER BY ts
```

E: Solar Energy Production Forecasting

	Historical Radiation (kWh/m^2/day)	Historical Outside Temperature (°C)	Area (m^2)	Days	Q_daily (GJ/day)	Energy wasted percentage (%)	Efficiency factor	Predicted Monthly Production (GJ)
Jan	0.77	-19.80	28.7	31	0.08	31.99		0.70
Feb	1.81	-14.90	28.7	28	0.19	25.18		1.56
Mar	3.45	-7.90	28.7	31	0.36	16.82		3.54
Apr	4.82	2.80	28.7	30	0.50	12.06	0.31	4.16
May	5.53	10.10	28.7	31	0.57	0.16	0.45	8.04
Jun	5.84	14.60	28.7	30	0.60	0.00	0.36	6.45
Jul	5.63	16.60	28.7	31	0.58	0.21		6.73
Aug	4.66	15.20	28.7	31	0.48	0.63		5.54
Sep	3.02	9.10	28.7	30	0.31	3.20		3.39
Oct	1.79	3.30	28.7	31	0.18	6.78		2.01
Nev	0.87	-9.00	28.7	30	0.09	18.03		0.85
Dec	0.55	-17.30	28.7	31	0.06	28.42		0.51

F: Detail Calculations Results (weekly)

Power Usage Weekly Calculations:

PART 1: by subtraction (Data in 'bas_el_energy' is cumulative. Power usage in a specific time period = data at end time - data at start time)											
System	Name	From	Start date	End date	Power usage	Start date	End date	Power usage	Start date	End date	Power usage
			15/03/2013 0:00	21/03/2013 23:59	kwh	22/03/2013 0:00	28/03/2013 23:59	kwh	29/03/2013 0:00	04/04/2013 23:59	kwh
Geo field	P1-1	bas_el_energy: P-1-1	89444259	1236833034	319	1236833034	2369209878	315	2369209878	3513466902	318
Geo field	P1-2	bas_el_energy: P-1-2	72514686	1213751577	317	1213751577	2336403984	312	2336403984	3473599551	316
Heat pumps	HP-1	bas_el_energy: HP1	8265735	21430965	4	21430965	34782693	4	34782693	989247504	265
	HP-2	bas_el_energy: HP2	6685455	15721887	3	15721887	24449358	2	24449358	32738838	2
	HP-3	bas_el_energy: HP3	302088552	5185699422	1357	5185699422	11775453765	1830	11775453765	13093266021	366
	HP-4	bas_el_energy: HP4	207079311	2900525670	748	2900525670	4804787196	529	4804787196	10200092715	1499

System	Name	From	Start date	End date	Power usage	Start date	End date	Power usage	Start date	End date	Power usage
			05/04/2013 0:00	11/04/2013 23:59	kwh	12/04/2013 0:00	18/04/2013 23:59	kwh	19/04/2013 0:00	25/04/2013 23:59	kwh
Geo field	P1-1	bas_el_energy: P-1-1	3513466902	4659238551	318	4659238551	5802297408	318	5802297408	6937554813	315
Geo field	P1-2	bas_el_energy: P-1-2	3473599551	4611881670	316	4611881670	5748881136	316	5748881136	6874510764	313
Heat pumps	HP-1	bas_el_energy: HP1	989247504	1810837869	228	1810837869	3081338823	353	3081338823	6352232115	909
	HP-2	bas_el_energy: HP2	32738838	40208487	2	40208487	48268314	2	48268314	55246803	2
	HP-3	bas_el_energy: HP3	13093266021	13098262824	1	13098262824	13104643503	2	13104643503	13109158191	1
	HP-4	bas_el_energy: HP4	10200092715	16456256718	1738	16456256718	22290500706	1621	22290500706	29675309220	2051

System	Name	From	Start date	End date	Power usage	Start date	End date	Power usage	Start date	End date	Power usage
			26/04/2013 0:00	02/05/2013 23:59	kwh	03/05/2013 0:00	09/05/2013 23:59	kwh	10/05/2013 0:00	16/05/2013 23:59	kwh
Geo field	P1-1	bas_el_energy: P-1-1	6937554813	8067824886	314	8067824886	9196921023	314	9196921023	9945423288	208
Geo field	P1-2	bas_el_energy: P-1-2	6874510764	7991028045	310	7991028045	9107311641	310	9107311641	10244184612	316
Heat pumps	HP-1	bas_el_energy: HP1	6352232115	11523707439	1437	11523707439	15379225188	1071	15379225188	18222843693	790
	HP-2	bas_el_energy: HP2	55246803	2237549472	606	2237549472	3140294493	251	3140294493	3675847335	149
	HP-3	bas_el_energy: HP3	13109158191	13197902541	25	13197902541	13427061477	64	13427061477	13644680181	60
	HP-4	bas_el_energy: HP4	29675309220	33024261471	930	33024261471	33194258103	47	33194258103	33331358145	38

System	Name	From	Start date 17/05/2013 0:00	End date 23/05/2013 23:59	Power usage kwh	Start date 24/05/2013 0:00	End date 30/05/2013 23:59	Power usage kwh	Start date 31/05/2013 0:00	End date 06/06/2013 23:59	Power usage kwh
Geo field	P1-1	bas_el_energy：P-1-1	9945423288	10852960311	252	10852960311	11982400167	314	11982400167	13116774252	315
	P1-2	bas_el_energy：P-1-2	10244184612	11381716692	316	11381716692	12494386920	309	12494386920	13611675144	310
Heat pumps	HP-1	bas_el_energy：HP1	18222843693	19394915841	326	19394915841	20620493034	340	20620493034	20791015779	47
	HP-2	bas_el_energy：HP2	3675847335	3930527688	71	3930527688	4280197446	97	4280197446	5243920059	268
	HP-3	bas_el_energy：HP3	13644680181	13853408862	58	13853408862	14082644817	64	14082644817	14416928688	93
	HP-4	bas_el_energy：HP4	33331358145	33493533255	45	33493533255	33667803243	48	33667803243	33932087799	73

System	Name	From	Start date 07/06/2013 0:00	End date 13/06/2013 23:59	Power usage kwh	Start date 14/06/2013 0:00	End date 20/06/2013 23:59	Power usage kwh	Total
Geo field	P1-1	bas_el_energy：P-1-1	13116774252	14087209065	270	14087209065	15383522796	360	4248
	P1-2	bas_el_energy：P-1-2	13611675144	14569934109	266	14569934109	15847711158	355	4382
Heat pumps	HP-1	bas_el_energy：HP1	20791015779	20870467119	22	20870467119	21003840591	37	5832
	HP-2	bas_el_energy：HP2	5243920059	8341193370	860	8341193370	9508109322	324	2639
	HP-3	bas_el_energy：HP3	14416928688	14549557608	37	14549557608	14833904721	79	4037
	HP-4	bas_el_energy：HP4	33932087799	34040799303	30	34040799303	34256560272	60	9458

			1st week			2nd week			3rd week		
System	**Name**	**Power**	**Status**	**Power usage(kwh)**	**Subtotal**	**Status**	**Power usage(kwh)**	**Subtotal**	**Status**	**Power usage(kwh)**	**Subtotal**
Solar	SHTS	111.55	1.00	18.74	19	1.00	18.74	18.74	1.00	18.74	18.74
DWHR	P7-1	714	1.00	119.95	260.11	1.00	119.95	260.14	1.00	119.95	260.12
	on stack	75.9	10.99	140.16		10.99	140.18		10.99	140.16	
Heat pumps_cir	P2-1	785	0.00	0.00	83.59	0.00	0.00	91.66	0.10	13.72	85.37
	P2-2	785	0.00	0.00		0.00	0.00		0.00	0.00	
	P2-3	785	0.40	53.16		0.54	71.87		0.03	4.56	
	P2-4	785	0.23	30.44		0.15	19.79		0.51	67.09	
Boilers	P4-1	870	0.31	45.20	107.17	0.00	0.00	0.00	0.00	0.00	0.00
	P4-2	870	0.23	32.89		0.00	0.00		0.00	0.00	
	BLR-1	324	0.31	16.83		0.00	0.00		0.00	0.00	
	BLR-2	324	0.23	12.25		0.00	0.00		0.00	0.00	
Heating loop	P3-1	2460	0.82	337.51	675.04	0.82	337.32	674.65	0.81	335.73	671.46
	P3-2	2460	0.82	337.53		0.82	337.32		0.81	335.73	

			4th week			5th week			6th week		
System	**Name**	**Power**	**Status**	**Power usage(kwh)**	**Subtotal**	**Status**	**Power usage(kwh)**	**Subtotal**	**Status**	**Power usage(kwh)**	**Subtotal**
Solar	SHTS	111.55	1.00	18.74	18.74	1.00	18.74	18.74	1.00	18.74	18.74
DWHR	P7-1	714	1.00	119.95	260.17	1.00	119.95	260.13	1.00	119.95	260.11
	on stack	75.9	11.00	140.22		10.99	140.18		10.99	140.16	
Heat pumps_cir	P2-1	785	0.08	10.51	77.66	0.12	15.61	78.61	0.29	38.65	116.93
	P2-2	785	0.00	0.00		0.00	0.00		0.00	0.00	
	P2-3	785	0.00	0.00		0.00	0.00		0.00	0.00	
	P2-4	785	0.51	67.14		0.48	63.00		0.59	78.29	
Boilers	P4-1	870	0.00	0.00	0.00	0.00	0.00	0.00	0.00	0.00	0.00
	P4-2	870	0.00	0.00		0.00	0.00		0.00	0.00	
	BLR-1	324	0.00	0.00		0.00	0.00		0.00	0.00	
	BLR-2	324	0.00	0.00		0.00	0.00		0.00	0.00	
Heating loop	P3-1	2460	0.84	347.16	694.32	0.80	331.16	662.31	0.80	329.58	659.17
	P3-2	2460	0.84	347.16		0.80	331.16		0.80	329.58	

PART 2: by calculation

System	Name	Power	7th week			8th week			9th week		
			Status	Power usage(kwh)	Subtotal	Status	Power usage(kwh)	Subtotal	Status	Power usage(kwh)	Subtotal
Solar	SHTS	111.55	1.00	18.74	18.74	1.00	18.74	18.74	1.00	18.74	18.74
DWHR	P7-1	714	1.00	119.95	260.10	1.00	119.95	260.11	1.00	119.95	260.05
	on stack	75.9	10.99	140.14		10.99	140.16		10.99	140.10	
Heat pumps_cir	P2-1	785	0.44	58.17	120.00	0.33	43.15	58.74	0.24	32.13	42.38
	P2-2	785	0.19	25.25		0.09	11.33		0.05	6.44	
	P2-3	785	0.01	0.98		0.02	2.45		0.02	2.37	
	P2-4	785	0.27	35.60		0.01	1.80		0.01	1.45	
Boilers	P4-1	870	0.00	0.00	0.00	0.00	0.00	0.00	0.00	0.00	0.00
	P4-2	870	0.00	0.00		0.00	0.00		0.00	0.00	
	BLR-1	324	0.00	0.00		0.00	0.00		0.00	0.00	
	BLR-2	324	0.00	0.00		0.00	0.00		0.00	0.00	
Heating loop	P3-1	2460	0.76	313.47	626.94	0.82	337.51	675.04	0.82	338.11	676.23
	P3-2	2460	0.76	313.47		0.82	337.53		0.82	338.11	

System	Name	Power	10th week			11th week			12th week		
			Status	Power usage(kwh)	Subtotal	Status	Power usage(kwh)	Subtotal	Status	Power usage(kwh)	Subtotal
Solar	SHTS	111.55	1.00	18.74	18.74	1.00	18.74	18.74	1.00	18.74	18.74
DWHR	P7-1	714	1.00	119.95	259.61	1.00	119.95	260.03	1.00	119.95	259.84
	on stack	75.9	10.95	139.66		10.99	140.08		10.97	139.89	
Heat pumps_cir	P2-1	785	0.10	13.40	20.28	0.11	14.08	22.34	0.01	1.89	19.36
	P2-2	785	0.02	2.86		0.03	3.94		0.08	11.18	
	P2-3	785	0.02	2.28		0.02	2.46		0.03	3.52	
	P2-4	785	0.01	1.73		0.01	1.86		0.02	2.76	
Boilers	P4-1	870	0.00	0.00	0.00	0.00	0.00	0.00	0.00	0.00	0.00
	P4-2	870	0.00	0.00		0.00	0.00		0.00	0.00	
	BLR-1	324	0.00	0.00		0.00	0.00		0.00	0.00	
	BLR-2	324	0.00	0.00		0.00	0.00		0.00	0.00	
Heating loop	P3-1	2460	0.81	335.17	670.33	0.84	347.16	694.32	0.80	331.16	662.31
	P3-2	2460	0.81	335.17		0.84	347.16		0.80	331.16	

System	Name	Power	13th week			14th week			15th week		
			Status	Power usage(kwh)	Subtotal	Status	Power usage(kwh)	Subtotal	Status	Power usage(kwh)	Subtotal
Solar	SHTS	111.55	1.00	18.74	18.74	1.00	18.74	18.74	1.00	18.74	18.74
DWHR	P7-1	714	1.00	119.95	260.14	1.00	119.95	259.37	1.00	119.95	259.02
	on stack	75.9	10.99	140.18		10.93	139.42		10.91	139.07	
Heat pumps_cir	P2-1	785	0.01	0.82	40.24	0.01	1.42	18.76	0.01	1.63	15.64
	P2-2	785	0.28	36.99		0.09	12.17		0.07	8.63	
	P2-3	785	0.01	1.37		0.02	2.93		0.02	3.23	
	P2-4	785	0.01	1.06		0.02	2.24		0.02	2.15	
Boilers	P4-1	870	0.00	0.00	0.00	0.00	0.00	0.00	0.00	0.00	0.00
	P4-2	870	0.00	0.00		0.00	0.00		0.00	0.00	
	BLR-1	324	0.00	0.00		0.00	0.00		0.00	0.00	
	BLR-2	324	0.00	0.00		0.00	0.00		0.00	0.00	
Heating loop	P3-1	2460	0.80	329.58	659.17	0.76	313.47	626.94	0.52	213.64	427.27
	P3-2	2460	0.80	329.58		0.76	313.47		0.52	213.64	

System	Name	Power	16th week		
			Status	Power usage(kwh)	Subtotal
Solar	SHTS	111.55	1.00	18.74	18.74
DWHR	P7-1	714	1.00	119.95	259.12
	on stack	75.9	10.91	139.17	
Heat pumps _cir	P2-1	785	0.01	1.23	5.85
	P2-2	785	0.01	1.52	
	P2-3	785	0.01	1.65	
	P2-4	785	0.01	1.46	
Boilers	P4-1	870	0.00	0.00	0.00
	P4-2	870	0.00	0.00	
	BLR-1	324	0.00	0.00	
	BLR-2	324	0.00	0.00	
Heating loop	P3-1	2460	0.45	187.11	374.23
	P3-2	2460	0.45	187.11	

Electricity Consumption Summary:

95	1st week(kwh)	2nd week(kwh)	3rd week(kwh)	4th week(kwh)	5th week(kwh)	6th week(kwh)	7th week(kwh)	8th week(kwh)	9th week(kwh)	10th week(kwh)
Electricity usage (solar)	19	19	19	19	19	19	19	19	19	19
Electricity usage (DWHR)	260	260	260	260	260	260	260	260	260	260
Electricity usage (HPs)	2111	2366	2132	1970	1978	2963	2998	1433	1037	499

	11th week(kwh)	12th week(kwh)	13th week(kwh)	14th week(kwh)	15th week(kwh)	16th week(kwh)	Total			
Electricity usage (solar)	19	19	19	19	19	19	300			
Electricity usage (DWHR)	260	260	260	259	259	259	4158			
Electricity usage (HPs)	550	481	949	500	389	156	22511			

Energy Production Calculations:

Systems	1st week(GJ)	2nd week(GJ)	3rd week(GJ)	4th week(GJ)	5th week(GJ)	6th week(GJ)	7th week(GJ)	8th week(GJ)	9th week(GJ)	10th week(GJ)
Solar	0.5	1.2	1.2	0.7	1.2	1.0	1.0	1.5	1.8	2.1
solar-revise	0.6	1.4	1.2	0.9	1.4	1.0	1.1	1.5	1.8	2.1
DWHR	6.9	6.6	7.6	6.2	7.0	6.9	6.7	5.6	6.4	5.6
GHE	4.3	5.1	2.7	3.7	2.5	8.2	8.5	0.2	-3.3	-5.6
Heat Pumps	19.28	21.53	19.09	17.75	17.82	26.74	26.96	12.42	8.65	3.85
Boilers 1&2	16.41	0.00	0.00	0.00	0.00	0.00	0.00	0.00	0.00	0.00
	11.92	0.00	0.00	0.00	0.00	0.00	0.00	0.00	0.00	0.00

Systems	11th week(GJ)	12th week(GJ)	13th week(GJ)	14th week(GJ)	15th week(GJ)	16th week(GJ)	Total
Solar	1.9	2.0	0.8	1.7	1.5	2.0	22.0
solar-revise	1.9	2.0	0.8	1.7	1.5	2.0	22.8
DWHR	5.9	5.7	5.0	3.8	3.4	3.7	93.0
GHE	-5.4	-5.8	0.6	-4.2	-2.9	-5.0	3.7
Heat Pumps	4.37	3.65	9.78	3.11	3.45	1.28	199.7
Boilers 1&2	0.00	0.00	-0.59	-1.38	0.00	0.00	25.06
	0.00	0.00	-0.39	-0.90	0.00	0.00	

	3.15-3.21, 2013	3.22-3.28, 2013	3.29 -4.4, 2013	4.5-4.11, 2013	4.12-4.18, 2013	4.19-4.25, 2013	4.26-5.2, 2013	5.3-5.9, 2013	5.10-5.16, 2013	5.17-5.23, 2013
Renewable (Solar+DWHR+GHE)	12.27	14.38	12.66	11.58	12.08	17.12	17.23	8.72	6.70	4.12
Paid (Electricity)	7.60	8.52	7.68	7.09	7.12	10.67	10.79	5.16	3.73	1.80
Paid (Natural Gas)	28.33	0.00	0.00	0.00	0.00	0.00	0.00	0.00	0.00	0.00
Outside Temperature	-14.57	-4.08	-2.09	-4.24	2.40	1.80	1.29	11.37	13.57	19.46
	5.24-5.30, 2013	**5.31-6.6, 2013**	**6.7-6.13, 2013**	**6.14-6.20, 2013**	**6.21-6.27, 2013**	**6.28-7.04, 2013**	**Total**			
Renewable (Solar+DWHR+GHE)	4.29	3.93	7.18	3.03	3.50	2.70	141.49			
Paid (Electricity)	1.98	1.73	3.42	1.80	1.40	0.56	81.04			
Paid (Natural Gas)	0.00	0.00	-0.98	-2.28	0.00	0.00	25.06			
Outside Temperature	9.79	19.82	13.12	19.39	19.31	24.77				

97

COP and Improvement:

	1st week	2nd week	3rd week	4th week	5th week	6th week	7th week	8th week	9th week	10th week
COP of solar	7.1	18.5	17.1	11.1	18.4	14.2	14.6	21.6	26.4	30.5
solar-revise	8.7	20.3	18.4	13.7	20.4	15.5	15.6	21.6	26.5	30.5
COP of DWHR	7.3	7.1	8.1	6.7	7.4	7.3	7.2	6.0	6.9	6.0
DWHR_revise	17.4	18.2	19.3	17.9	18.0	18.5	17.2	17.0	17.7	17.4
COP of HP(39GPM)	2.2	2.2	2.2	2.2	2.2	2.2	2.2	2.1	2.0	1.9
COP of HP(45GPM)	2.5	2.5	2.5	2.5	2.5	2.5	2.5	2.4	2.3	2.1
	11th week	12th week	13th week	14th week	15th week	16th week	Total			
COP of solar	28.2	29.8	12.1	25.5	21.6	29.4	20.4			
solar-revise	28.2	29.8	12.1	25.5	21.6	29.4	21.1			
COP of DWHR	6.2	6.1	5.3	4.1	3.7	4.0	6.2			
DWHR_revise	17.1	17.7	17.0	15.1	12.8	12.8	17.1			
COP of HP(39GPM)	1.9	1.8	2.5	1.5	2.1	2.0	2.1			
COP of HP(45GPM)	2.2	2.1	2.9	1.7	2.5	2.3	2.5			

Production Cost (Natural gas and electricity):

	1st week	2nd week	3rd week	4th week	5th week	6th week	7th week	8th week	9th week	10th week
	$/GJ	$/GJ	$/GJ	$/GJ	$/GJ	$/GJ	$/GJ	$/GJ	$/GJ	$/GJ
Electricity(39GPM)	9.2	9.3	11.0	10.9	10.9	10.9	10.9	11.3	11.8	12.7
Electricity(45GPM)	8.0	8.0	8.2	8.1	8.1	8.1	8.1	8.4	8.8	9.5
Electricity(60GPM)	6.0	6.0	7.1	7.1	7.1	7.1	7.1	7.4	7.6	8.3
Natural Gas	3.4	3.8	3.8	4.0	4.2	4.1	4.2	3.9	3.9	4.0

	11th week	12th week	13th week	14th week	15th week	16th week	Total			
Electricity(39GPM)	12.3	12.9	9.5	15.8	11.1	12.0	11.4			
Electricity(45GPM)	9.2	9.6	7.1	11.7	8.2	8.9	8.6			
Electricity(60GPM)	8.0	8.4	6.2	10.2	7.2	7.8	7.4			
Natural Gas	4.1	4.1	3.6	3.8	3.8	3.8	3.9			

Expected Production Cost with COP improvement (Electricity):

COP improved	1st week	2nd week	3rd week	4th week	5th week	6th week	7th week	8th week	9th week	10th week
Electricity(min)	6.1	6.1	7.2	7.2	7.2	7.2	7.2	7.2	7.2	7.2
Electricity(max)	6.3	6.3	7.4	7.4	7.4	7.4	7.4	7.4	7.4	7.4

COP improved	11th week	12th week	13th week	14th week	15th week	16th week	Total			
Electricity(min)	7.2	7.2	7.2	7.2	7.2	7.2	7.0			
Electricity(max)	7.4	7.4	7.4	7.4	7.4	7.4	7.2			

G: Detail Calculations Results (monthly)

Power Usage Monthly Calculations:

System	Name	From	April			May			June		
			Start date	End date	Power usage	Start date	End date	ower usag	Start date	End date	ower usag
			01/04/2013 0:00	30/04/2013 23:59	kwh	01/05/2013 0:00	31/05/2013 23:59	kwh	01/06/2013 0:00	30/06/2013 23:59	kwh
Geo field	P1-1	bas_el_energy：P-1-1	2859316080	7743297981	1357	7743297981	12144613650	1223	12144613650	17013658803	1353
	P1-2	bas_el_energy：P-1-2	2823397335	7670857098	1347	7670857098	12654096357	1384	12654096357	17455817394	1334
Heat pumps	HP-1	bas_el_energy：HP1	180782670	9829932156	2680	9829932156	20645930013	3004	20645930013	21219372384	159
	HP-2	bas_el_energy：HP2	28488660	1394368425	379	1394368425	4369849254	827	4369849254	10345428798	1660
	HP-3	bas_el_energy：HP3	13090596066	13114678884	7	13114678884	14124961791	281	14124961791	15231585783	307
	HP-4	bas_el_energy：HP4	6516431607	32983995273	7352	32983995273	33702384621	200	33702384621	34551344751	236

System	Name	Power	April			May			June		
			Status	Power usage(kwh)	Subtotal	Status	Power usage(kwh)	Subtotal	Status	Power usage(kwh)	Subtotal
Solar	SHTS	111.55	1.00	80.32	80.32	1.00	82.99	82.99	1.00	80.32	80.32
DWHR	P7-1	714	1.00	514.08	654.26	1.00	531.22	671.21	1.00	514.08	653.56
	on stack	75.9	10.99	140.18		10.98	140.00		10.94	139.48	
Heat pumps_cir	P2-1	785	0.20	26.62	96.24	0.21	27.49	39.72	0.01	1.45	22.30
	P2-2	785	0.03	3.58		0.06	8.02		0.12	16.10	
	P2-3	785	0.00	0.00		0.02	2.48		0.02	2.71	
	P2-4	785	0.50	66.04		0.01	1.72		0.02	2.04	
Boilers	P4-1	870	0.00	0.00	0.00	0.00	0.00	0.00	0.00	0.00	0.00
	P4-2	870	0.00	0.00		0.00	0.00		0.00	0.00	
	BLR-1	324	0.00	0.00		0.00	0.00		0.00	0.00	
	BLR-2	324	0.00	0.00		0.00	0.00		0.00	0.00	
Heating loop	P3-1	2460	0.81	334.71	669.42	0.81	335.21	670.42	0.69	286.81	573.63
	P3-2	2460	0.81	334.71		0.81	335.21		0.69	286.81	

Energy production calculation and COP (monthly):

	April (GJ)	May (GJ)	June (GJ)
Solar	4.2	8.0	6.5
solar-revise	4.7	8.1	6.5
DWHR	29.1	26.0	19.1
GHE	23.1	-13.3	-13.6
Heat Pumps	93.82	36.30	20.41
Boilers 1&2	0.00	0.00	-1.97
	0.00	0.00	-1.29

	April (GJ)	May (GJ)	June (GJ)
Renewable (Solar+DWHR+GHE)	60.97	28.84	18.36
Paid (Electricity)	37.51	15.52	8.50
Paid (Natural Gas)	0.00	0.00	-3.26
Outside Temperature	-0.33	13.25	18.35
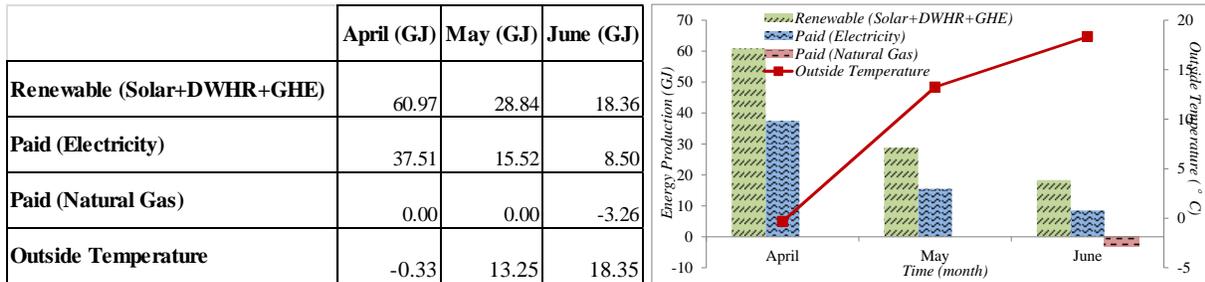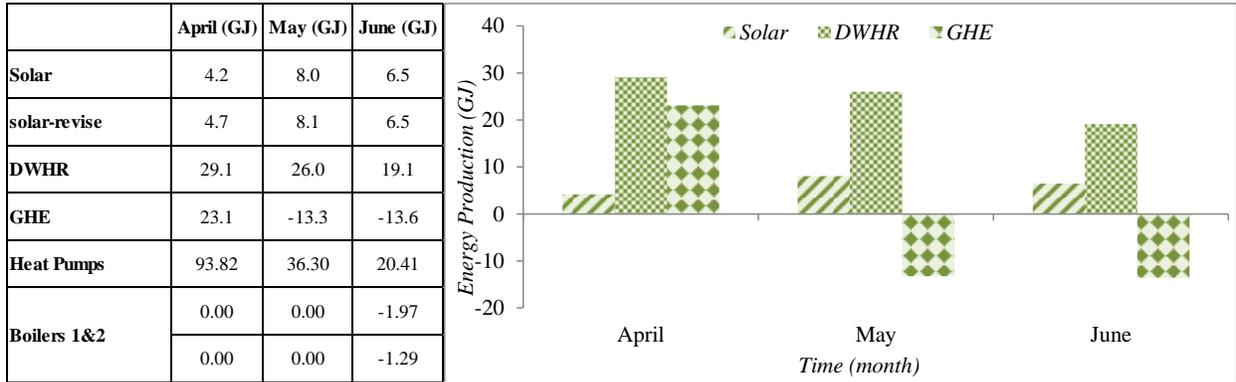
	April(kwh)	May(kwh)	June(kwh)
Electricity usage (solar)	80	83	80
Electricity usage (DWHR)	654	671	654
Electricity usage (HPs)	10419	4311	2362

	April	May	June
	$/GJ	$/GJ	$/GJ
Electricity	9.4	10.0	9.7
Electricity(45GPM)	8.1	8.7	8.4
Electricity(60GPM)	6.1	6.5	6.3
Natural Gas	3.5	3.4	3.4

	April	May	June
COP of solar	14.4	26.9	22.3
solar-revise	16.1	27.0	22.3
COP of DWHR	12.3	10.8	8.1
DWHR_revise	17.4	18.2	19.3
COP of HP(39GPM)	2.2	2.0	2.1
COP of HP(45GPM)	2.5	2.3	2.4

COP improved	April	May	June
Electricity	6.1	6.1	7.2
Electricity(60GPM)	6.3	6.3	7.4